Exploring the partonic phase at finite chemical potential within heavy-ion collisions

Pierre Moreau, Olga Soloveva, Lucia Oliva, Taesoo Song, Wolfgang Cassing, Elena Bratkovskaya

Rencontres QGP-France, Etretat, July 1, 2019

arXiv:1903.10257

Outline

- **Introduction / motivations**
- **The Dynamical QuasiParticle model (DQPM)**
- **Implementation of the (T, μ_B)-dependent EoS in PHSD**
- **Results for heavy-ion collisions**
- **Summary / outlook**

Motivations

- **Explore the QCD phase diagram at finite temperature and chemical potential through heavy-ion collisions**

- **Available information:**
  - **Experimental data at SPS, BES at RHIC**
  - **Lattice QCD calculation**

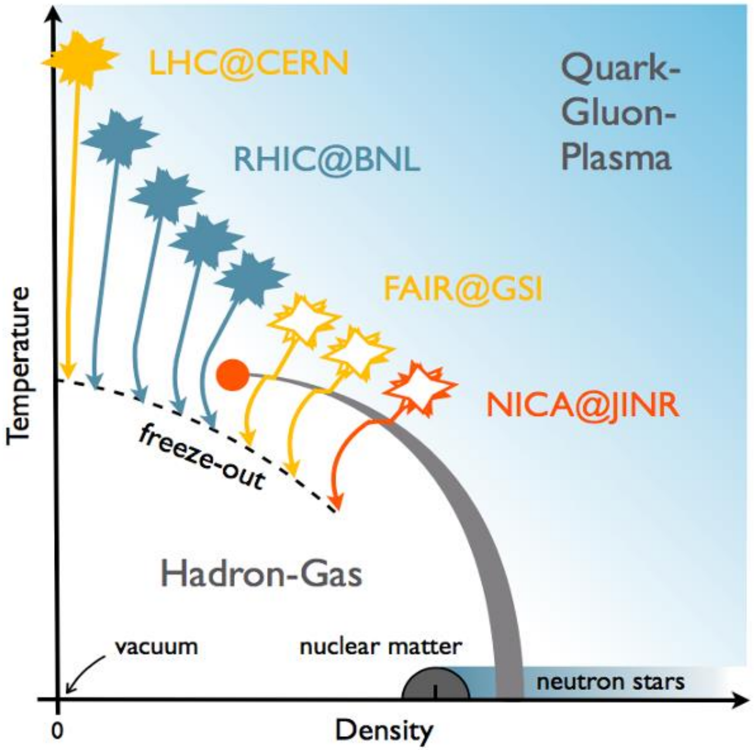

Probes of the QGP at finite (T, μ_B)

Dynamical description of HIC

- **Goal:** **Study the properties of strongly interacting matter under extreme conditions from a microscopic point of view**
- **Realization: dynamical many-body transport approach**

Parton-Hadron-String-Dynamics (PHSD)

- **Explicit parton-parton interactions, explicit transiton from hadronic to partonic degrees of freedom**
- **Transport theory: off-shell transport equations in phase-space representation based on Kadanoff-Baym equations for the partonic and hadronic phase**

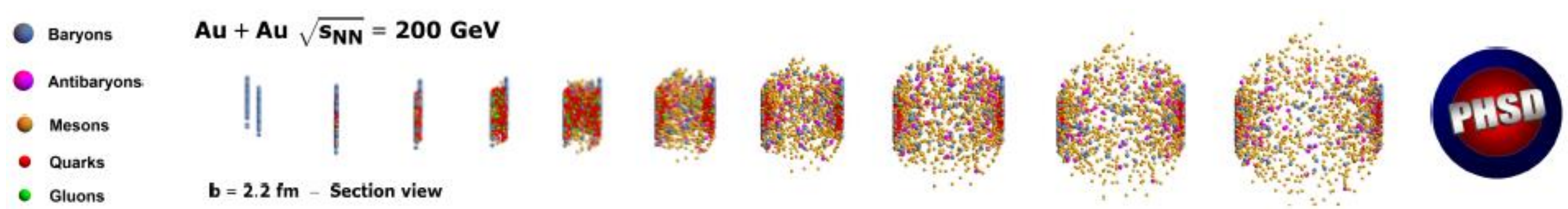

W.Cassing, E.Bratkovskaya, PRC 78 (2008) 034919; NPA831 (2009) 215; W.Cassing, EPJ ST 168 (2009) 3

Stages of a collision in PHSD

Initial A+A collision

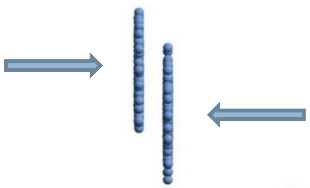

Partonic phase

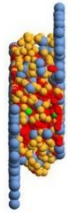

Hadronization

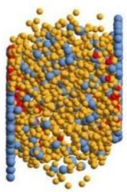

Hadronic phase

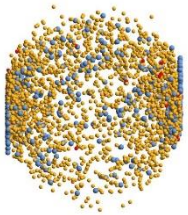

- **String formation in primary NN collisions**

→ decays to pre-hadrons (baryons and mesons)

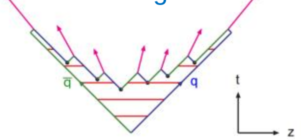

Stages of a collision in PHSD

Initial A+A collision

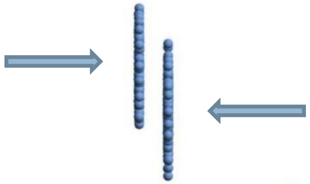

Partonic phase

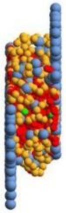

Hadronization

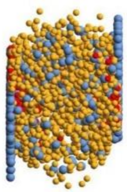

Hadronic phase

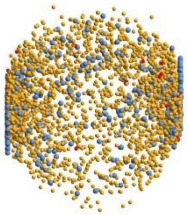

- **String formation in primary NN collisions**

→ **decays to pre-hadrons (baryons and mesons)**

LUND string model

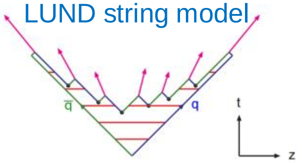

- **Formation of a QGP state if $\varepsilon > \varepsilon_{critical}$:**

Dissolution of pre-hadrons → DQPM

→ massive quarks/gluons and mean-field energy

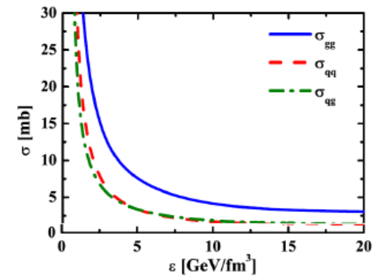

(quasi-)elastic collisions :

$$g+q \to g+q \qquad g+q \to g+q$$
$$g+\bar{q} \to g+\bar{q} \qquad g+\bar{q} \to g+\bar{q}$$
$$g+g \to g+g \qquad g+g \to g+g$$

inelastic collisions :

$$q+\bar{q} \to g+g \qquad q+\bar{q} \to g+g$$
$$g \to g+g \qquad g \to g+g$$

Stages of a collision in PHSD

Initial A+A collision

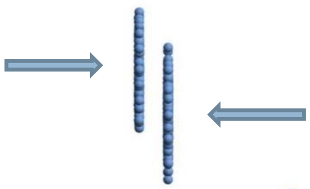

Partonic phase

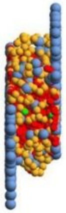

Hadronization

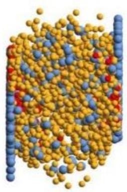

Hadronic phase

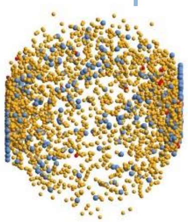

- **String formation in primary NN collisions**

→ decays to pre-hadrons (baryons and mesons)

LUND string model

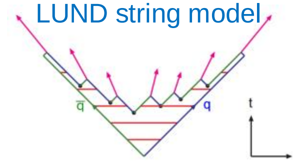

- **Formation of a QGP state if $\varepsilon > \varepsilon_{critical}$:**

  Dissolution of pre-hadrons → DQPM

  → massive quarks/gluons and mean-field energy

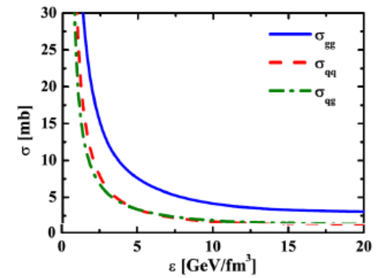

(quasi-)elastic collisions :

$$g+q \to g+q \qquad g+q \to g+q$$
$$g+\bar{q} \to g+\bar{q} \qquad g+\bar{q} \to g+\bar{q}$$
$$g+g \to g+g \qquad g+g \to g+g$$

inelastic collisions :

$$q+\bar{q} \to g+g \qquad q+\bar{q} \to g+g$$
$$g \to g+g \qquad g \to g+g$$

- **Hadronization to colorless off-shell mesons and baryons**

$$g \to q+\bar{q}, \quad q+\bar{q} \leftrightarrow meson\ ('\,string\,')$$
$$q+q+q \leftrightarrow baryon\ ('\,string\,')$$

Strict 4-momentum and quantum number conservation

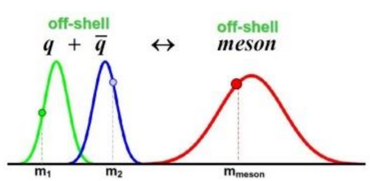

Stages of a collision in PHSD

Initial A+A collision

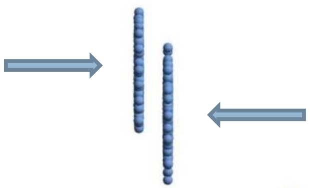

Partonic phase

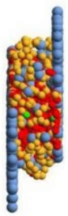

Hadronization

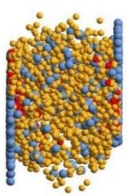

Hadronic phase

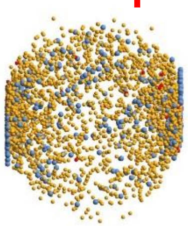

- **String formation in primary NN collisions**
  → decays to pre-hadrons (baryons and mesons)

LUND string model

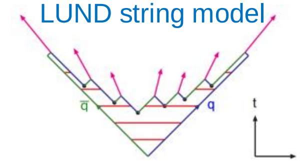

- **Formation of a QGP state if $\varepsilon > \varepsilon_{critical}$:**
  Dissolution of pre-hadrons → DQPM
  → massive quarks/gluons and mean-field energy

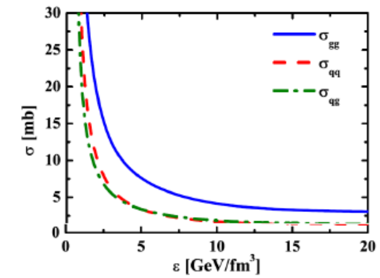

(quasi-)elastic collisions :

$$g+q \rightarrow g+q \qquad g+q \rightarrow g+q$$
$$g+\bar{q} \rightarrow g+\bar{q} \qquad g+\bar{q} \rightarrow g+\bar{q}$$
$$g+g \rightarrow g+g \qquad g+g \rightarrow g+g$$

inelastic collisions :

$$q+\bar{q} \rightarrow g+g \qquad q+\bar{q} \rightarrow g+g$$
$$g \rightarrow g+g \qquad g \rightarrow g+g$$

- **Hadronization to colorless off-shell mesons and baryons**

$$g \rightarrow q+\bar{q}, \quad q+\bar{q} \leftrightarrow meson\ ('string')$$
$$q+q+q \leftrightarrow baryon\ ('string')$$

Strict 4-momentum and quantum number conservation

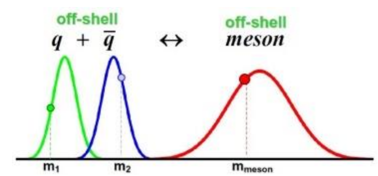

- **Hadron-string interactions – off-shell HSD**

CRC-TR 211
Strong-interaction matter under extreme conditions

Stages of a collision in PHSD

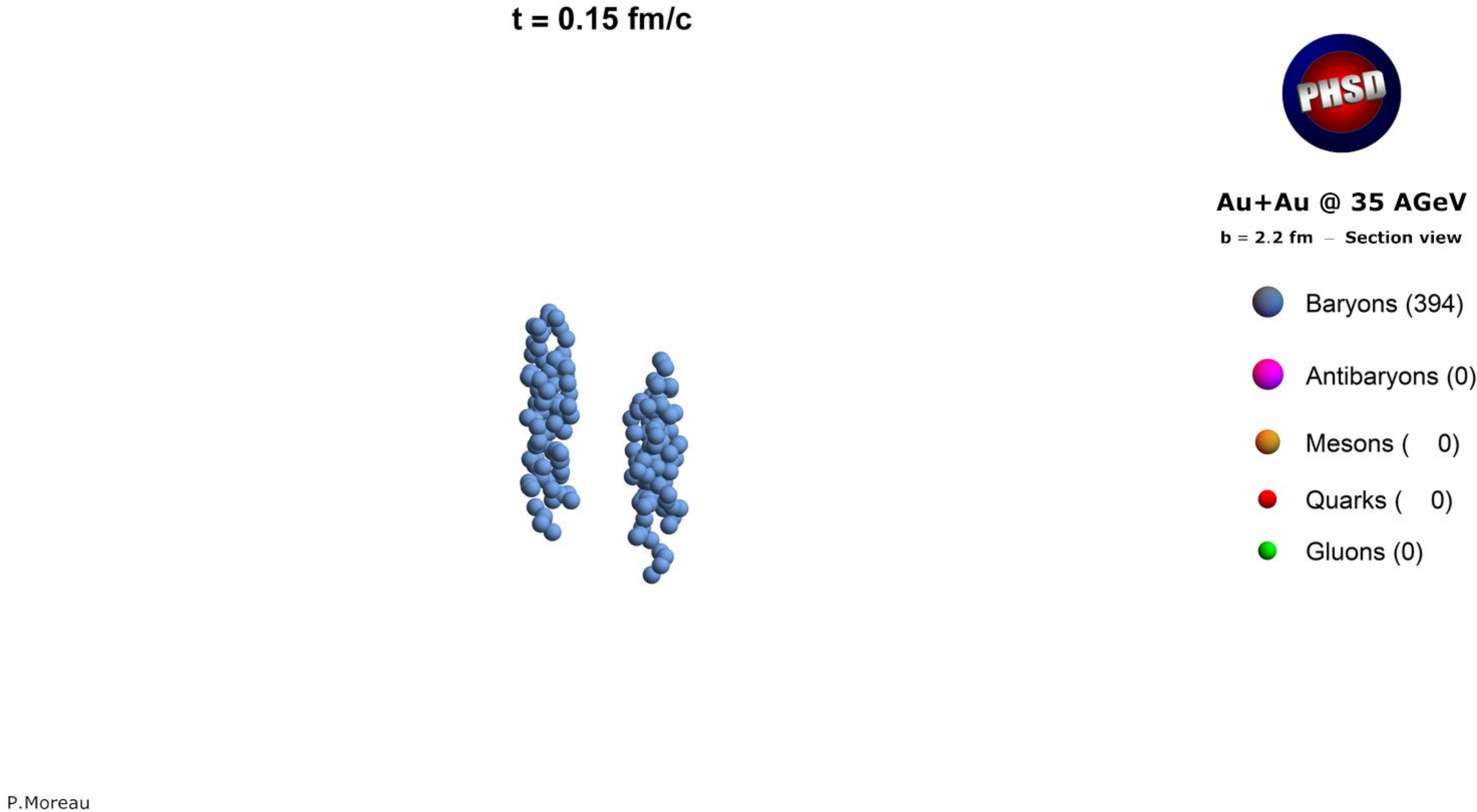

Stages of a collision in PHSD

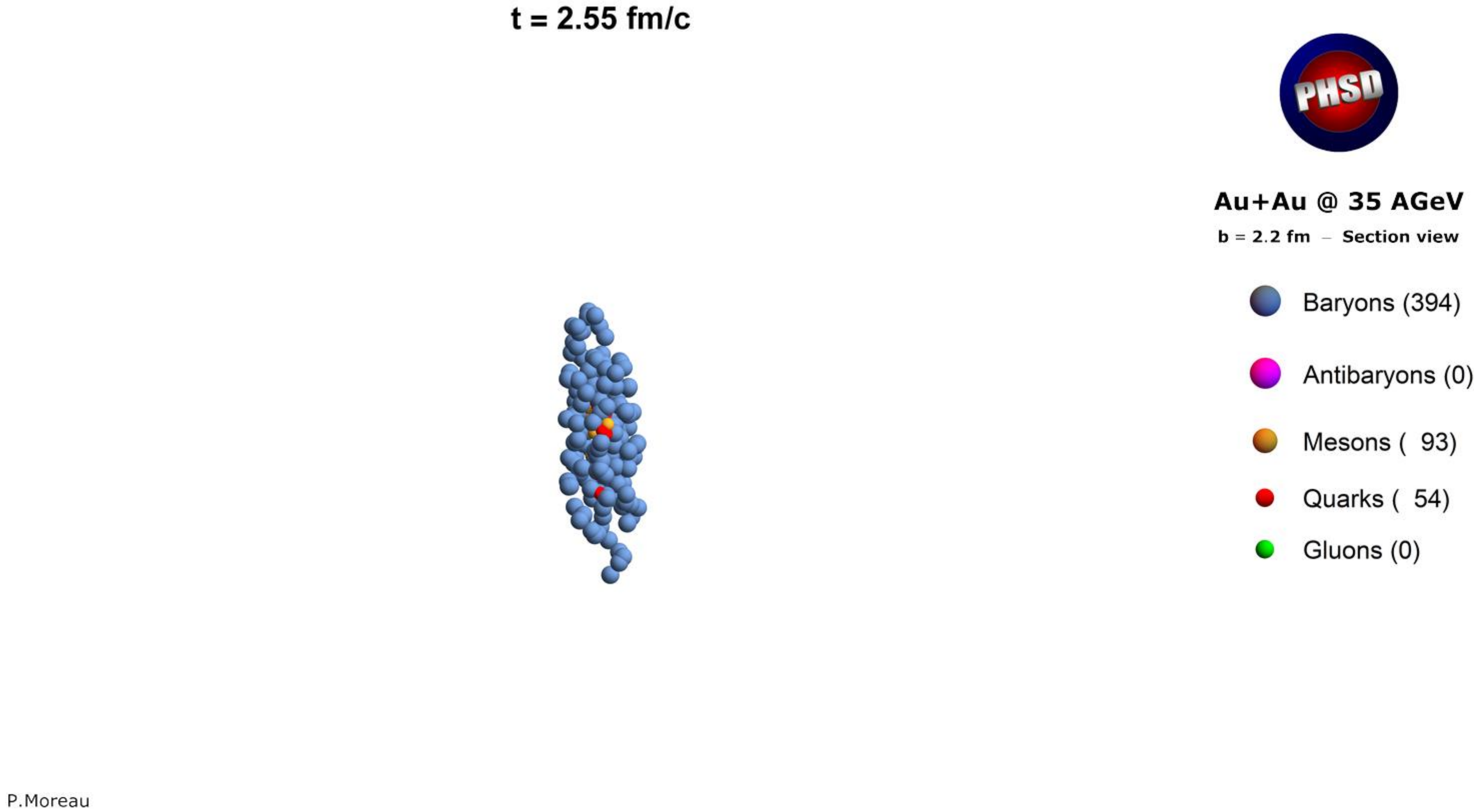

Stages of a collision in PHSD

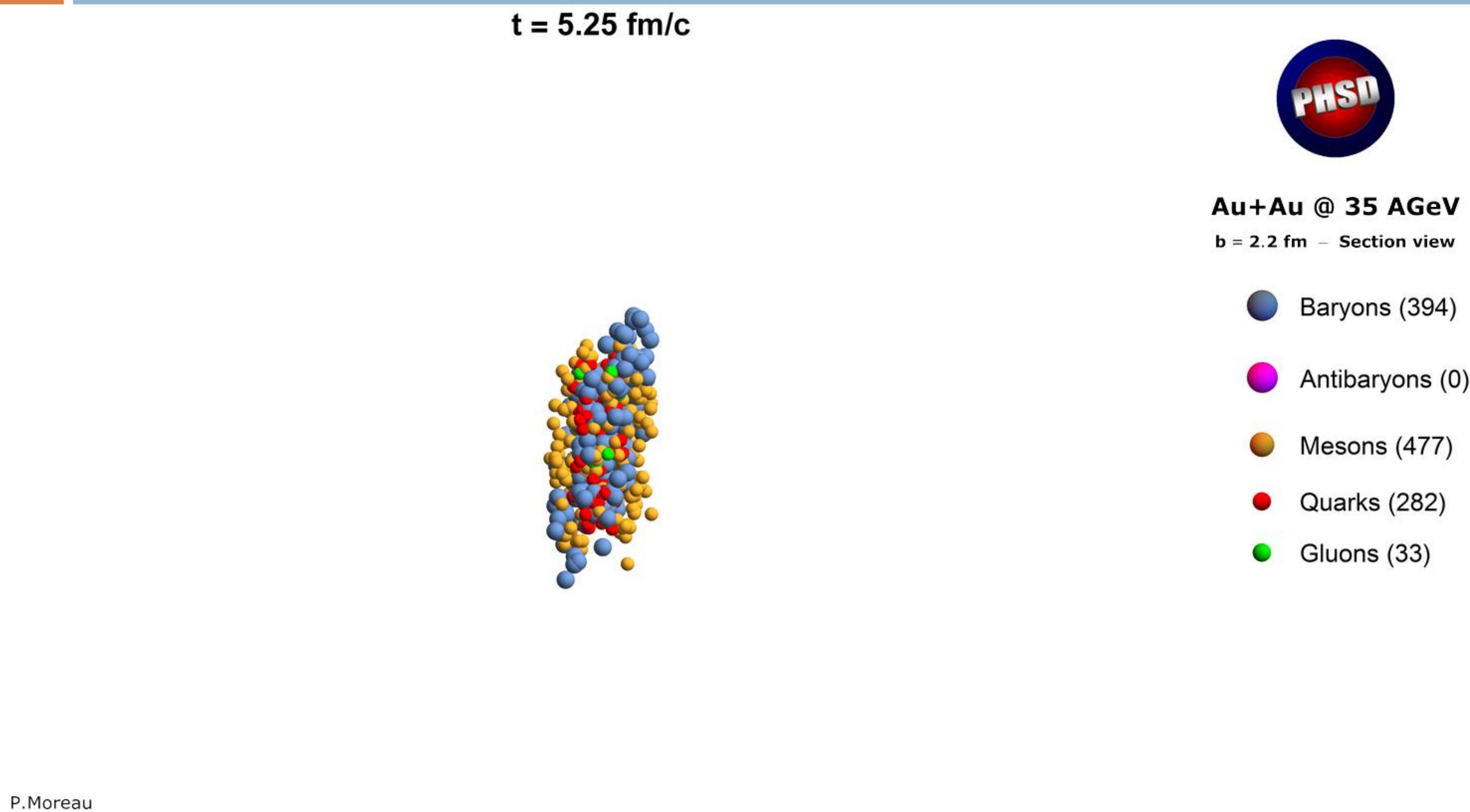

Stages of a collision in PHSD

CRC-TR 211
Strong-interaction matter under extreme conditions

t = 6.55001 fm/c

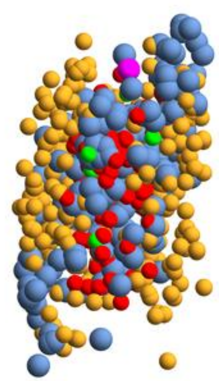

PHSD

Au+Au @ 35 AGeV

b = 2.2 fm – Section view

Baryons (397)

Antibaryons (3)

Mesons (554)

Quarks (199)

Gluons (20)

P.Moreau

Stages of a collision in PHSD

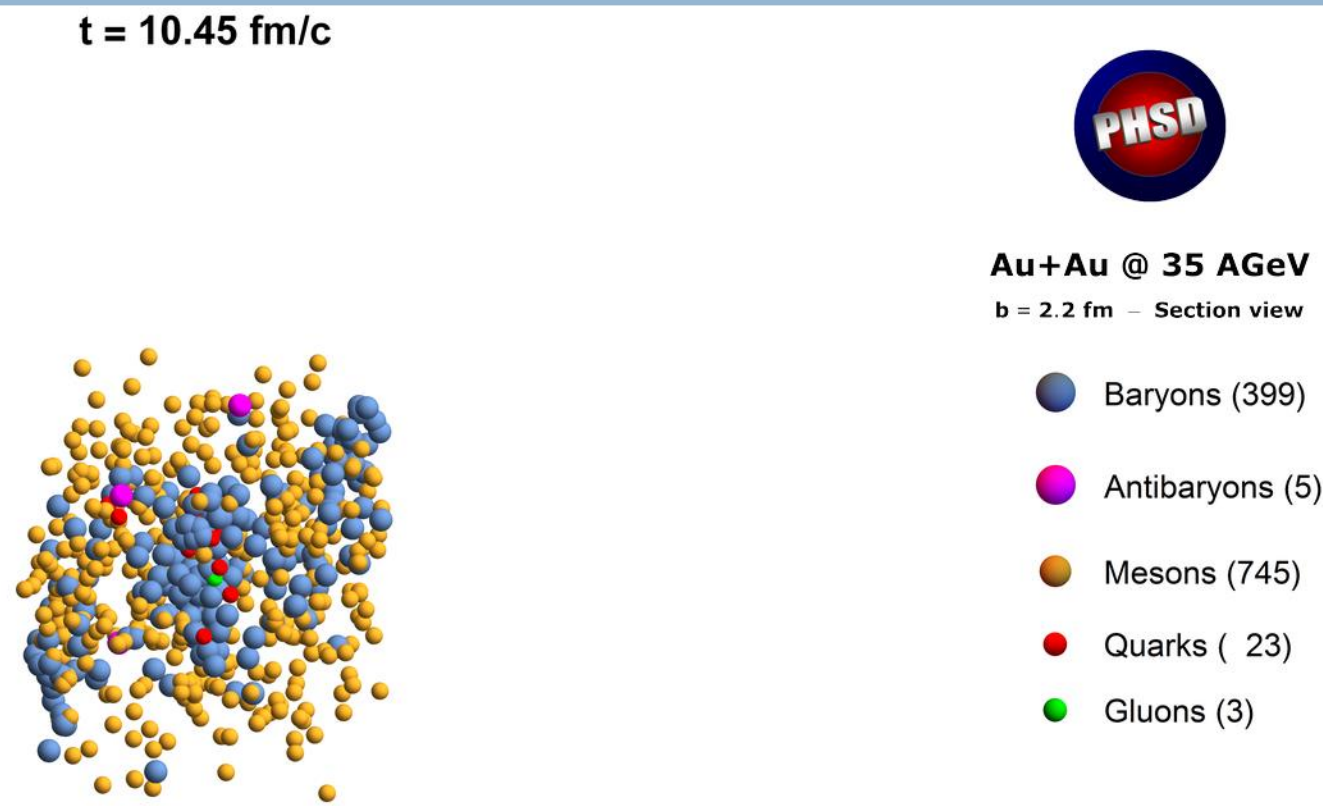

P.Moreau

Stages of a collision in PHSD

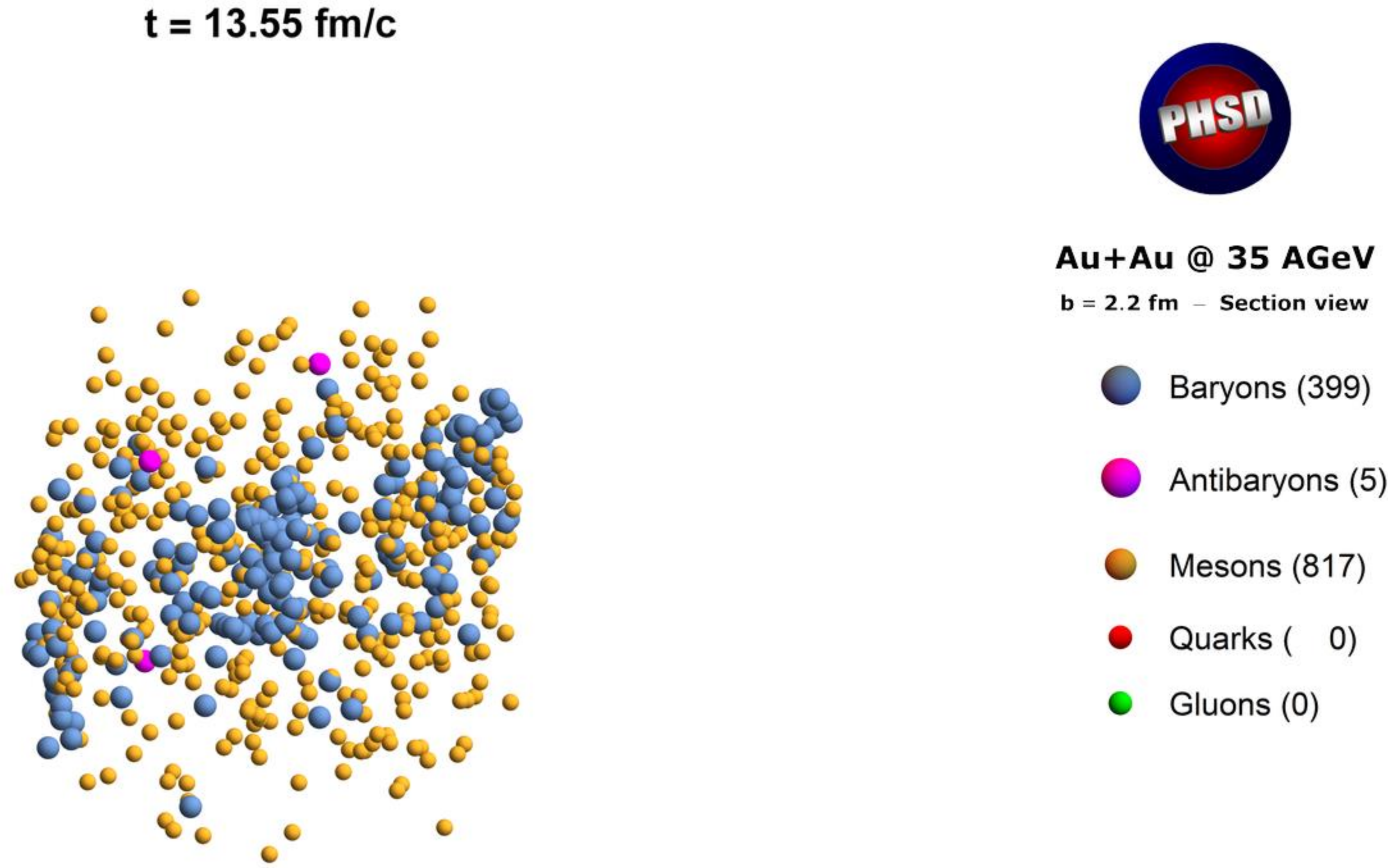

P.Moreau

Stages of a collision in PHSD

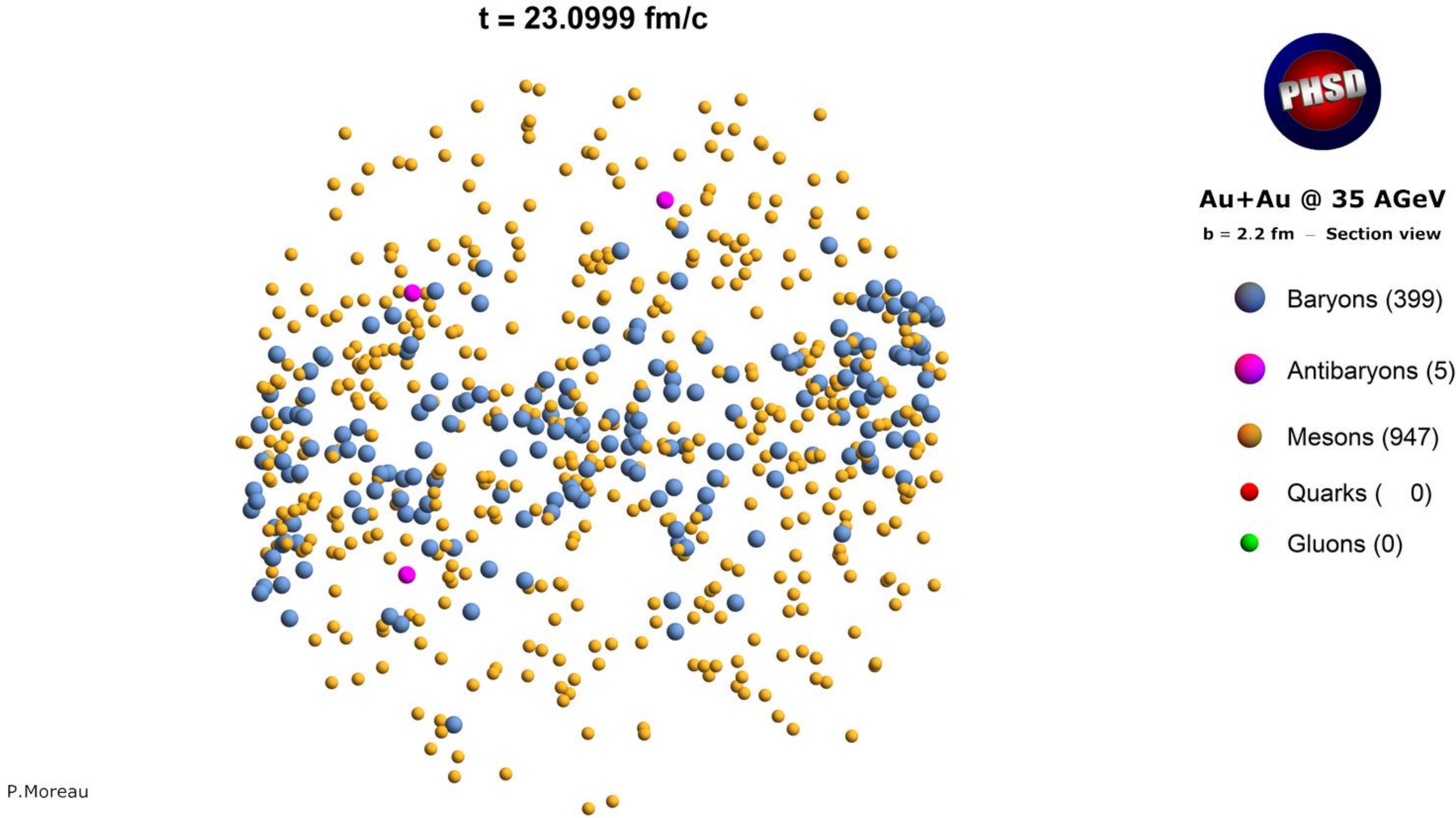

Stages of a collision in PHSD

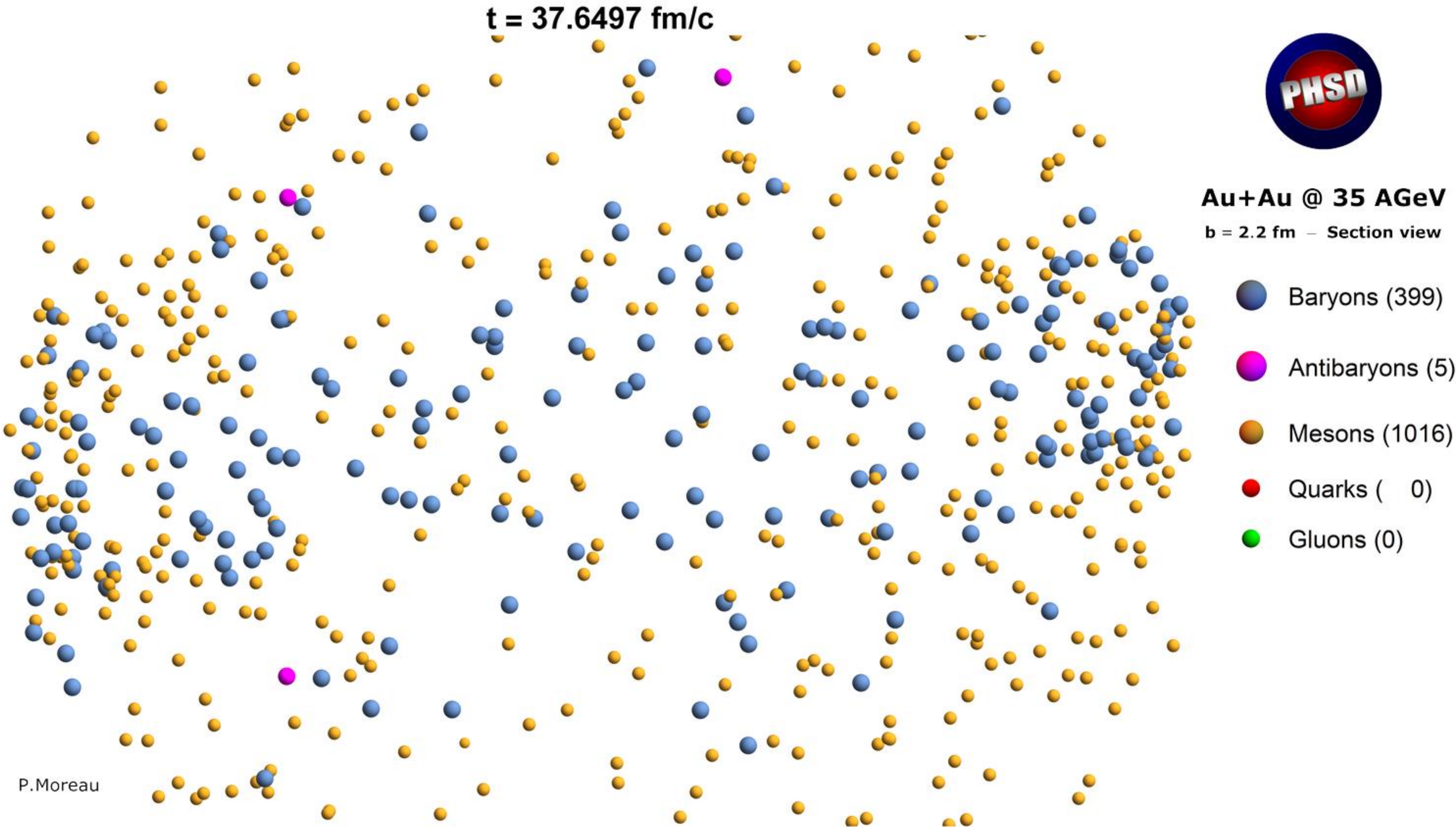

DQPM (T, μ_B)

QCD EoS, partonic interactions

Lattice data for $\mu_B = 0$ and $\neq 0$

CRC-TR 211
Strong-interaction matter under extreme conditions

- **Lattice QCD data: well known at $\mu_B = 0$**
  - **Crossover from hadron gas to QGP**

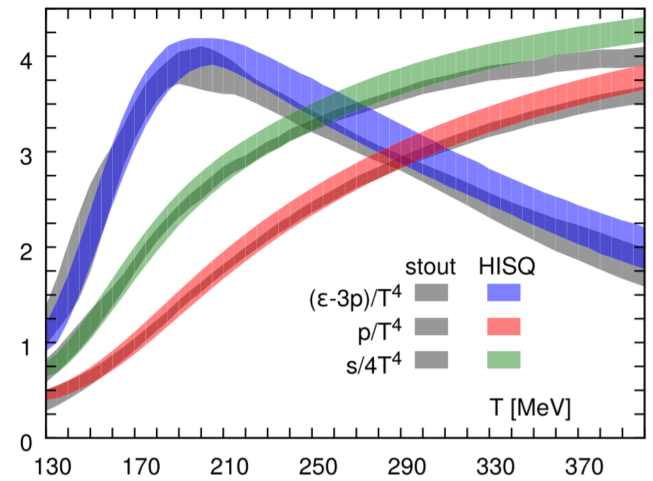

- **Results available at finite μ_B from analytical continuation or from a series expansion in terms of the susceptibilities**

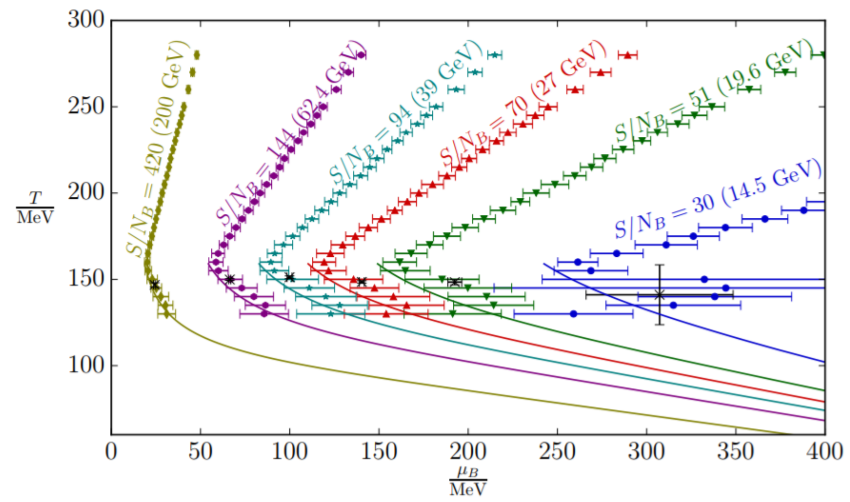

Lattice results from: Phys.Rev. D90 (2014) 094503; PoS CPOD2017 (2018) 032

Lattice data at finite (T, μ_B)

- Taylor series of thermodynamic quantities in terms of (μ_B/T)

- For the pressure, we get:

$$\frac{P}{T^4} = c_0(T) + c_2(T)\left(\frac{\mu_B}{T}\right)^2 + c_4(T)\left(\frac{\mu_B}{T}\right)^4 + c_6(T)\left(\frac{\mu_B}{T}\right)^6 + \mathcal{O}\left(\mu_B^8\right)$$

- Conditions of heavy-ion collisions

$$\langle \mathrm{n_S} \rangle = 0 \text{ and } \langle \mathrm{n_Q} \rangle = 0.4\ \langle \mathrm{n_B} \rangle$$

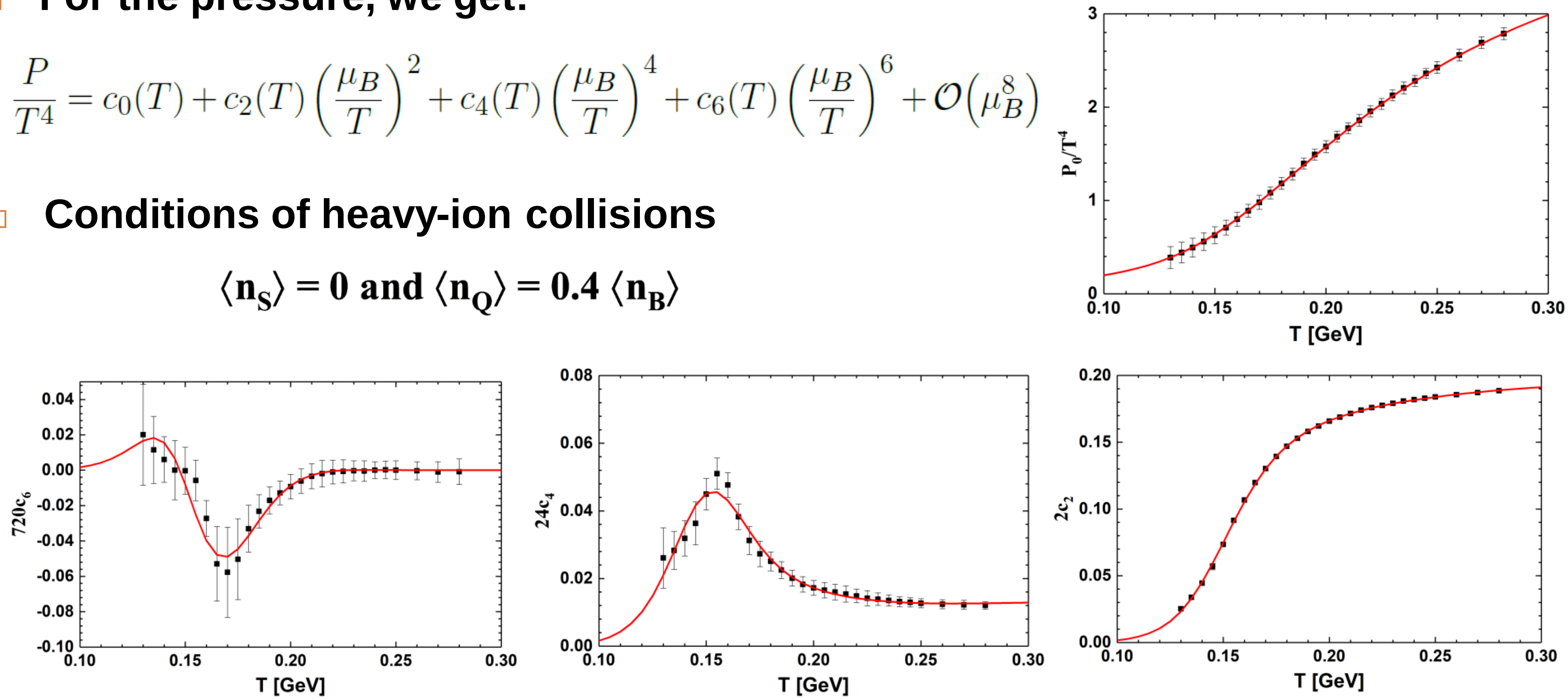

EPJ Web Conf. 137 (2017) 07008

Isentropic trajectories for (T, μ_B)

CRC-TR 211
Strong-interaction matter under extreme conditions

- Correspondance $s/n_B \leftrightarrow$ collisional energy

s/n_B = 420 ↔ 200 GeV

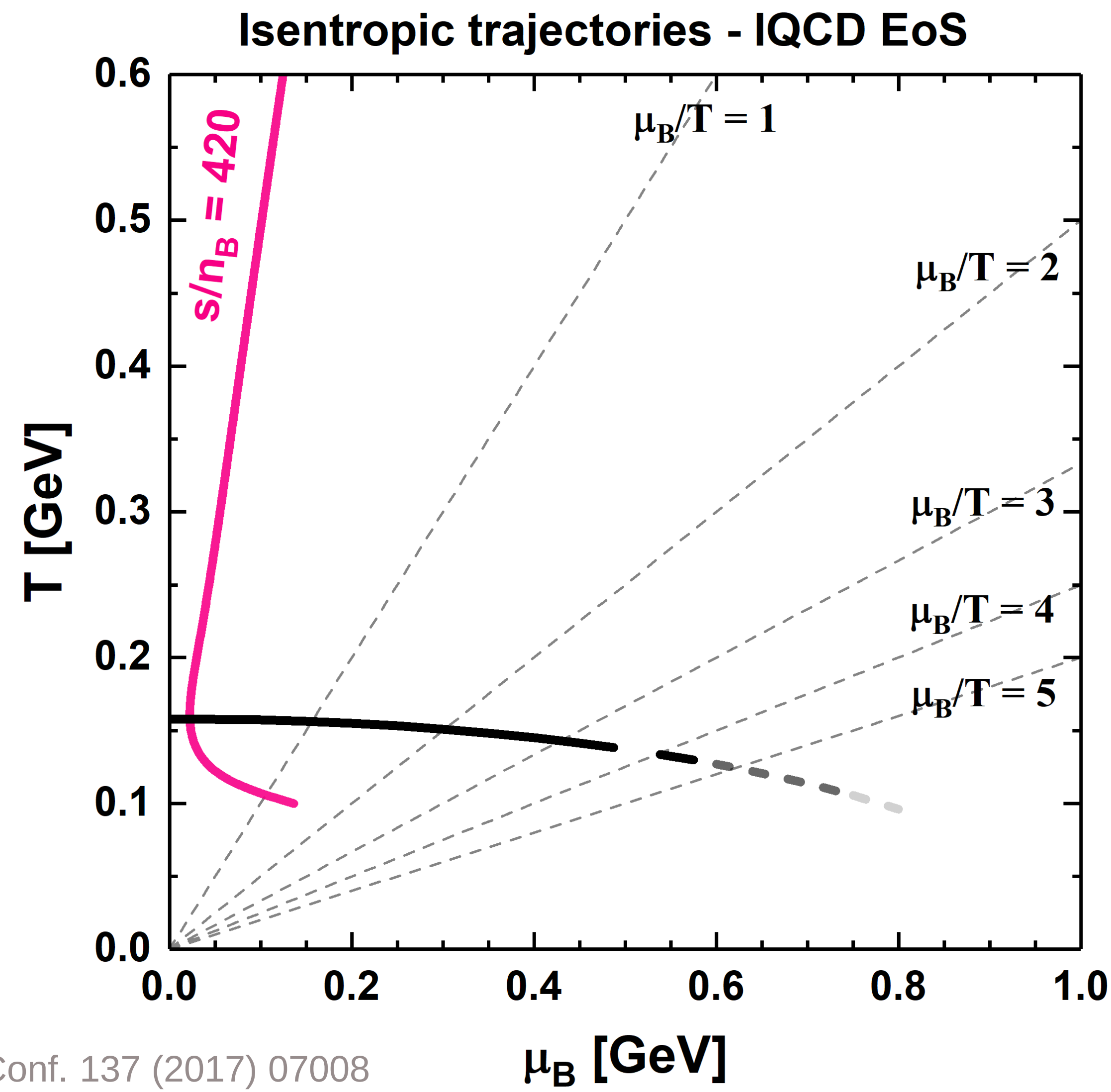

EPJ Web Conf. 137 (2017) 07008

Isentropic trajectories for (T, μ_B)

- Correspondance $s/n_B \leftrightarrow$ collisional energy

s/n_B = 420 ↔ 200 GeV

= 144 ↔ 62.4 GeV

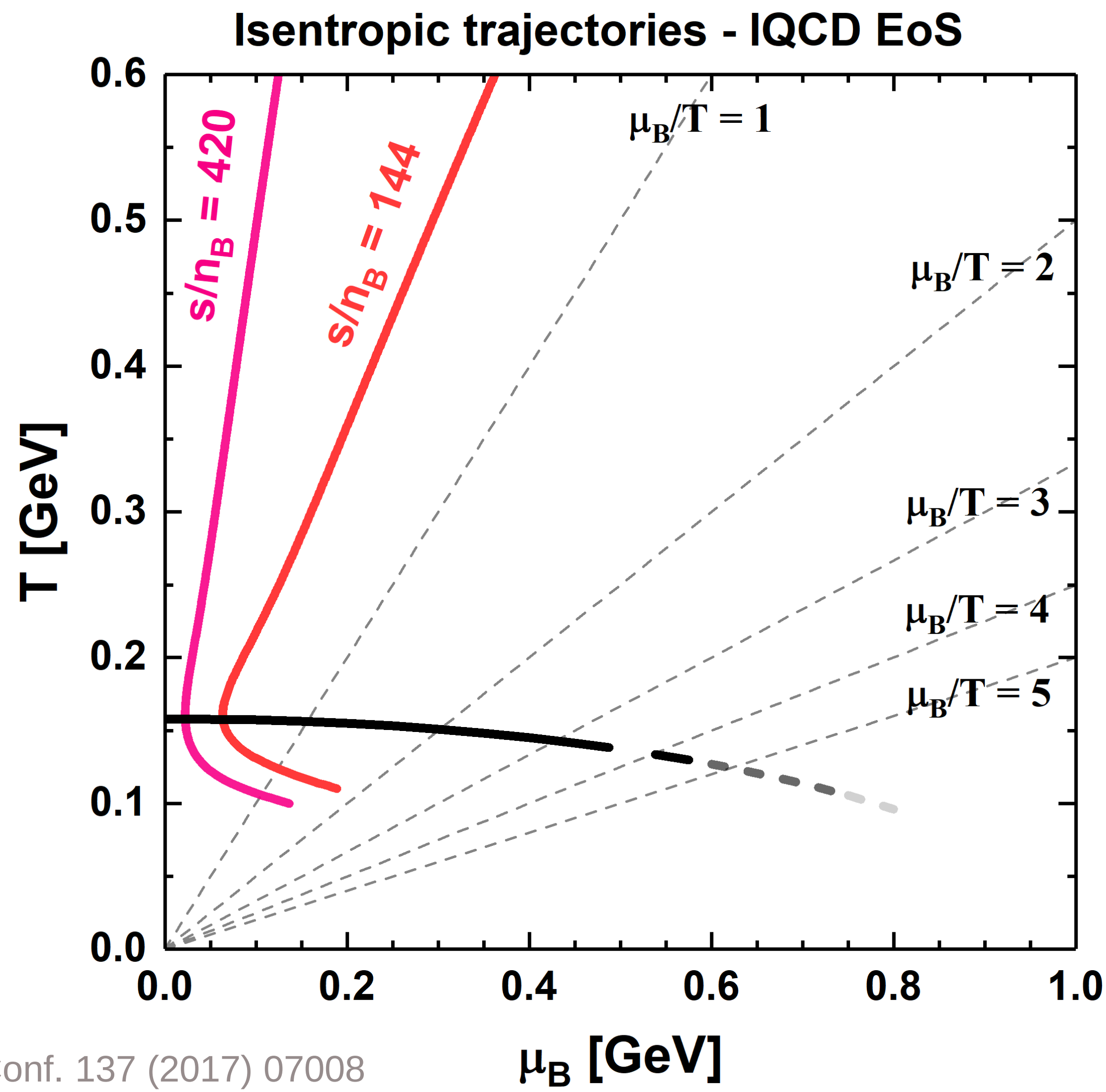

EPJ Web Conf. 137 (2017) 07008

Isentropic trajectories for (T, μ_B)

- Correspondance $s/n_B \leftrightarrow$ collisional energy

s/n_B = 420 ↔ 200 GeV

= 144 ↔ 62.4 GeV

= 94 ↔ 39 GeV

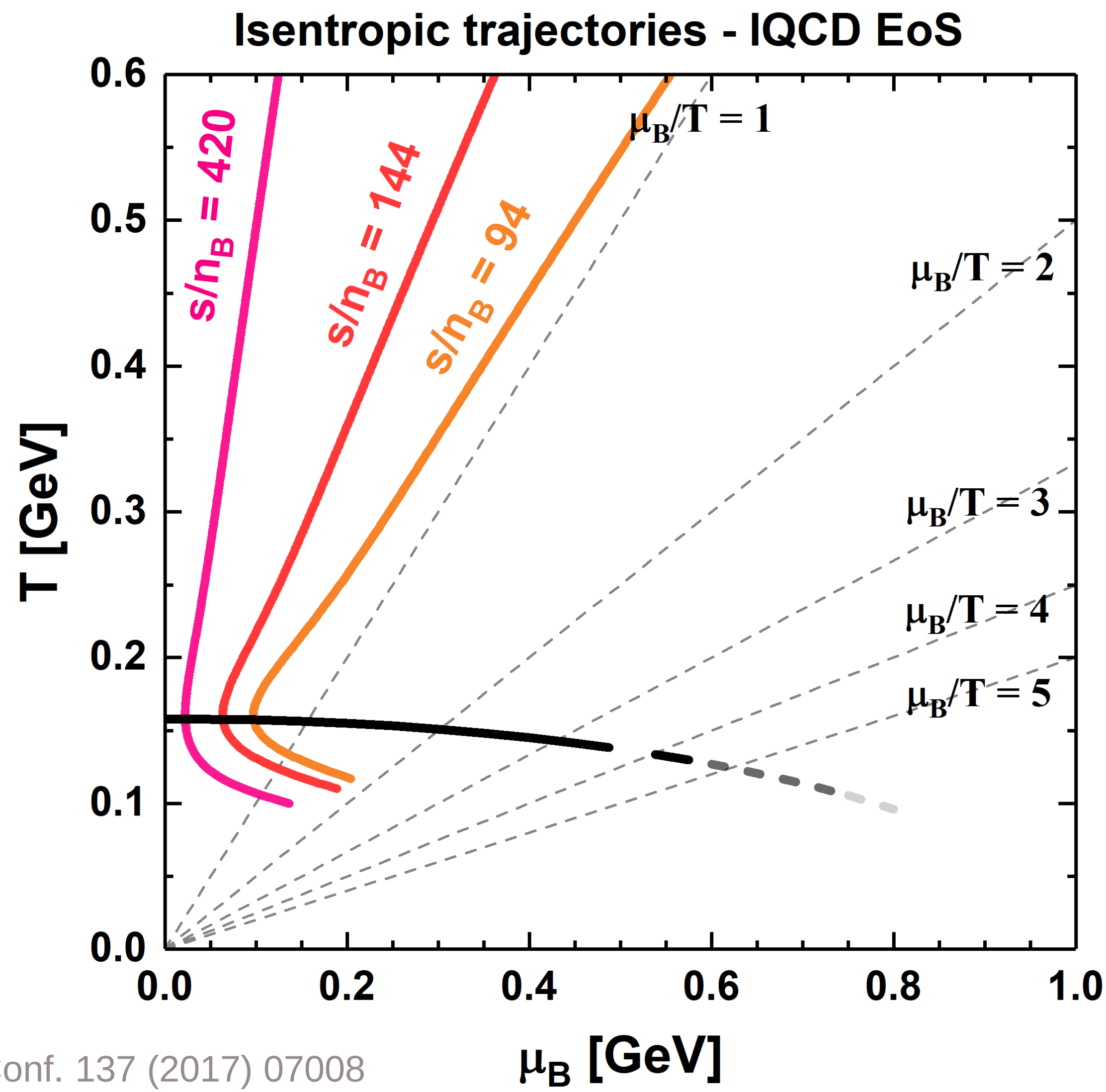

EPJ Web Conf. 137 (2017) 07008

Isentropic trajectories for (T, μ_B)

- Correspondance $s/n_B \leftrightarrow$ collisional energy

s/n_B = 420 ↔ 200 GeV

= 144 ↔ 62.4 GeV

= 94 ↔ 39 GeV

= 70 ↔ 27 GeV

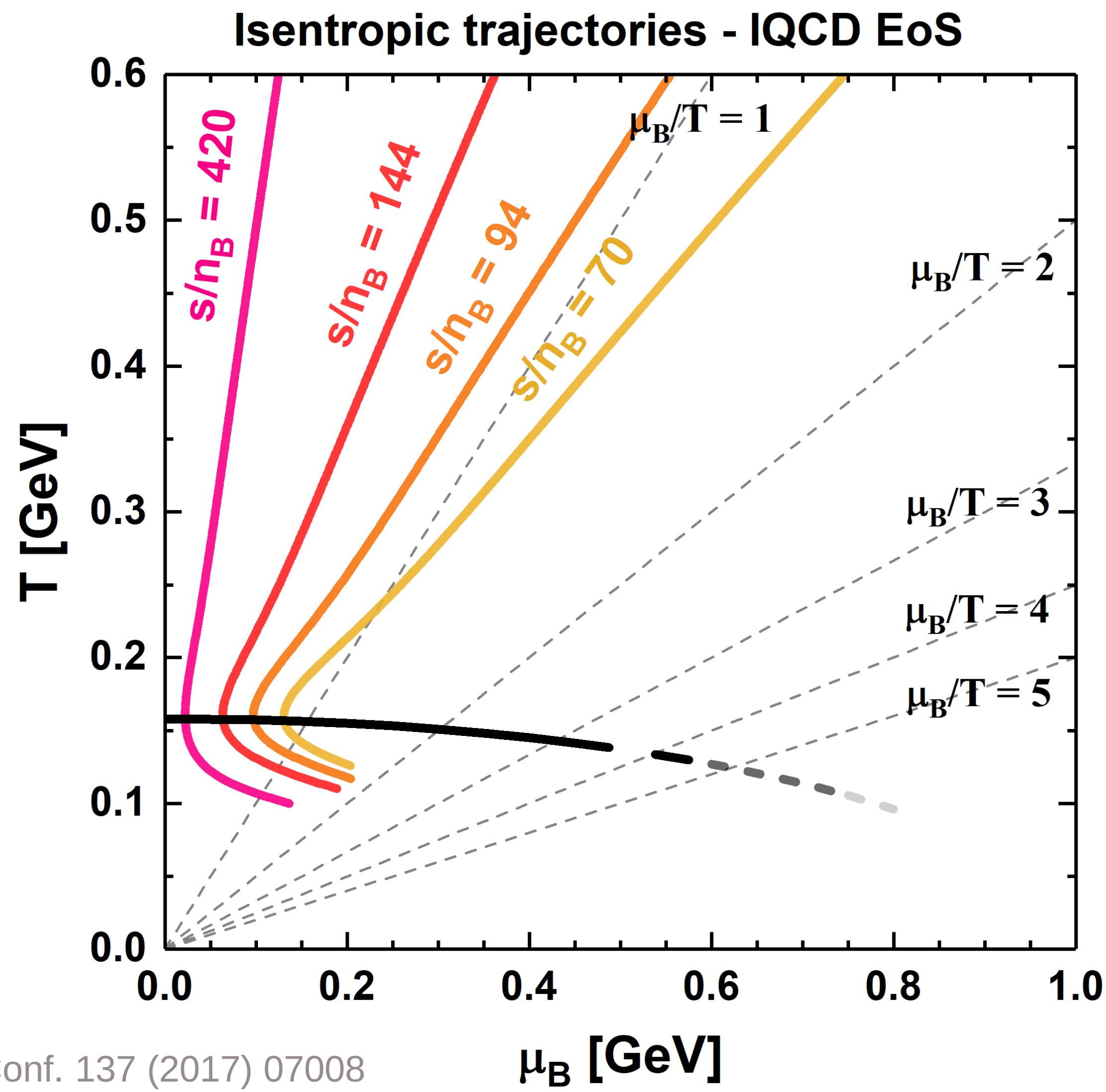

EPJ Web Conf. 137 (2017) 07008

CRC–TR 211 Strong-interaction matter under extreme conditions

Isentropic trajectories for (T, μ_B)

- Correspondance $s/n_B \leftrightarrow$ collisional energy

s/n_B = 420 ↔ 200 GeV

= 144 ↔ 62.4 GeV

= 94 ↔ 39 GeV

= 70 ↔ 27 GeV

= 51 ↔ 19.6 GeV

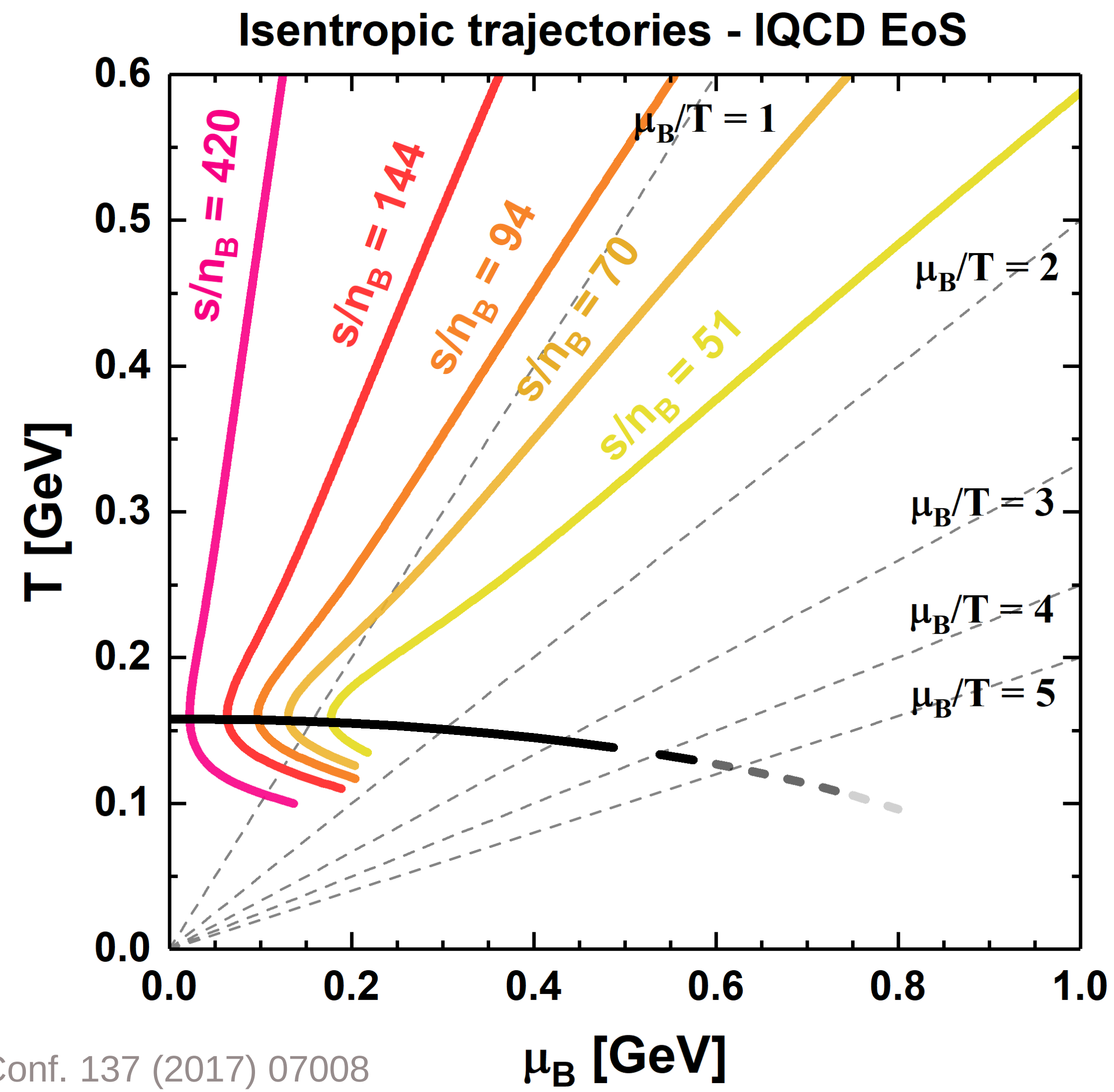

EPJ Web Conf. 137 (2017) 07008

Isentropic trajectories for (T, μ_B)

- Correspondance $s/n_B \leftrightarrow$ collisional energy

s/n_B = 420 ↔ 200 GeV

= 144 ↔ 62.4 GeV

= 94 ↔ 39 GeV

= 70 ↔ 27 GeV

= 51 ↔ 19.6 GeV

= 30 ↔ 14.5 GeV

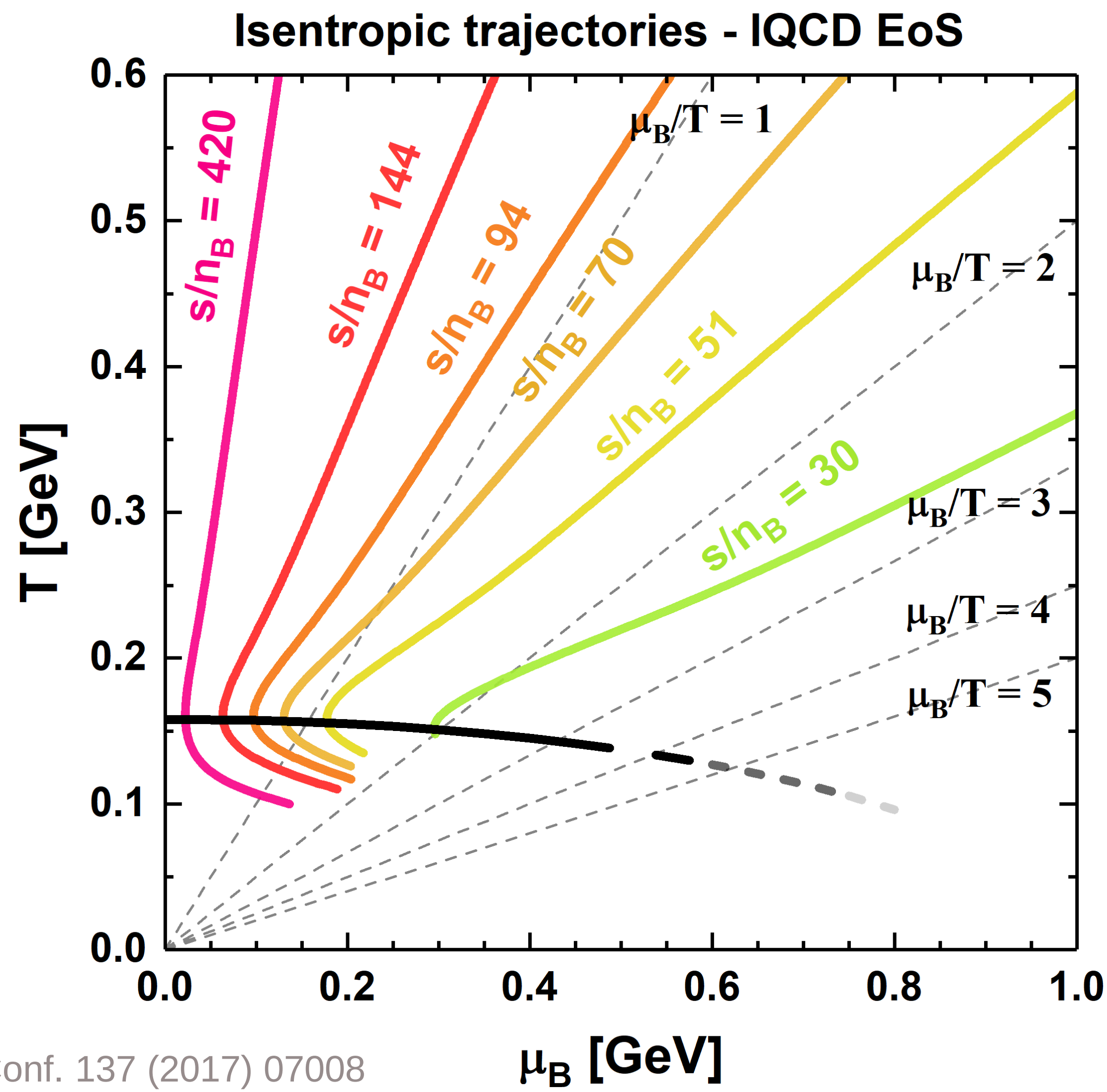

EPJ Web Conf. 137 (2017) 07008

Isentropic trajectories for (T, μ_B)

CRC-TR 211
Strong-interaction matter under extreme conditions

- Correspondance $s/n_B \leftrightarrow$ collisional energy

s/n_B = 420 ↔ 200 GeV

= 144 ↔ 62.4 GeV

= 94 ↔ 39 GeV

= 70 ↔ 27 GeV

= 51 ↔ 19.6 GeV

= 30 ↔ 14.5 GeV

- **Safe for $(\mu_B/T) < 3$**

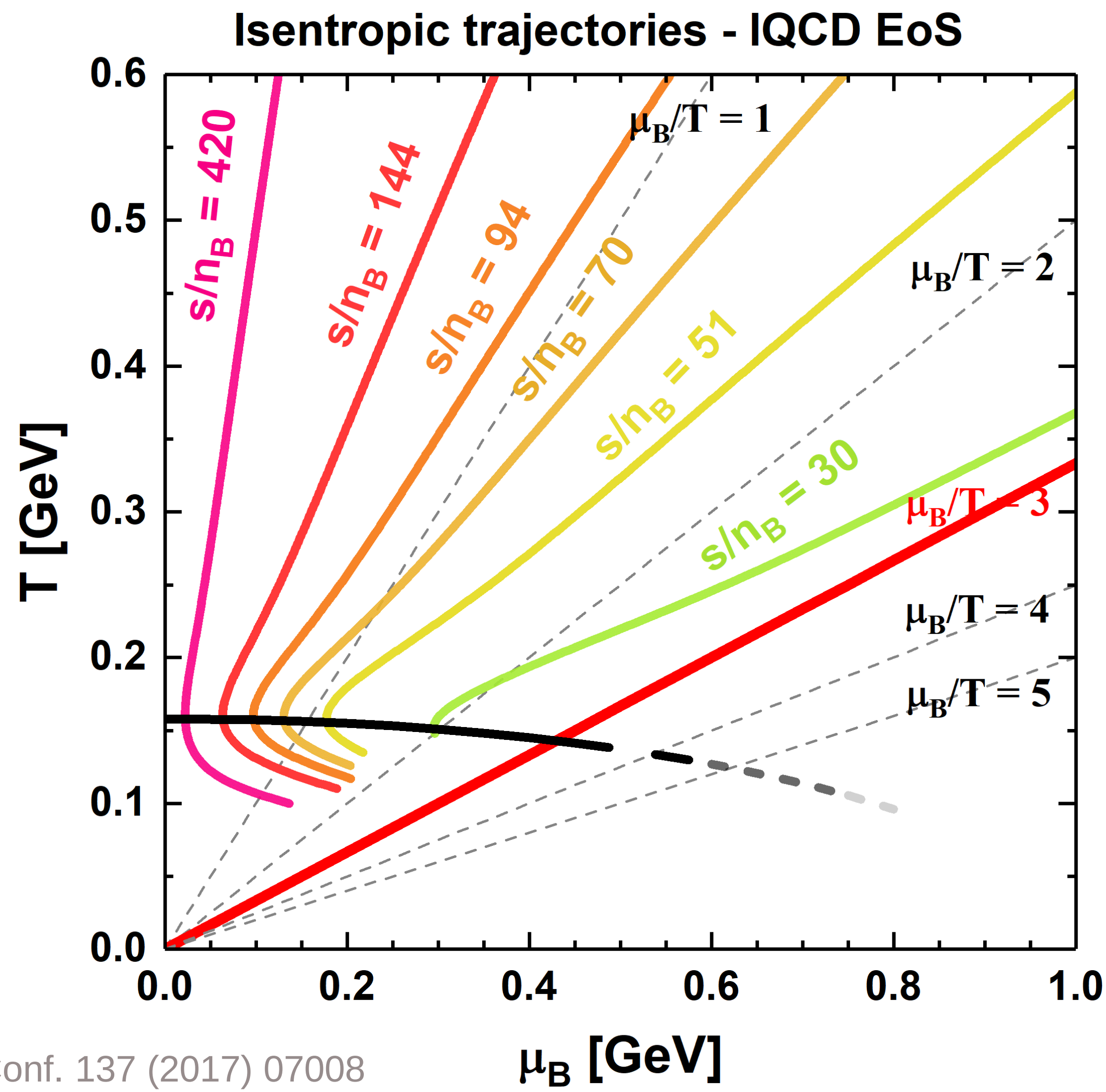

EPJ Web Conf. 137 (2017) 07008

CRC–TR 211
Strong-interaction matter under extreme conditions

Isentropic trajectories for (T, μ_B)

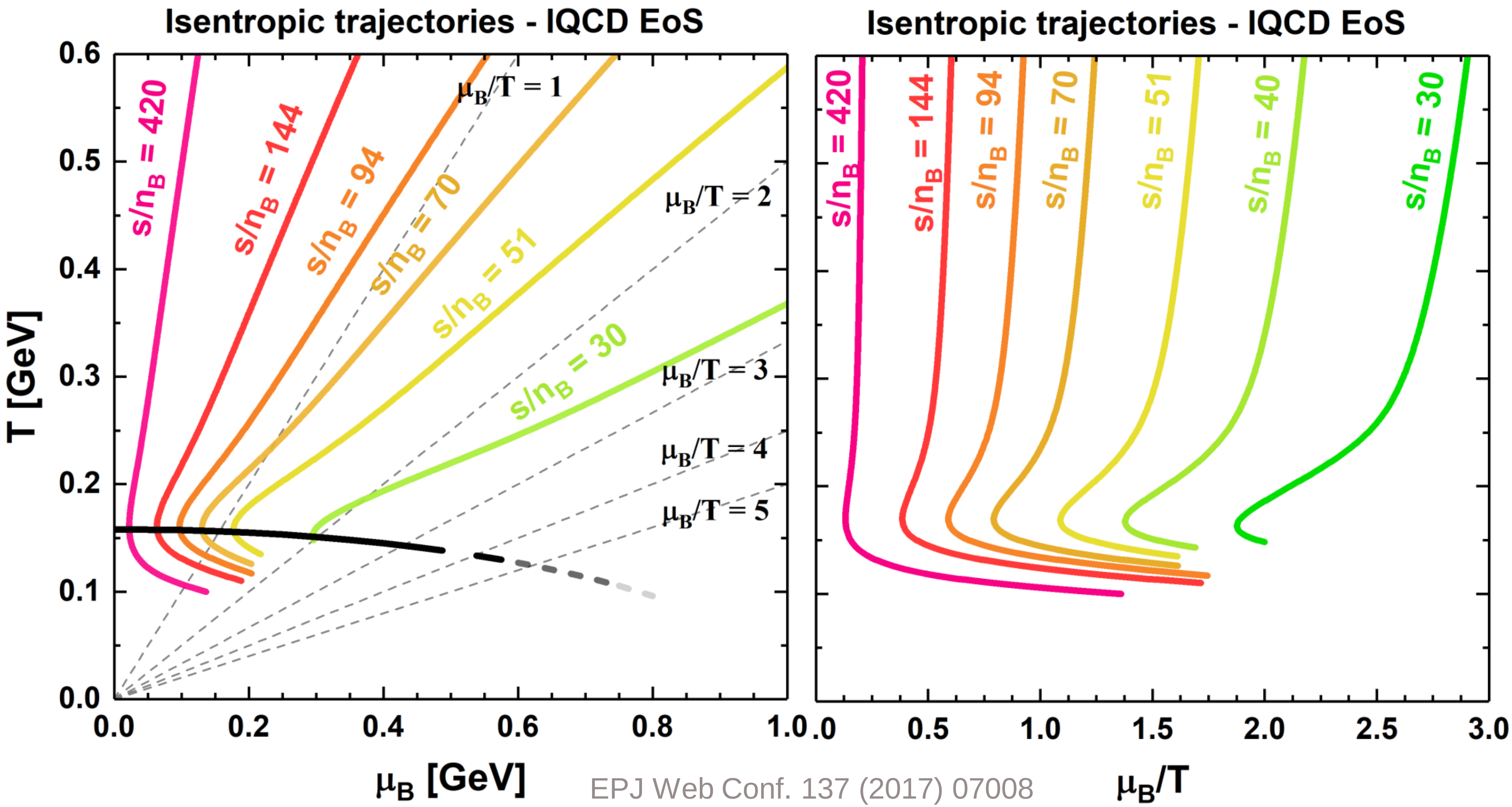

EPJ Web Conf. 137 (2017) 07008

Dynamical QuasiParticle Model (DQPM)

CRC-TR 211 Strong-interaction matter under extreme conditions

- Information from lQCD can constrain effective models for the QGP

Need to be interpreted in terms of degrees-of-freedom

- The QGP phase is described in terms of **interacting quasiparticles: quarks and gluons** with Lorentzian spectral functions:

$$\rho_j(\omega,\mathbf{p}) = \frac{\gamma_j}{\tilde{E}_j}\left(\frac{1}{(\omega-\tilde{E}_j)^2+\gamma_j^2} - \frac{1}{(\omega+\tilde{E}_j)^2+\gamma_j^2}\right)$$
$$\equiv \frac{4\omega\gamma_j}{\left(\omega^2-\mathbf{p}^2-M_j^2\right)^2+4\gamma_j^2\omega^2}$$

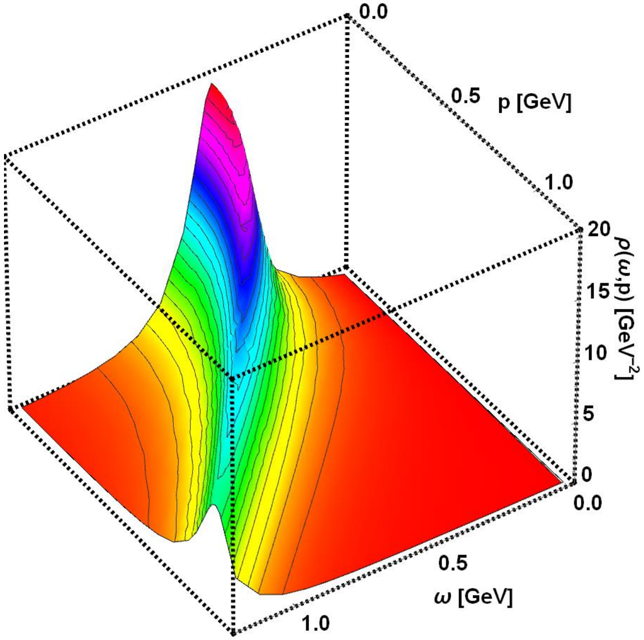

- Corresponding retarded propagator:

$$G^R(\omega,\mathbf{p}) = \frac{1}{\omega^2-\mathbf{p}^2-M^2+2i\gamma\omega}$$

Peshier, Cassing, PRL 94 (2005) 172301; Cassing, NPA 791 (2007) 365: NPA 793 (2007)

Dynamical QuasiParticle Model (DQPM)

- The QGP phase is described in terms of **interacting quasiparticles: quarks and gluons** with Lorentzian spectral functions:

$$\rho_j(\omega,\mathbf{p}) = \frac{\gamma_j}{\tilde{E}_j}\left(\frac{1}{(\omega-\tilde{E}_j)^2+\gamma_j^2} - \frac{1}{(\omega+\tilde{E}_j)^2+\gamma_j^2}\right)$$
$$\equiv \frac{4\omega\gamma_j}{\left(\omega^2-\mathbf{p}^2-M_j^2\right)^2+4\gamma_j^2\omega^2}$$

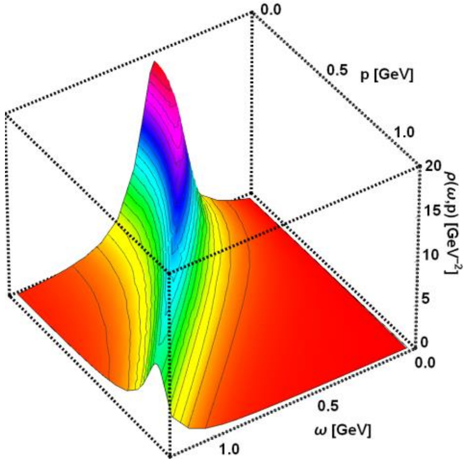

- **Resummed properties of the quasiparticles are specified by scalar complex self-energies:**

gluon propagator: $\Delta^{-1} = P^2 - \Pi$	&	quark propagator $S_q^{-1} = P^2 - \Sigma_q$
gluon self-energy: $\Pi = M_g^2 - i2g_g\omega$	&	quark self-energy: $\Sigma_q = M_q^2 - i2g_q\omega$

- **Real part of the self-energy: thermal mass (M_g, M_q)**
- **Imaginary part of the self-energy: interaction width of partons (γ_g, γ_q)**

Peshier, Cassing, PRL 94 (2005) 172301; Cassing, NPA 791 (2007) 365: NPA 793 (2007)

CRC-TR 211
Strong-interaction matter under extreme conditions

Parton properties

- **Modeling of the quark/gluon masses and widths (inspired by HTL calculations)**

$$M_g^2(T,\mu_B) = \frac{g^2(T,\mu_B)}{6}\left(\left(N_c + \frac{1}{2}N_f\right)T^2 + \frac{N_c}{2}\sum_q \frac{\mu_q^2}{\pi^2}\right)$$

$$M_{q(\bar{q})}^2(T,\mu_B) = \frac{N_c^2-1}{8N_c} g^2(T,\mu_B)\left(T^2 + \frac{\mu_q^2}{\pi^2}\right)$$

$$\gamma_{q(\bar{q})}(T,\mu_B) = \frac{1}{3}\frac{N_c^2-1}{2N_c}\frac{g^2(T,\mu_B)T}{8\pi}\ln\left(\frac{2c}{g^2(T,\mu_B)}+1\right)$$

$$\gamma_g(T,\mu_B) = \frac{1}{3}N_c\frac{g^2(T,\mu_B)T}{8\pi}\ln\left(\frac{2c}{g^2(T,\mu_B)}+1\right)$$

- **Only one parameter (c = 14.4) + (T,μ_B)- dependent coupling constant to determine from lattice results**

DQPM coupling constant

- Input: entropy density as a function of temperature for $\mu_B = 0$

$$g^2(s/s_{SB}) = d\left((s/s_{SB})^e - 1\right)^f$$

$$s_{SB}^{QCD} = 19/9\pi^2 T^3$$

Fit to lattice data:

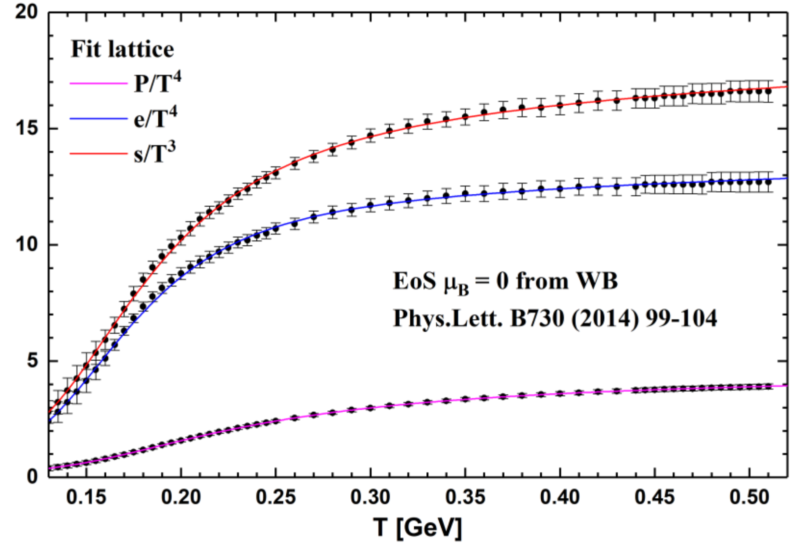

DQPM coupling constant

- Input: entropy density as a function of temperature for $\mu_B = 0$

$$g^2(s/s_{SB}) = d\left((s/s_{SB})^e - 1\right)^f$$

$$s_{SB}^{QCD} = 19/9\pi^2 T^3$$

- Scaling hypothesis at finite $\mu_B \approx 3\mu_q$

$$g^2(T/T_c, \mu_B) = g^2\left(\frac{T^*}{T_c(\mu_B)}, \mu_B = 0\right)$$

with the effective temperature

$$T^* = \sqrt{T^2 + \mu_q^2/\pi^2}$$

and the critical temperature at finite μ_B

$$T_c(\mu_B) = T_c\sqrt{1 - \alpha\mu_B^2}$$

Fit to lattice data:

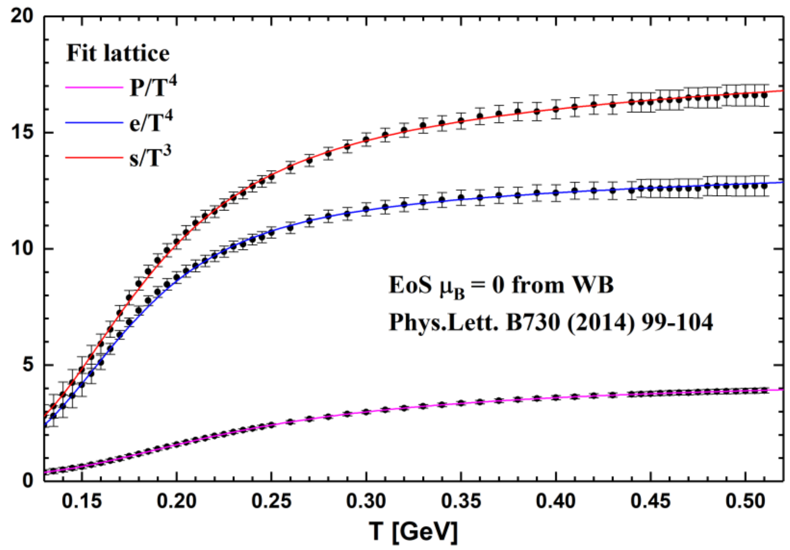

DQPM coupling constant

- Input: entropy density as a function of temperature for $\mu_B = 0$

$$g^2(s/s_{SB}) = d\left((s/s_{SB})^e - 1\right)^f$$

$$s_{SB}^{QCD} = 19/9\pi^2 T^3$$

Fit to lattice data:

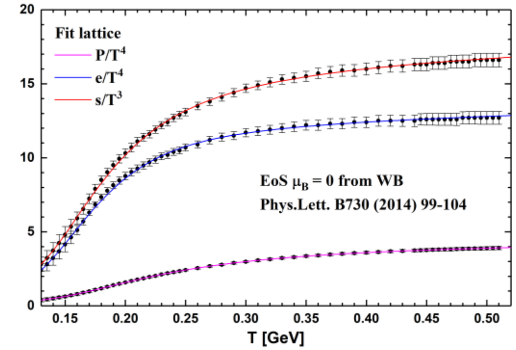

- Scaling hypothesis at finite $\mu_B \approx 3\mu_q$

$$g^2(T/T_c, \mu_B) = g^2\left(\frac{T^*}{T_c(\mu_B)}, \mu_B = 0\right)$$

with the effective temperature

$$T^* = \sqrt{T^2 + \mu_q^2/\pi^2}$$

and the critical temperature at finite μ_B

$$T_c(\mu_B) = T_c\sqrt{1 - \alpha\mu_B^2}$$

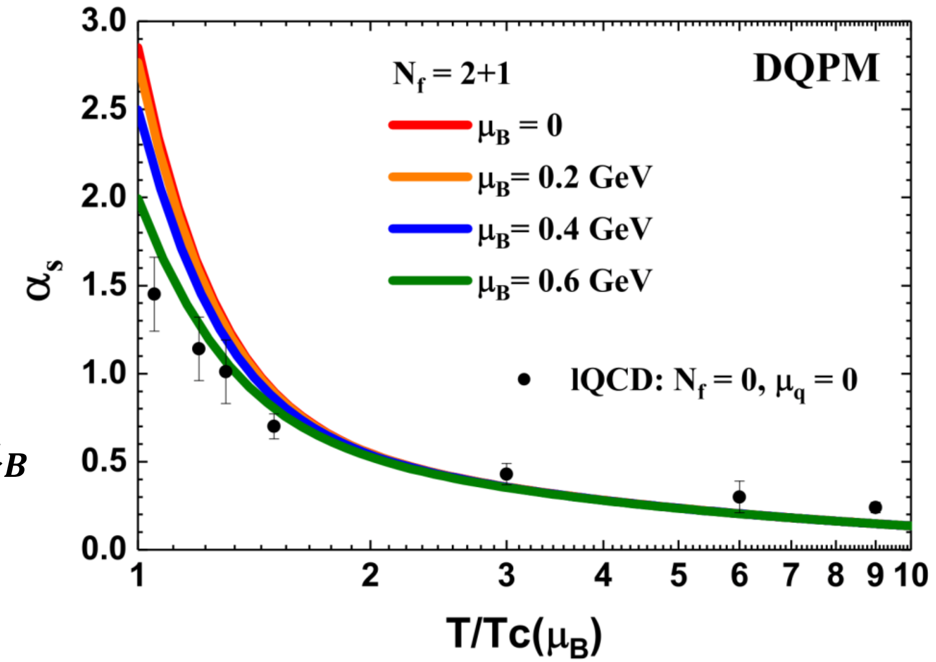

DQPM: parton properties

- DQPM masses and widths as a function of (T, μ_B)

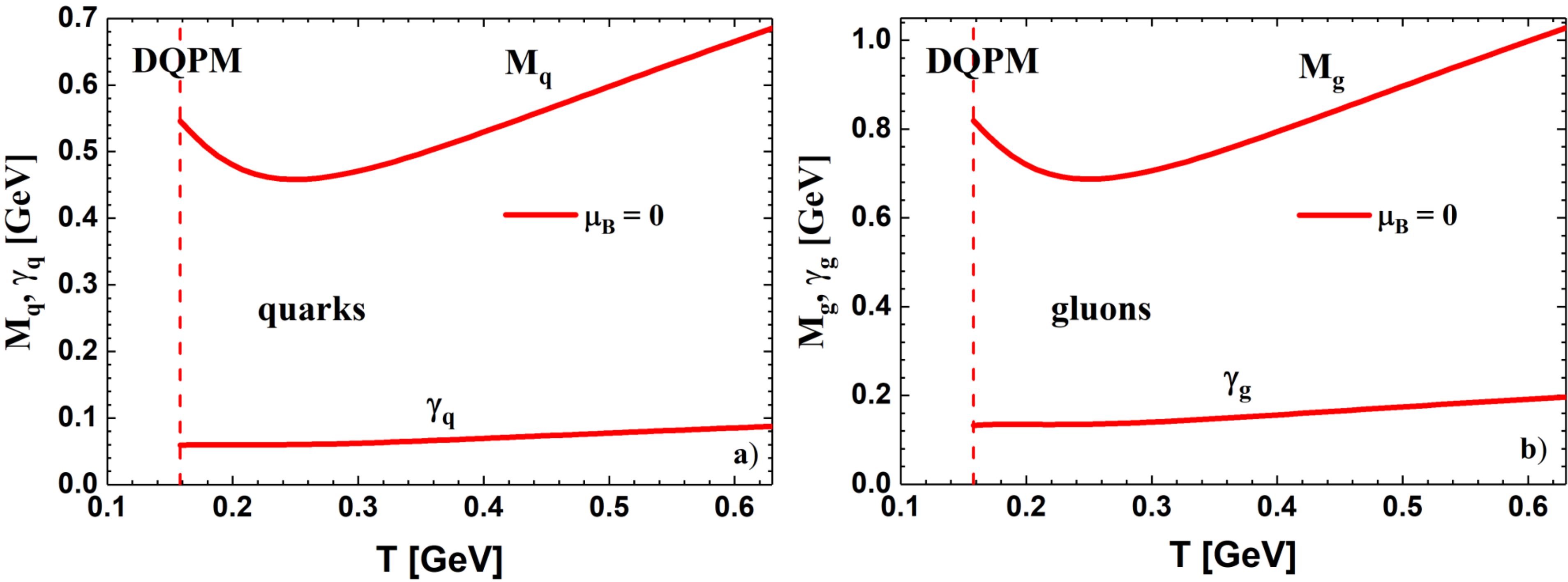

CRC-TR 211
Strong-interaction matter under extreme conditions

DQPM: parton properties

- DQPM masses and widths as a function of (T, μ_B)

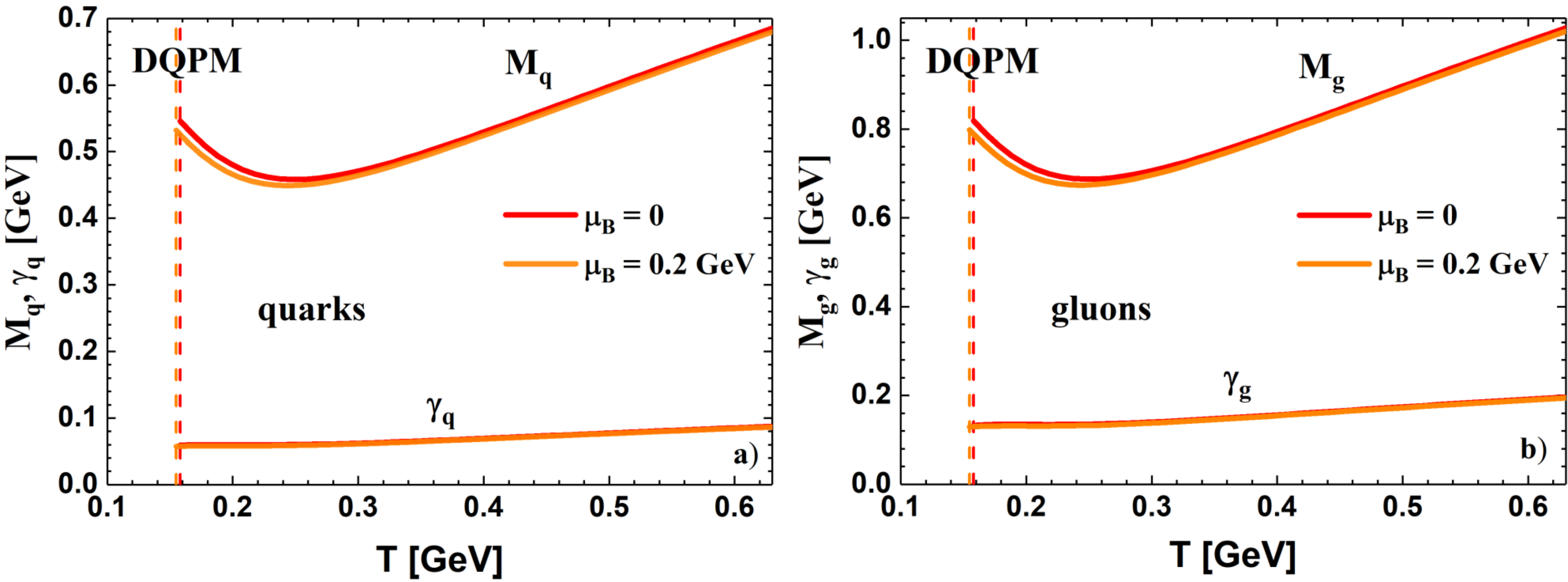

DQPM: parton properties

- DQPM masses and widths as a function of (T, μ_B)

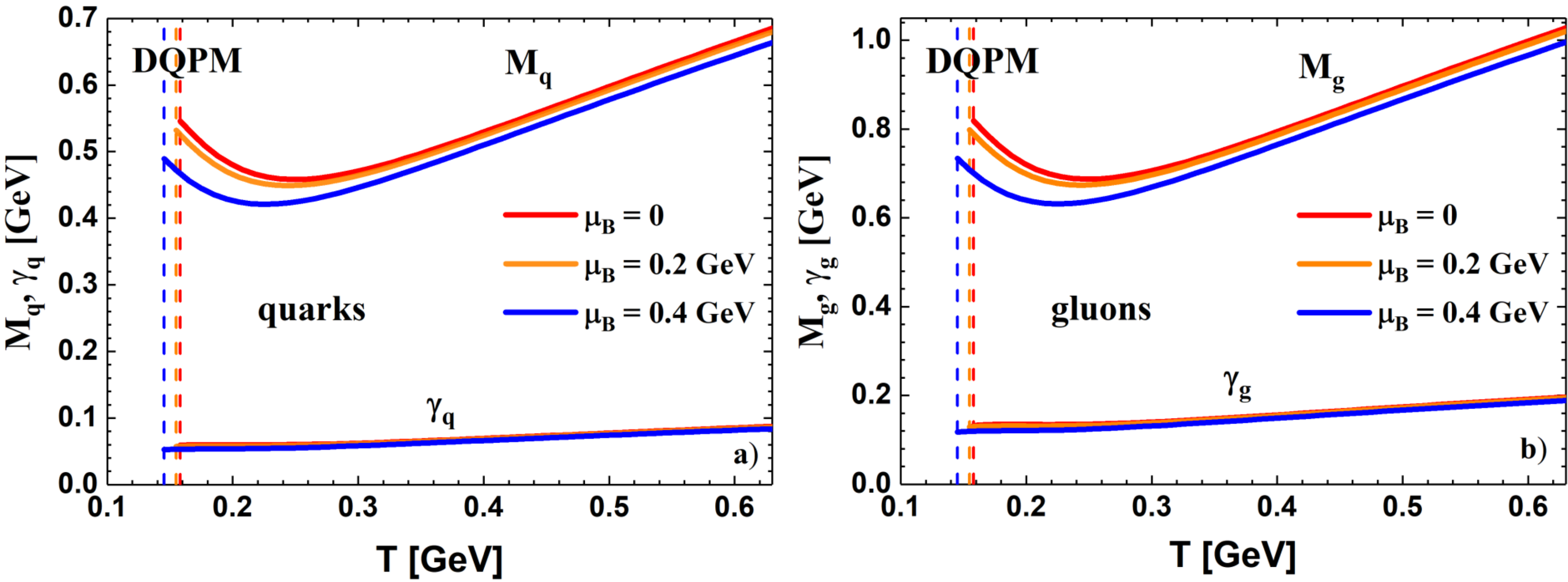

DQPM: parton properties

CRC-TR 211 Strong-interaction matter under extreme conditions

- DQPM masses and widths as a function of (T, μ_B)

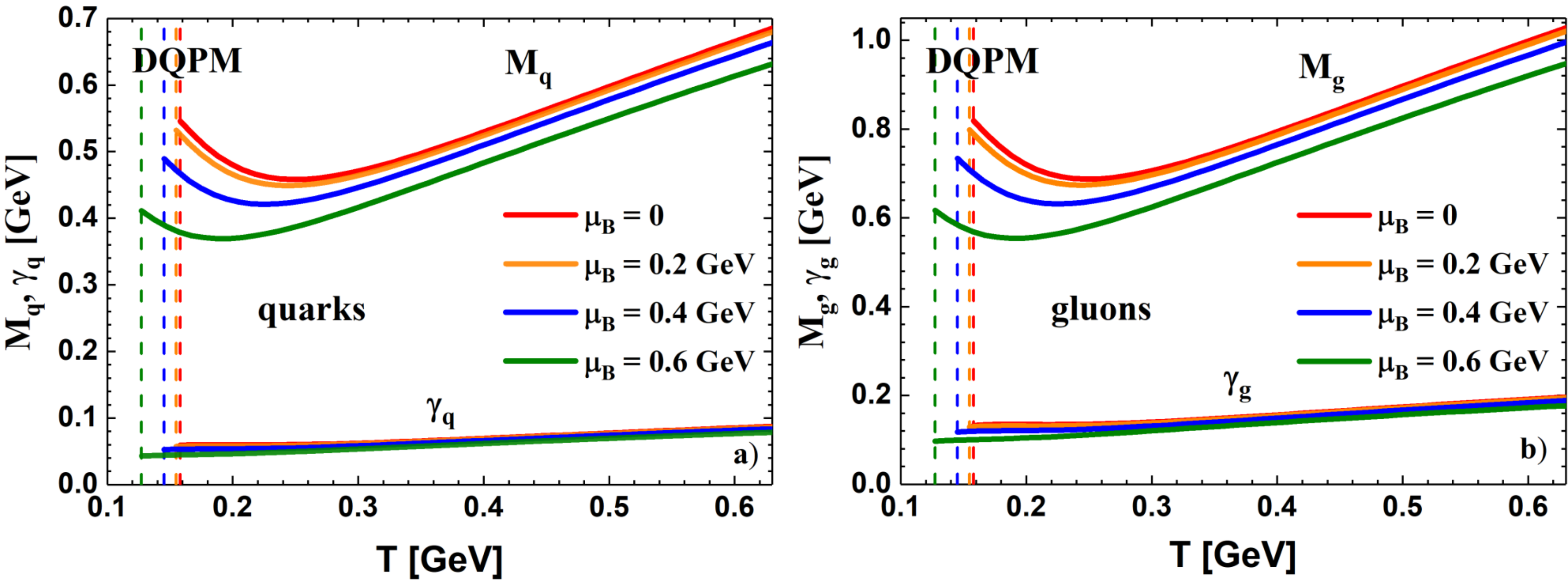

DQPM Thermodynamics

CRC-TR 211 Strong-interaction matter under extreme conditions

- **Entropy and baryon density in the quasiparticle limit:**

$$s^{dqp} =$$
$$-\int \frac{d\omega}{2\pi}\frac{d^3p}{(2\pi)^3}\left[d_g \frac{\partial n_B}{\partial T}\left(\mathrm{Im}(\ln -\Delta^{-1}) + \mathrm{Im}\,\Pi\,\mathrm{Re}\,\Delta\right)\right.$$
$$+\sum_{q=u,d,s} d_q \frac{\partial n_F(\omega-\mu_q)}{\partial T}\left(\mathrm{Im}(\ln -S_q^{-1}) + \mathrm{Im}\,\Sigma_q\,\mathrm{Re}\,S_q\right)$$
$$\left.+\sum_{\bar{q}=\bar{u},\bar{d},\bar{s}} d_{\bar{q}} \frac{\partial n_F(\omega+\mu_q)}{\partial T}\left(\mathrm{Im}(\ln -S_{\bar{q}}^{-1}) + \mathrm{Im}\,\Sigma_{\bar{q}}\,\mathrm{Re}\,S_{\bar{q}}\right)\right]$$

$$n^{dqp} = -\int \frac{d\omega}{2\pi}\frac{d^3p}{(2\pi)^3}$$
$$\left[\sum_{q=u,d,s} d_q \frac{\partial n_F(\omega-\mu_q)}{\partial \mu_q}\left(\mathrm{Im}(\ln -S_q^{-1}) + \mathrm{Im}\,\Sigma_q\,\mathrm{Re}\,S_q\right)\right.$$
$$\left.+\sum_{\bar{q}=\bar{u},\bar{d},\bar{s}} d_{\bar{q}} \frac{\partial n_F(\omega+\mu_q)}{\partial \mu_q}\left(\mathrm{Im}(\ln -S_{\bar{q}}^{-1}) + \mathrm{Im}\,\Sigma_{\bar{q}}\,\mathrm{Re}\,S_{\bar{q}}\right)\right]$$

Blaizot, Iancu, Rebhan, Phys. Rev. D 63 (2001) 065003

Note: The contribution of longitudinal gluons is neglected in the calculation of thermodynamic quantities

DQPM Thermodynamics

- **Entropy and baryon density in the quasiparticle limit:**

$$s^{dqp} = -\int \frac{d\omega}{2\pi}\frac{d^3p}{(2\pi)^3}\Big[d_g \frac{\partial n_B}{\partial T}\left(\mathrm{Im}(\ln -\Delta^{-1}) + \mathrm{Im}\,\Pi\,\mathrm{Re}\,\Delta\right) + \sum_{q=u,d,s} d_q \frac{\partial n_F(\omega-\mu_q)}{\partial T}\left(\mathrm{Im}(\ln -S_q^{-1}) + \mathrm{Im}\,\Sigma_q\,\mathrm{Re}\,S_q\right) + \sum_{\bar q=\bar u,\bar d,\bar s} d_{\bar q} \frac{\partial n_F(\omega+\mu_q)}{\partial T}\left(\mathrm{Im}(\ln -S_{\bar q}^{-1}) + \mathrm{Im}\,\Sigma_{\bar q}\,\mathrm{Re}\,S_{\bar q}\right)\Big]$$

$$n^{dqp} = -\int \frac{d\omega}{2\pi}\frac{d^3p}{(2\pi)^3}\Big[\sum_{q=u,d,s} d_q \frac{\partial n_F(\omega-\mu_q)}{\partial \mu_q}\left(\mathrm{Im}(\ln -S_q^{-1}) + \mathrm{Im}\,\Sigma_q\,\mathrm{Re}\,S_q\right) + \sum_{\bar q=\bar u,\bar d,\bar s} d_{\bar q} \frac{\partial n_F(\omega+\mu_q)}{\partial \mu_q}\left(\mathrm{Im}(\ln -S_{\bar q}^{-1}) + \mathrm{Im}\,\Sigma_{\bar q}\,\mathrm{Re}\,S_{\bar q}\right)\Big]$$

Blaizot, Iancu, Rebhan, Phys. Rev. D 63 (2001) 065003

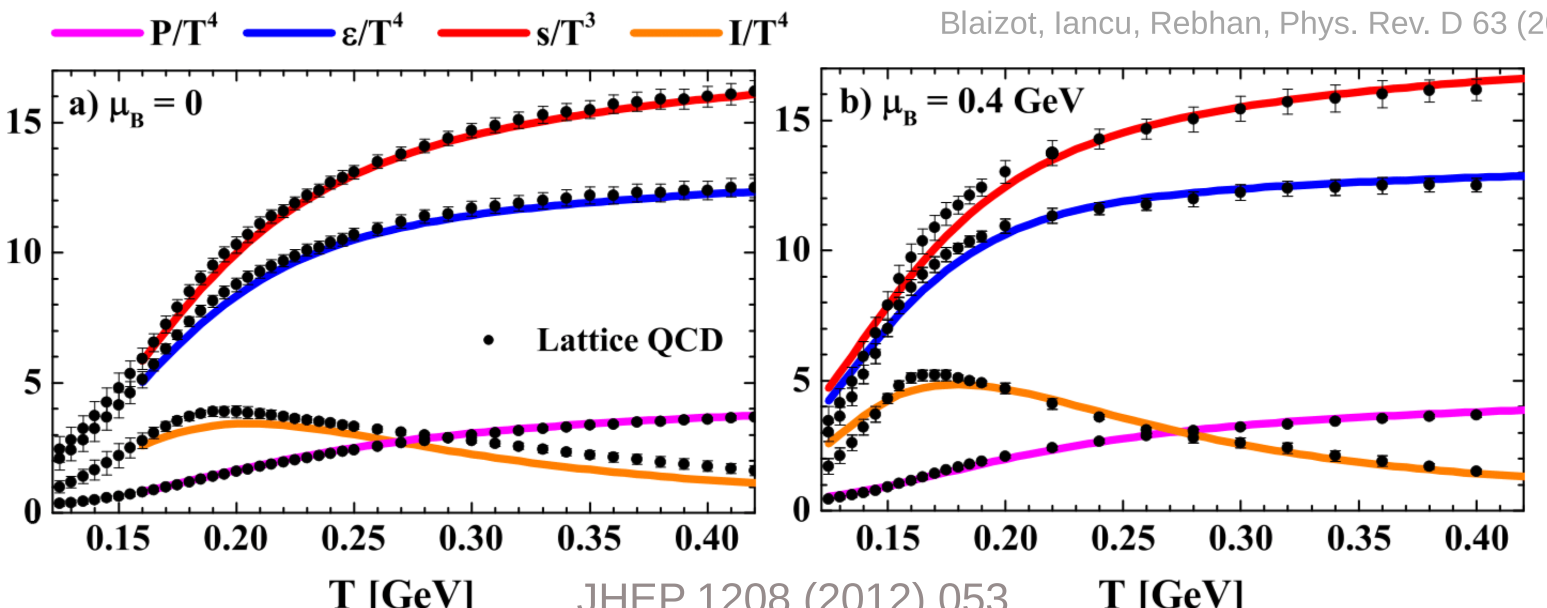

JHEP 1208 (2012) 053

Partonic interactions: cross sections

- **Definition of the off-shell cross section:**

$$F d\sigma^{\text{off}} = \frac{d^4p_3}{(2\pi)^4}\,\frac{d^4p_4}{(2\pi)^4}\;\tilde\rho_3(\omega_3,\mathbf{p}_3)\;\theta(\omega_3)\;\tilde\rho_4(\omega_4,\mathbf{p}_4)\;\theta(\omega_4)$$
$$(2\pi)^4\delta^{(4)}(p_1+p_2-p_3-p_4)\,|\bar{\mathcal{M}}|^2$$

- **Initial flux factor:** $F = v_{\text{rel}}\;2E_1\;2E_2$

- **Renormalized spectral-function for the timelike sector**

$$\tilde\rho_j(\omega_j,\mathbf{p}_j) = \frac{\rho(\omega_j,\mathbf{p}_j)\;\theta(p_j^2)}{\int_0^\infty \frac{d\omega_j}{(2\pi)}\;2\omega_j\;\rho(\omega_j,\mathbf{p}_j)\;\theta(p_j^2)}$$

normalized to 1 and

$$\lim_{\gamma_j\to 0}\rho_j(\omega,\mathbf{p}) = 2\pi\;\delta(\omega^2-\mathbf{p}^2-M_j^2)$$

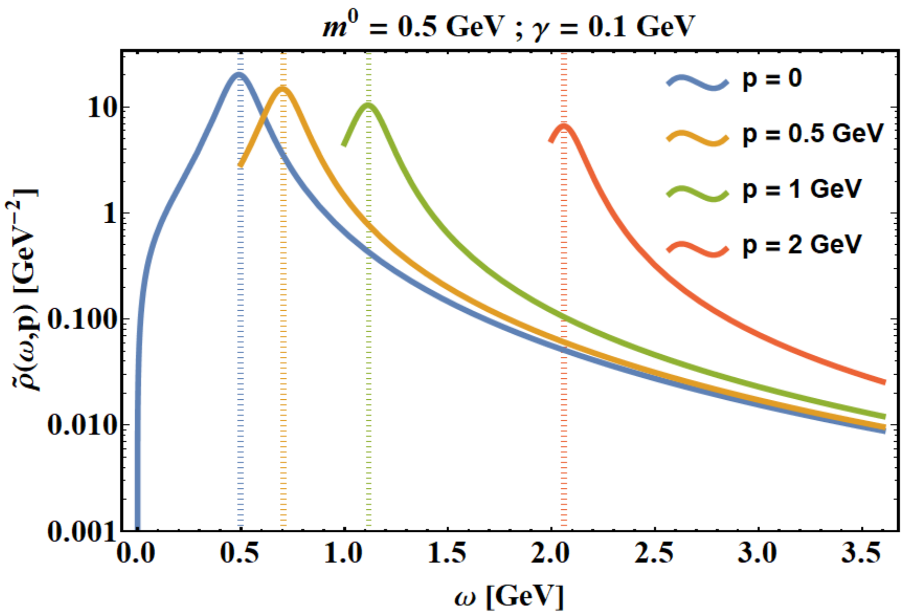

Partonic interactions: matrix elements

$qq', \ q\bar{q}$

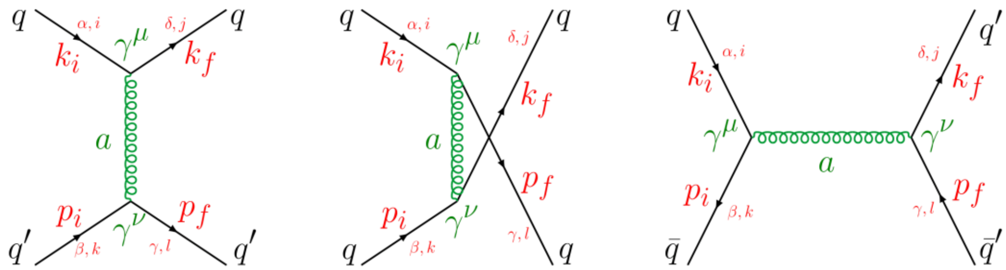

$t-$channel $u-$channel $s-$channel

gq

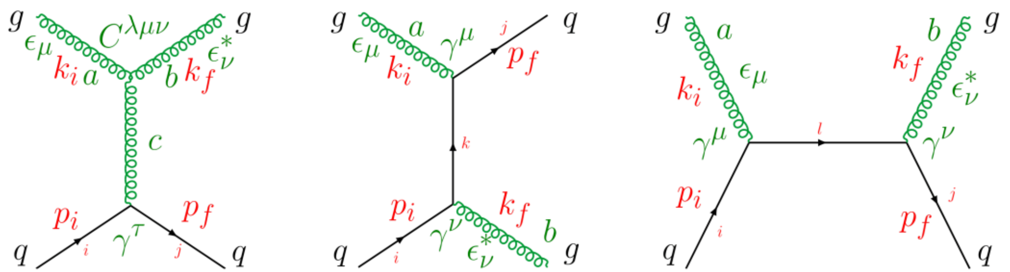

$t-$channel $u-$channel $s-$channel

gg

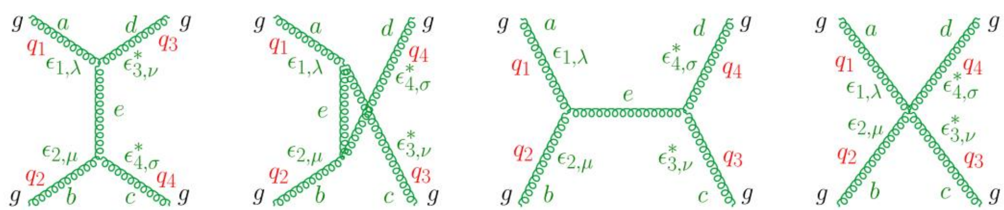

$t-$channel $u-$channel $s-$channel $4-$point

Differential cross section

- **On-shell:**

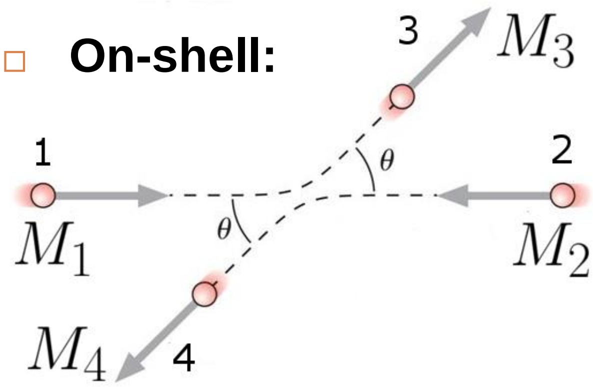

- **Off-shell:**

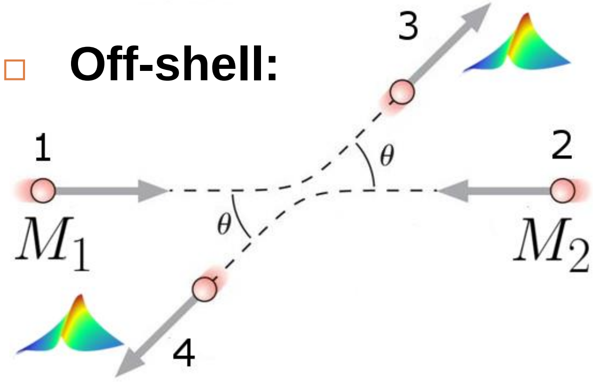

Differential cross section

- **On-shell:**

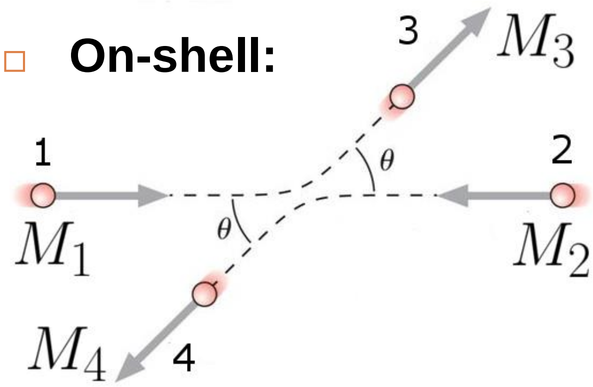

- **Off-shell:**

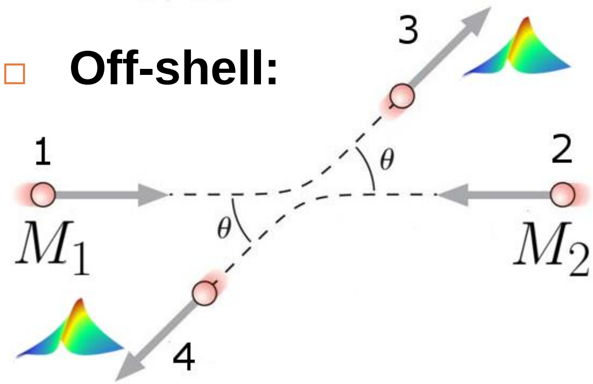

- **Off-shell σ < on-shell σ since $\omega_3 + \omega_4 < \sqrt{s}$**

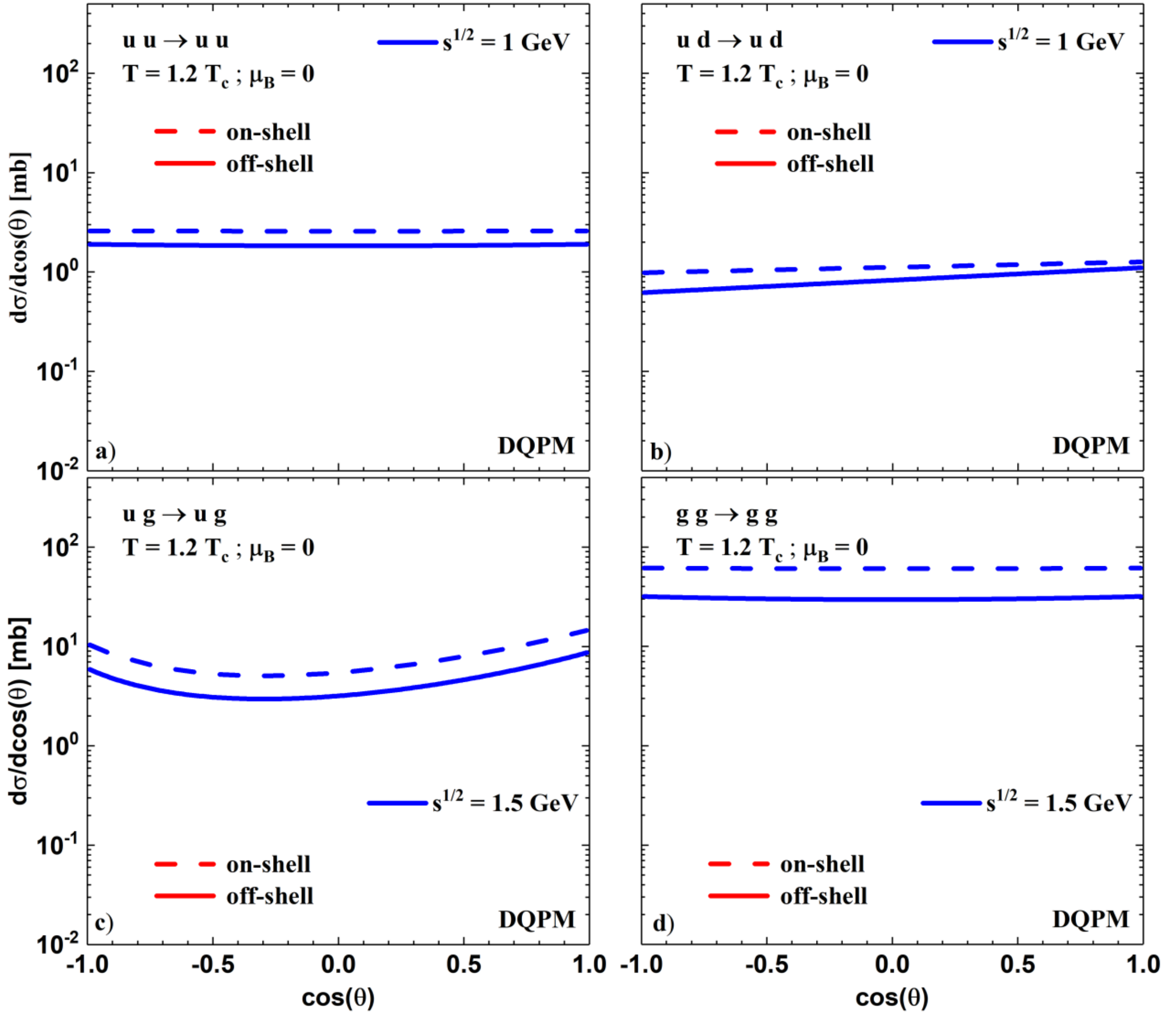

Differential cross section

- On-shell:
- Off-shell:

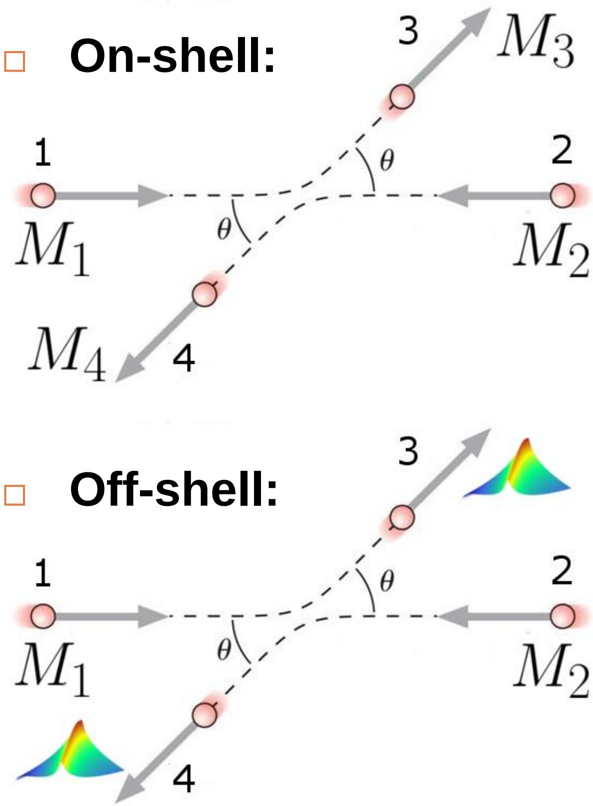

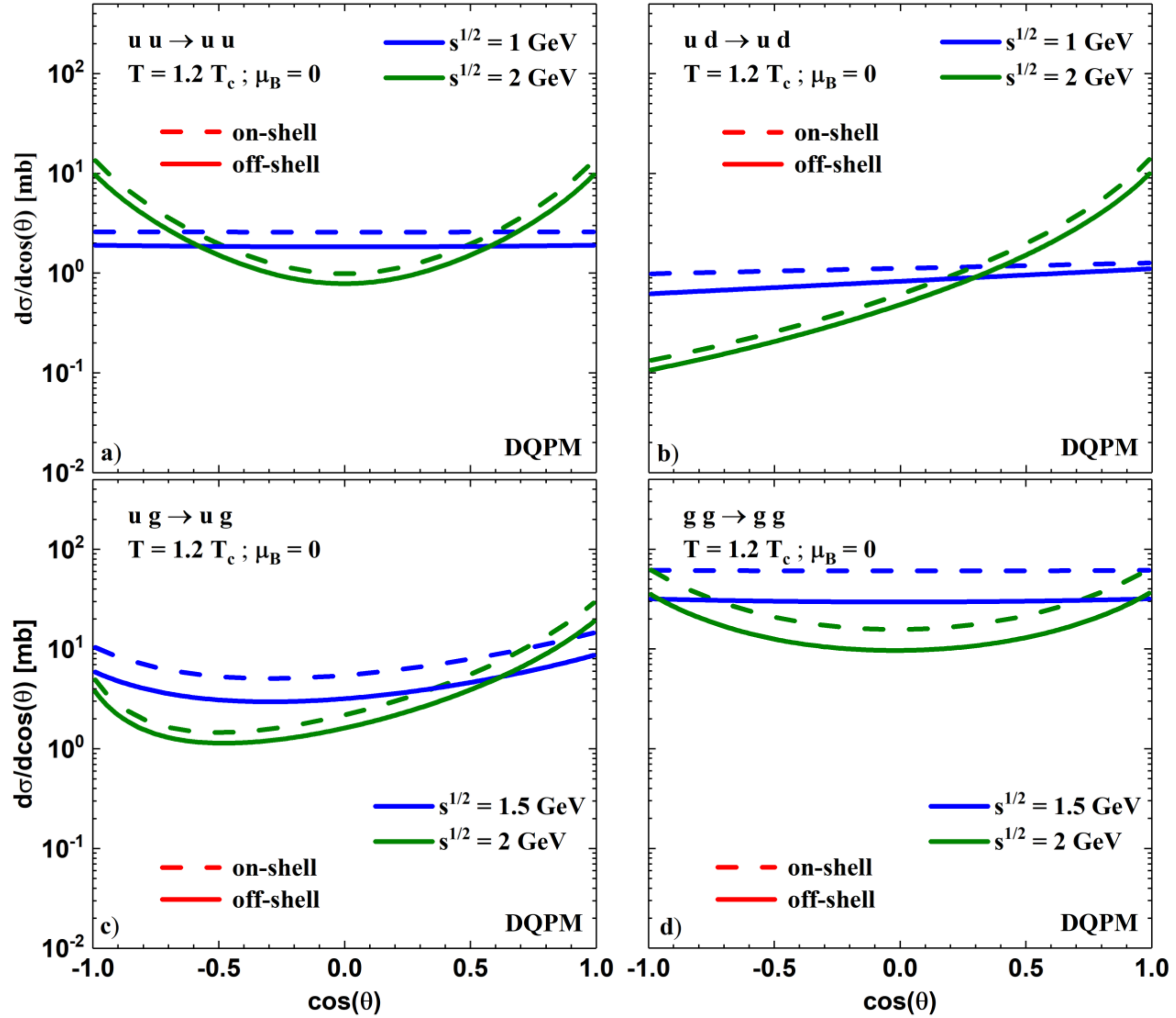

- **Off-shell σ < on-shell σ since $\omega_3 + \omega_4 < \sqrt{s}$**

Differential cross section

- **On-shell:**

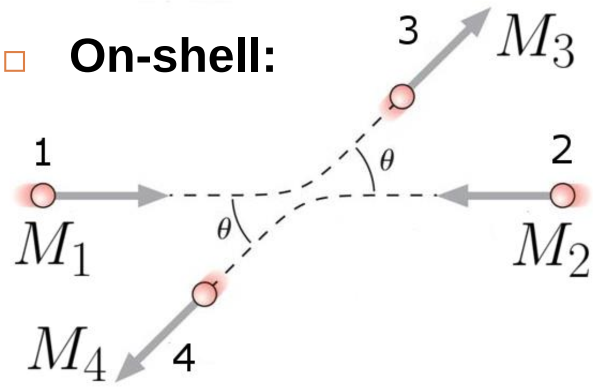

- **Off-shell:**

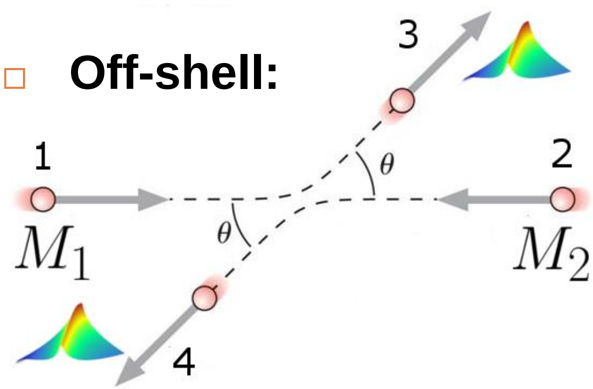

- **Off-shell σ < on-shell σ since $\omega_3 + \omega_4 < \sqrt{s}$**

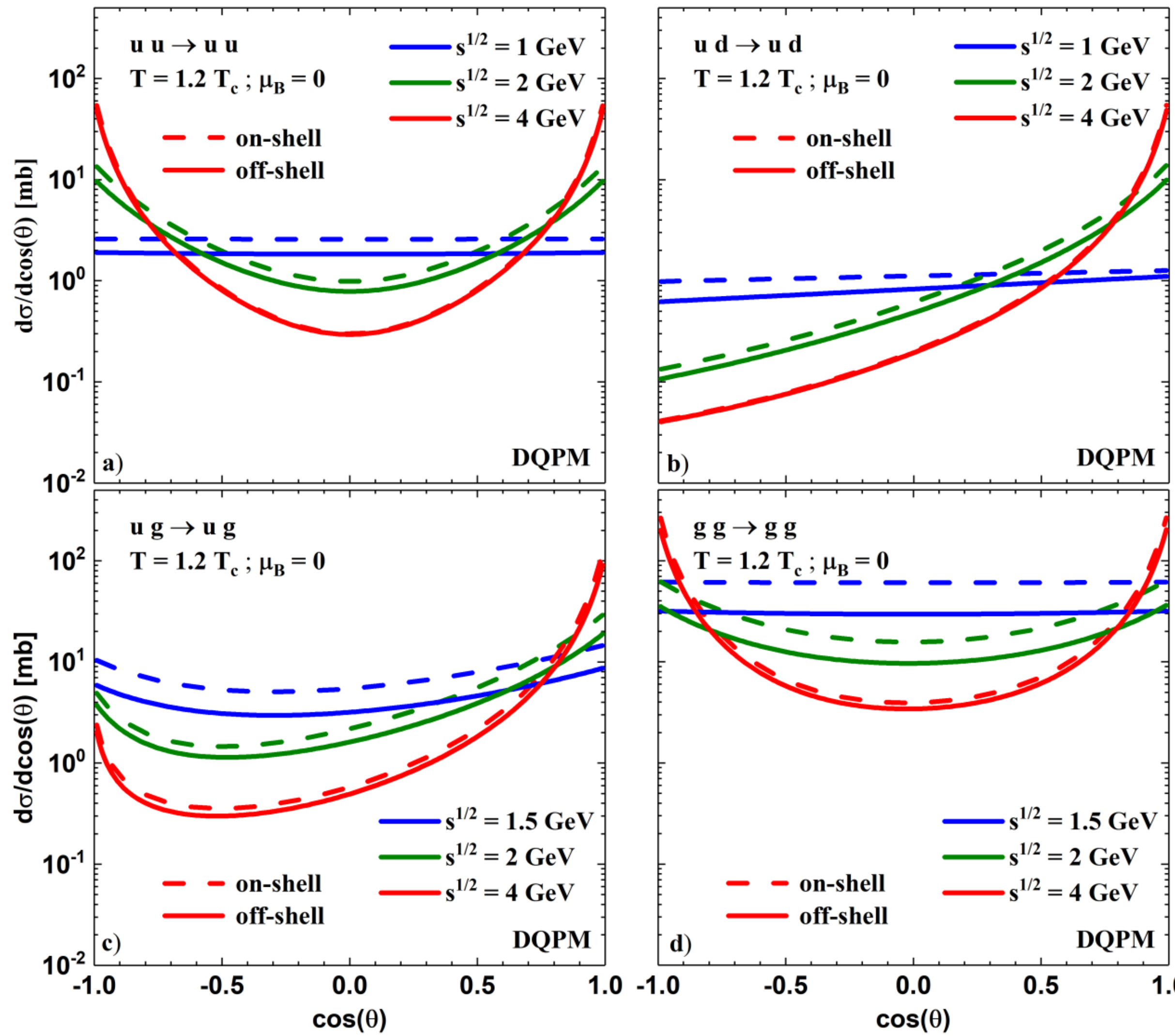

Total cross section

- On-shell:
- Off-shell:

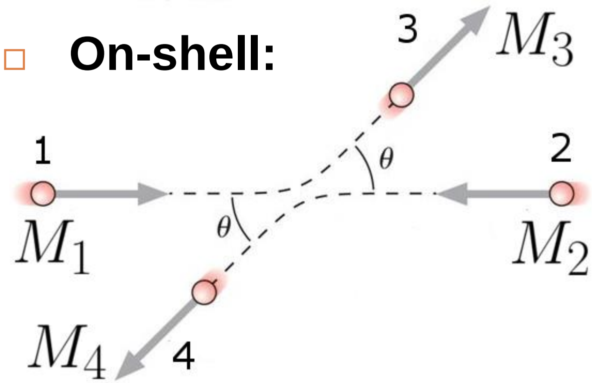

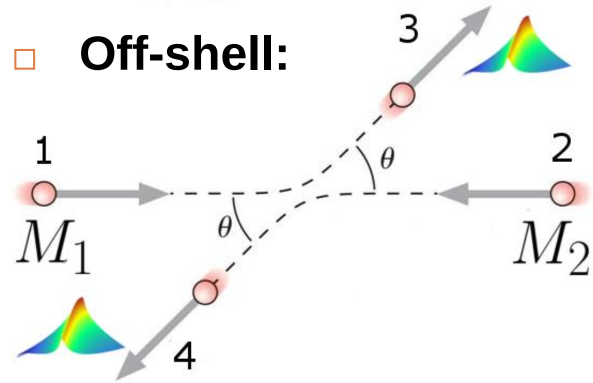

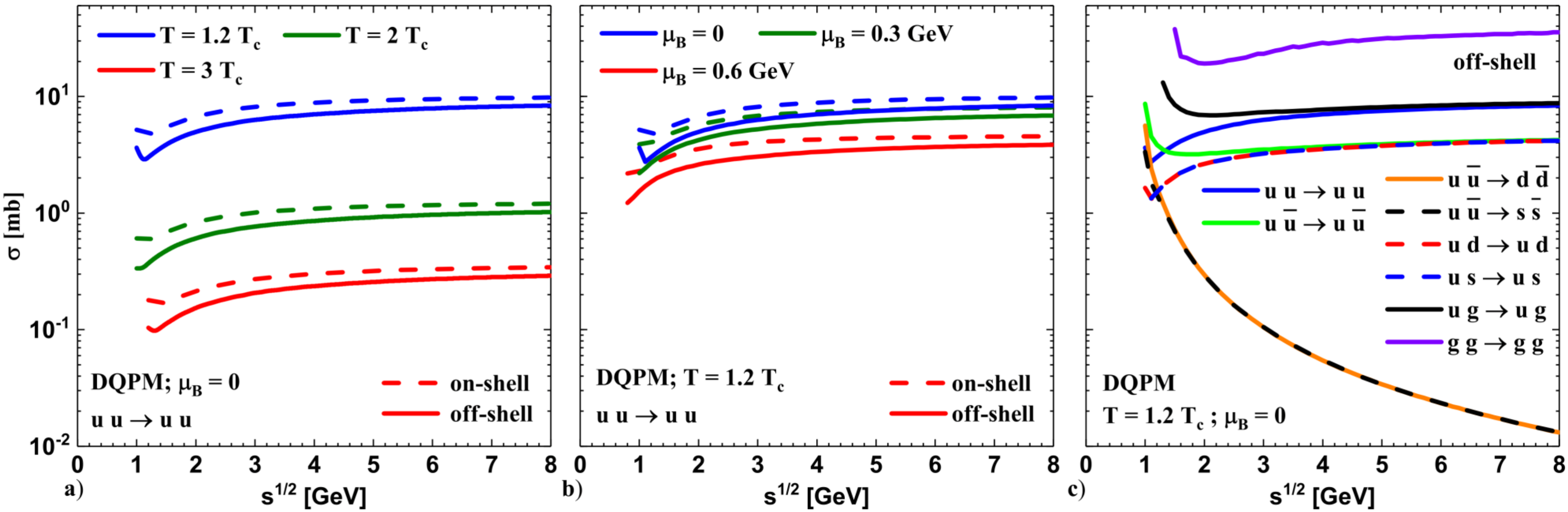

QGP:

in equilibrium → off equilibrium

Energy-momentum tensor in PHSD

CRC-TR 211
Strong-interaction matter under extreme conditions

- **In each space-time cell of the PHSD, the energy-momentum tensor is calculated by the formula:**

$$T^{\mu\nu} = \sum_i \frac{p_i^\mu p_i^\nu}{E_i}$$

- **Diagonalization of the energy-momentum tensor to get the energy density and pressure components expressed in the local rest frame (LRF)**

$$T^{\mu\nu} = \begin{pmatrix} T^{00} & T^{01} & T^{02} & T^{03} \\ T^{10} & T^{11} & T^{12} & T^{13} \\ T^{20} & T^{21} & T^{22} & T^{23} \\ T^{30} & T^{31} & T^{32} & T^{33} \end{pmatrix} \Rightarrow \begin{pmatrix} \epsilon^{LRF} & 0 & 0 & 0 \\ 0 & P_x^{LRF} & 0 & 0 \\ 0 & 0 & P_y^{LRF} & 0 \\ 0 & 0 & 0 & P_z^{LRF} \end{pmatrix}$$

Xu et al., Phys.Rev. C96 (2017), 024902

CRC-TR 211 Strong-interaction matter under extreme conditions

Energy-momentum tensor in PHSD

- **Diagonalization of the energy-momentum tensor to get the energy density and pressure components expressed in the local rest frame (LRF)**

$$T^{\mu\nu}\ (x_\nu)_i = \lambda_i\ (x^\mu)_i = \lambda_i\ g^{\mu\nu}\ (x_\nu)_i$$

- **Landau-matching condition:** Xu et al., Phys.Rev. C96 (2017), 024902

$$T^{\mu\nu} u_\nu = \epsilon u^\mu = (\epsilon g^{\mu\nu}) u_\nu$$

- **Evaluation of the characteristic polynomial:**

$$P(\lambda) = \begin{vmatrix} T^{00} - \lambda & T^{01} & T^{02} & T^{03} \\ T^{10} & T^{11} + \lambda & T^{12} & T^{13} \\ T^{20} & T^{21} & T^{22} + \lambda & T^{23} \\ T^{30} & T^{31} & T^{32} & T^{33} + \lambda \end{vmatrix}$$

- **The four solutions λ_i are identified to $(e, -P_1, -P_2, -P_3)$**

The pressure components P_i do not necessarily correspond to (P_x, P_y, P_z)

Baryon density in PHSD

- **Calculation of the baryon current in each cells of the PHSD**

$$J_B^\mu = \sum_i \frac{p_i^\mu}{E_i} \frac{(q_i - \bar{q}_i)}{3}$$

- **Lorentz transformation to obtain the local baryon density:**

$$n_B = \gamma_E \left(J_B^0 - \vec{\beta_E} \cdot \vec{J_B} \right) = \frac{J_B^0}{\gamma_E}$$

with $\vec{\beta_E} = \vec{J_B} / J_B^0$ **being the Eckart velocity.**

Illustration for HIC $(\sqrt{s_{NN}} = 17\ \mathrm{GeV})$

t = 0.005 fm/c

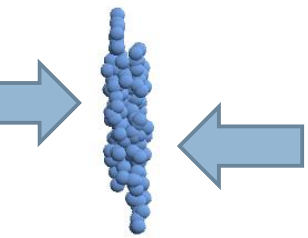

Baryons
Antibaryons
Mesons
Quarks
Gluons

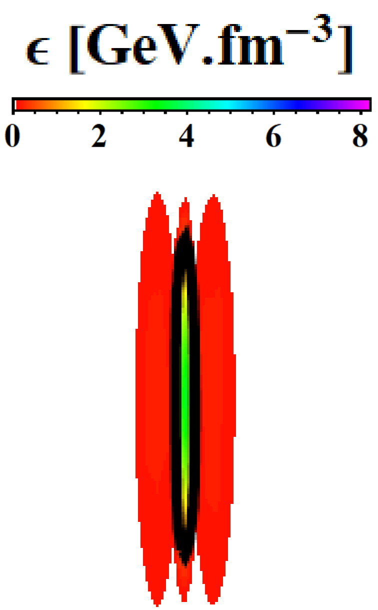

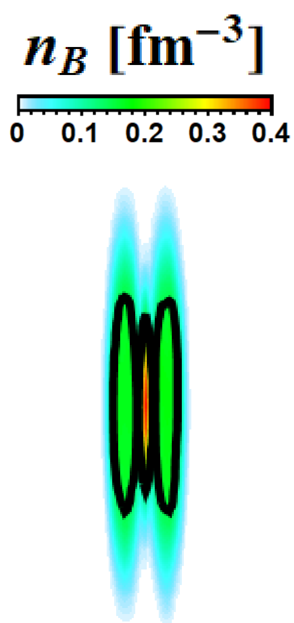

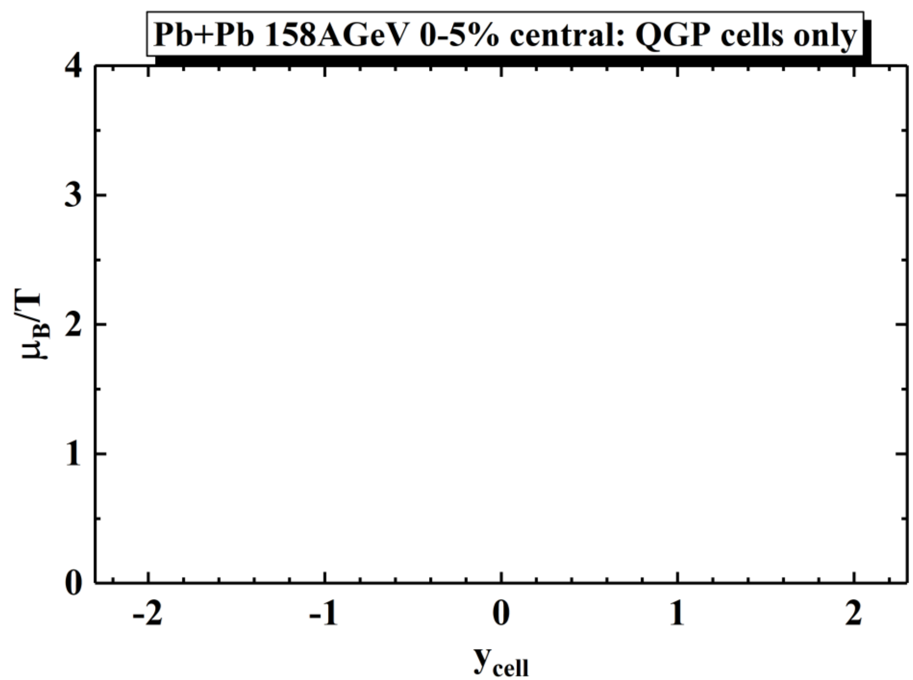

Illustration for HIC ($\sqrt{s_{NN}} = 17$ GeV)

t = 0.005 fm/c t = 1 fm/c

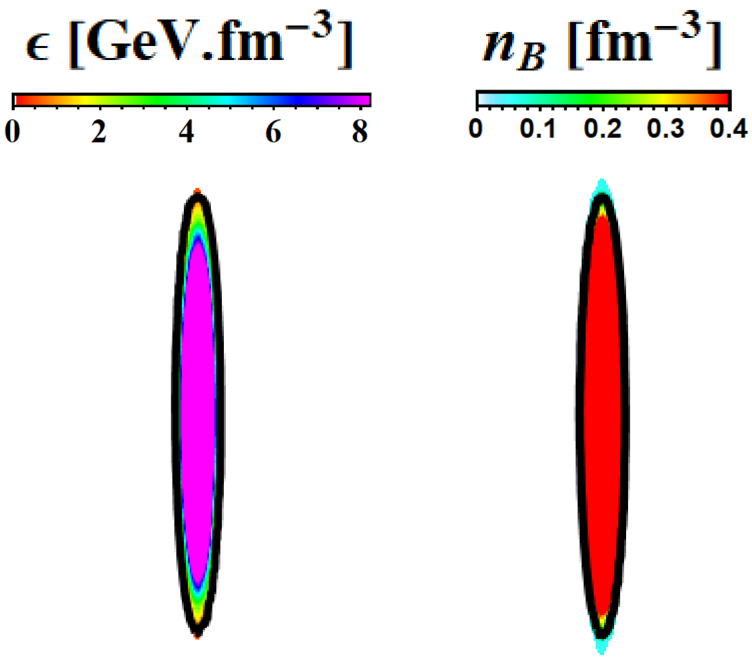

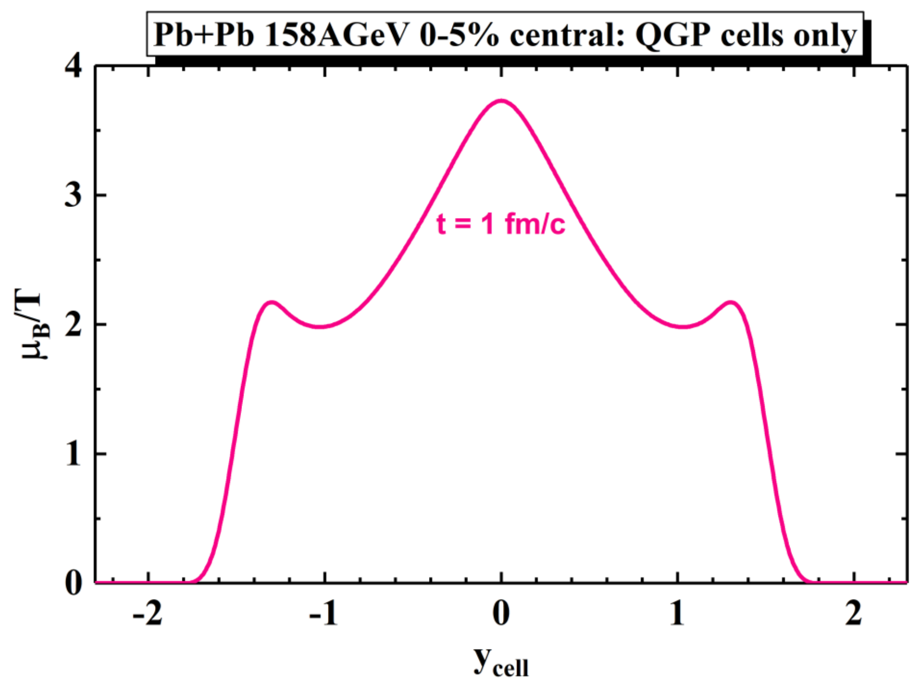

Illustration for HIC ($\sqrt{s_{NN}} = 17$ GeV)

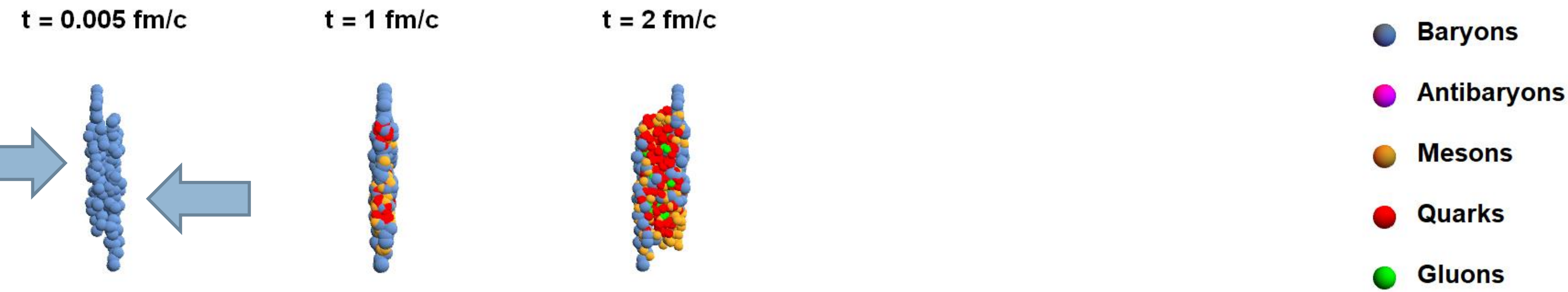

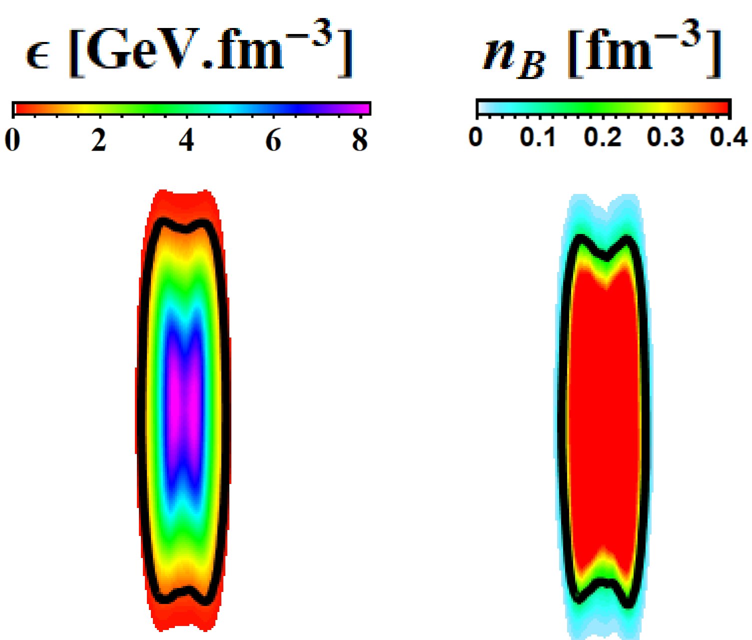

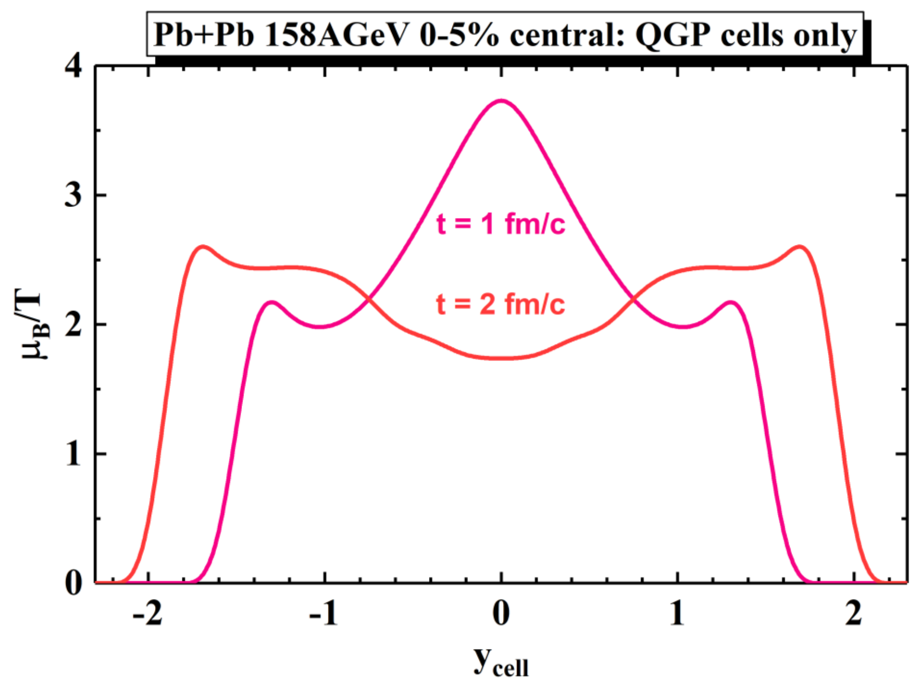

Illustration for HIC $(\sqrt{s_{NN}} = 17$ GeV$)$

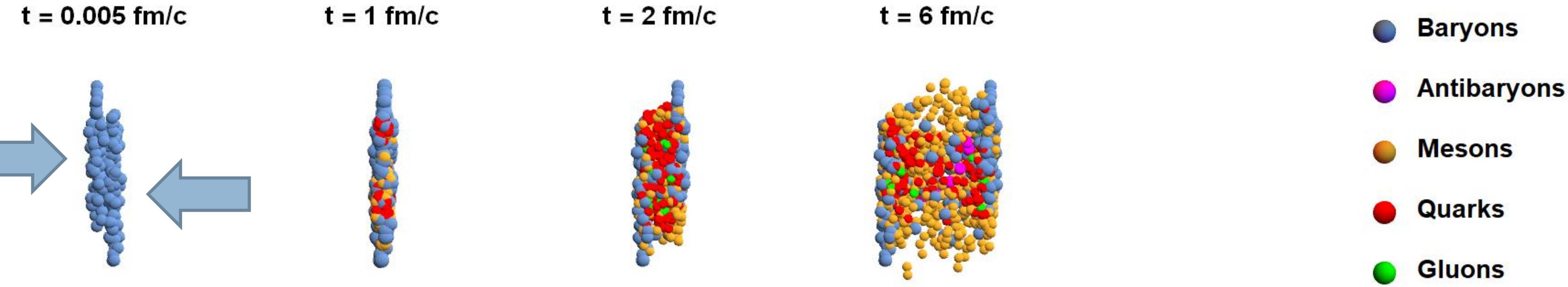

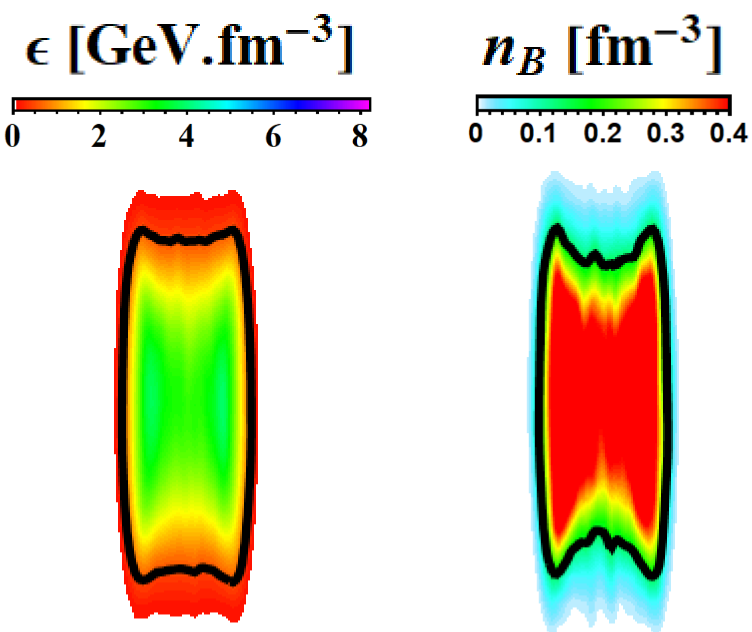

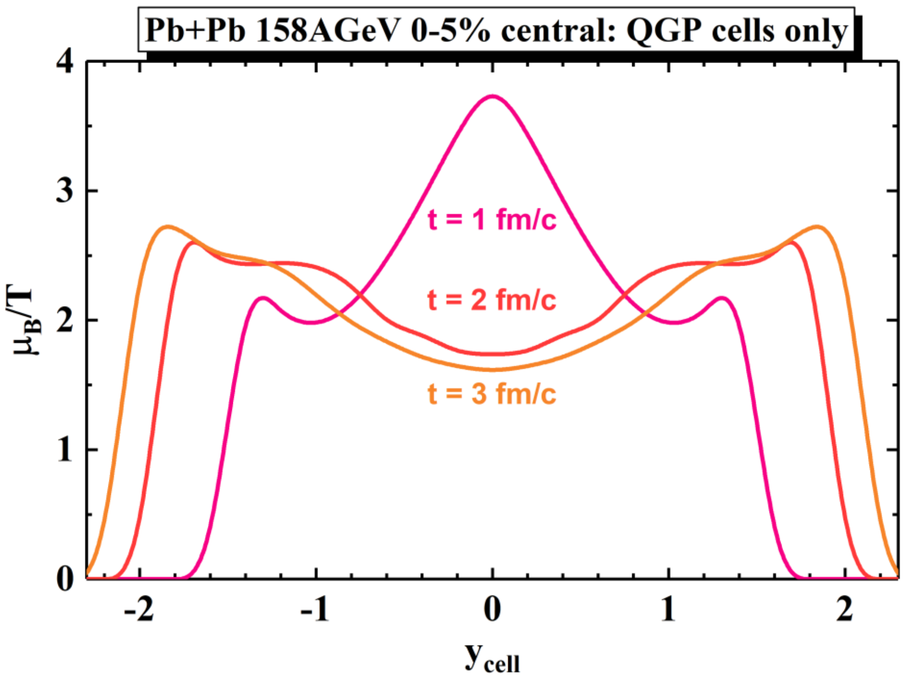

Illustration for HIC $(\sqrt{s_{NN}} = 17\text{ GeV})$

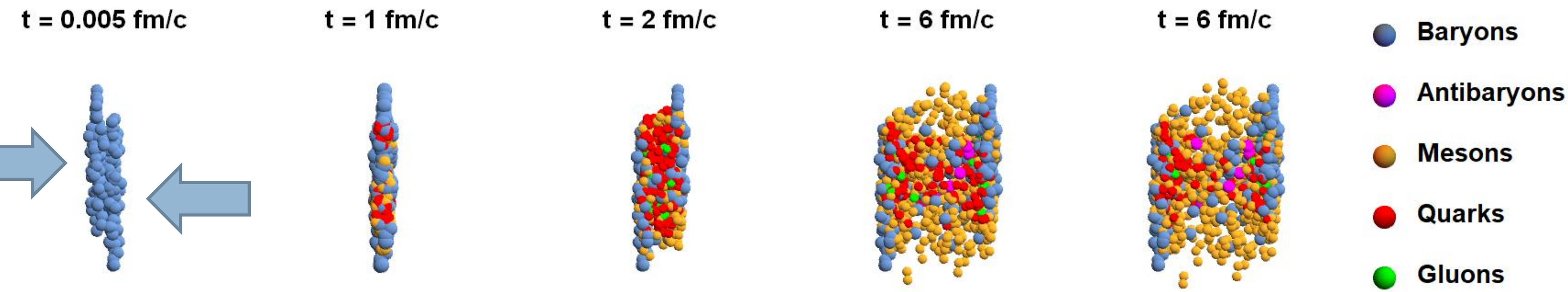

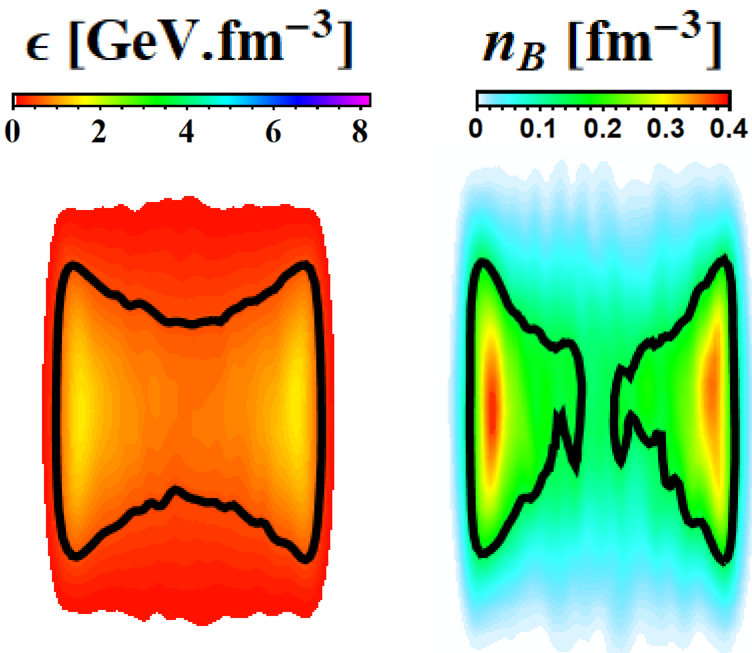

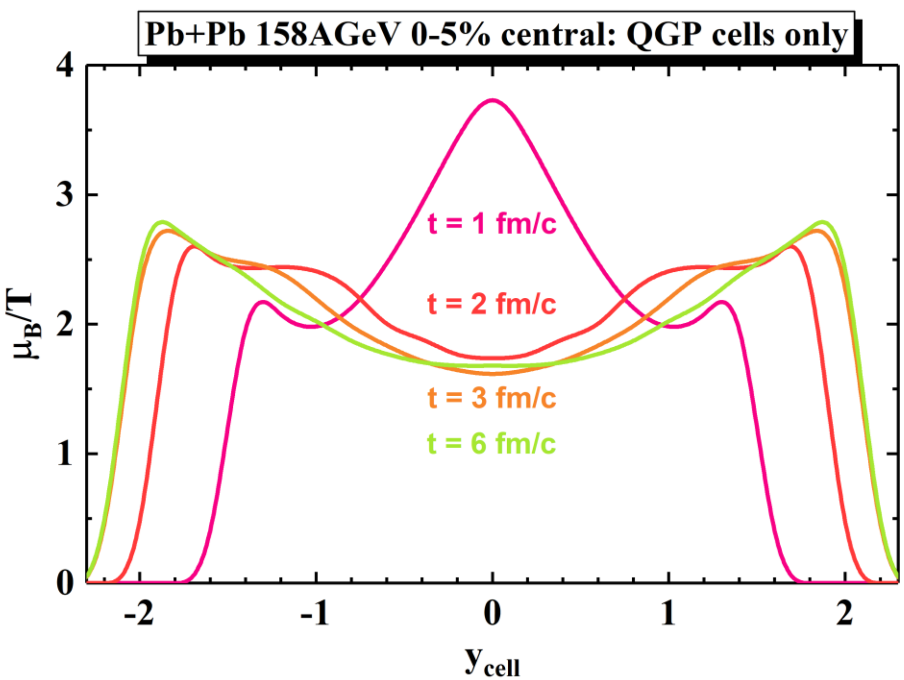

Illustration for HIC $(\sqrt{s_{NN}} = 17$ GeV)

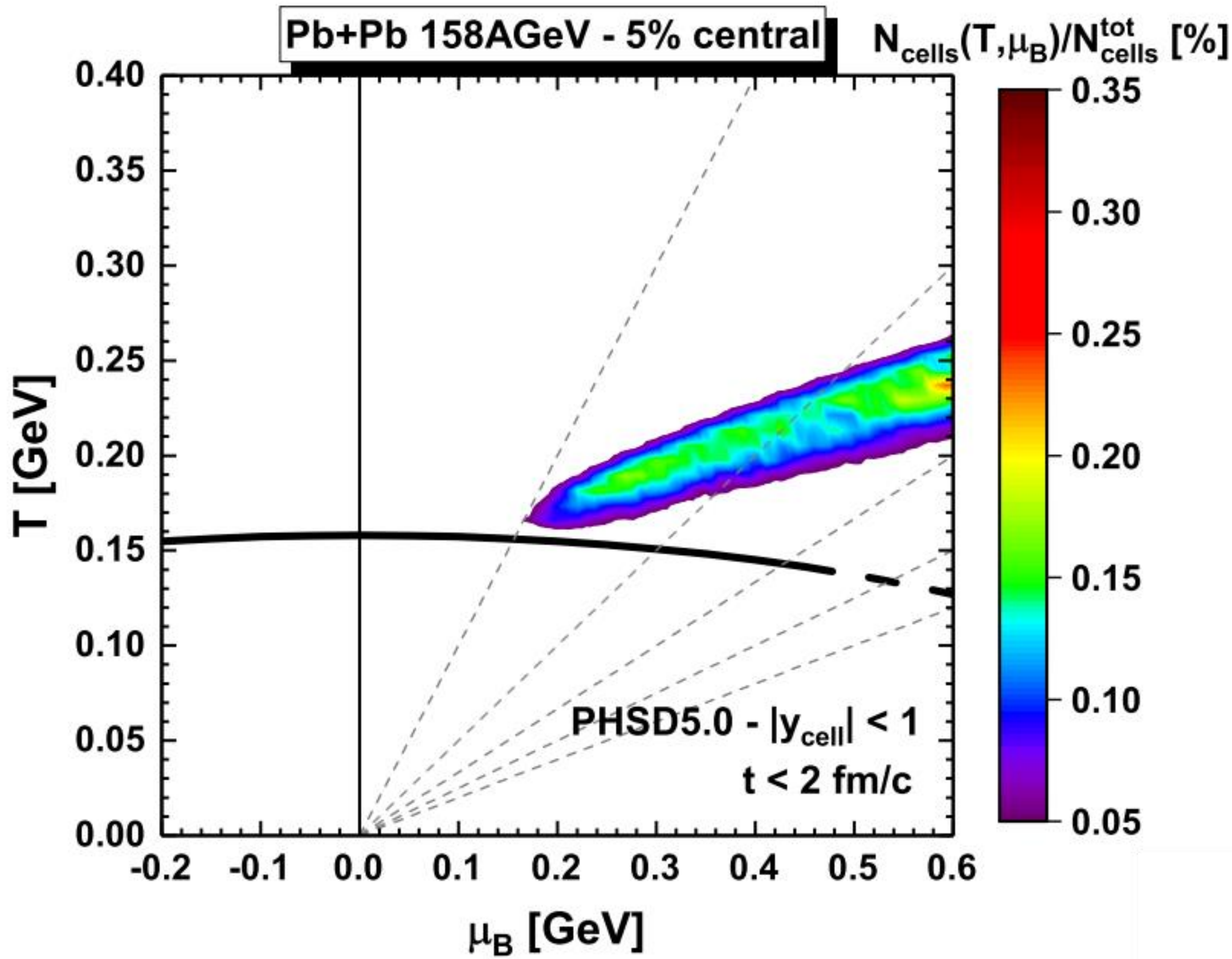

Illustration for HIC ($\sqrt{s_{NN}} = 17$ GeV)

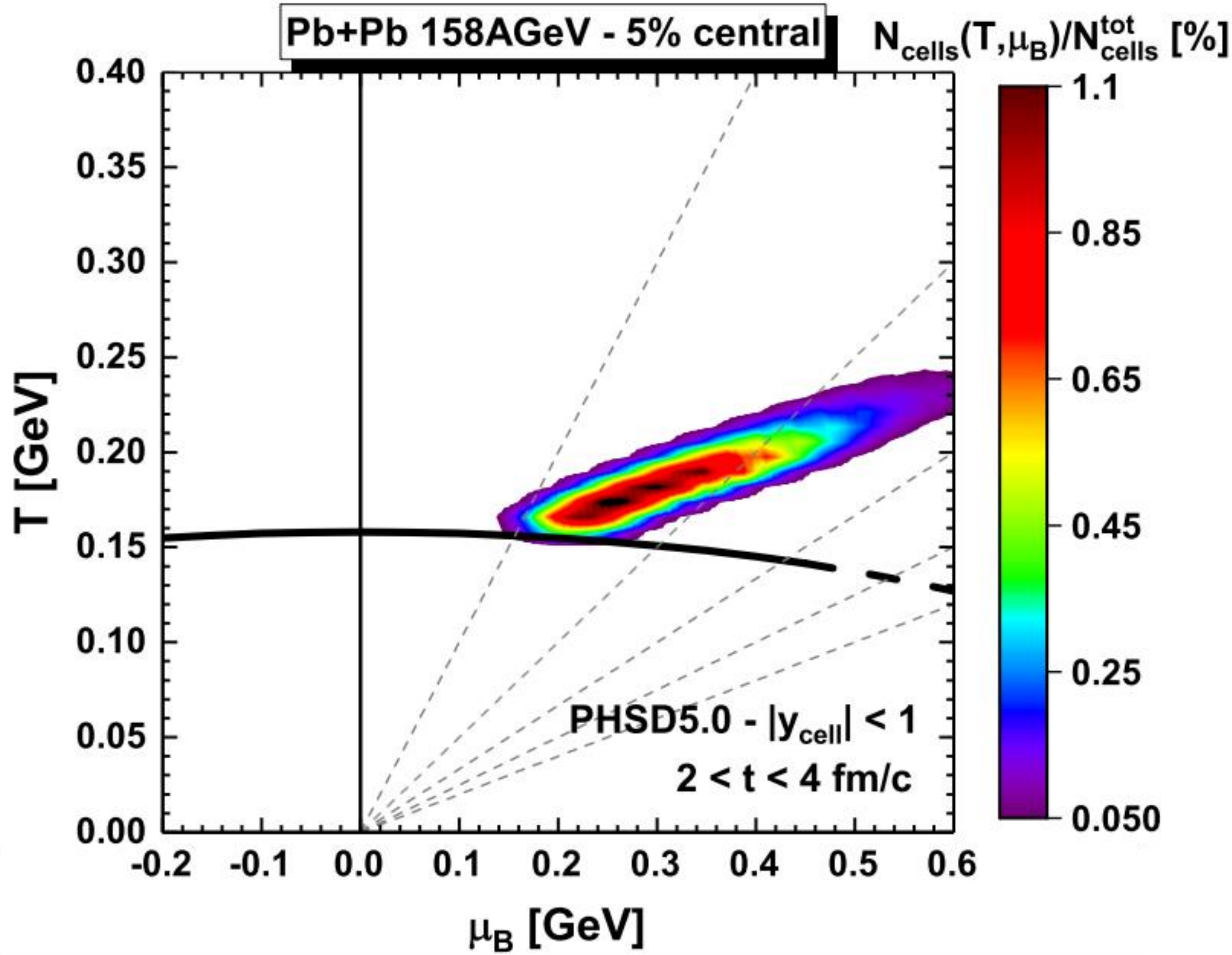

Illustration for HIC ($\sqrt{s_{NN}} = 17$ GeV)

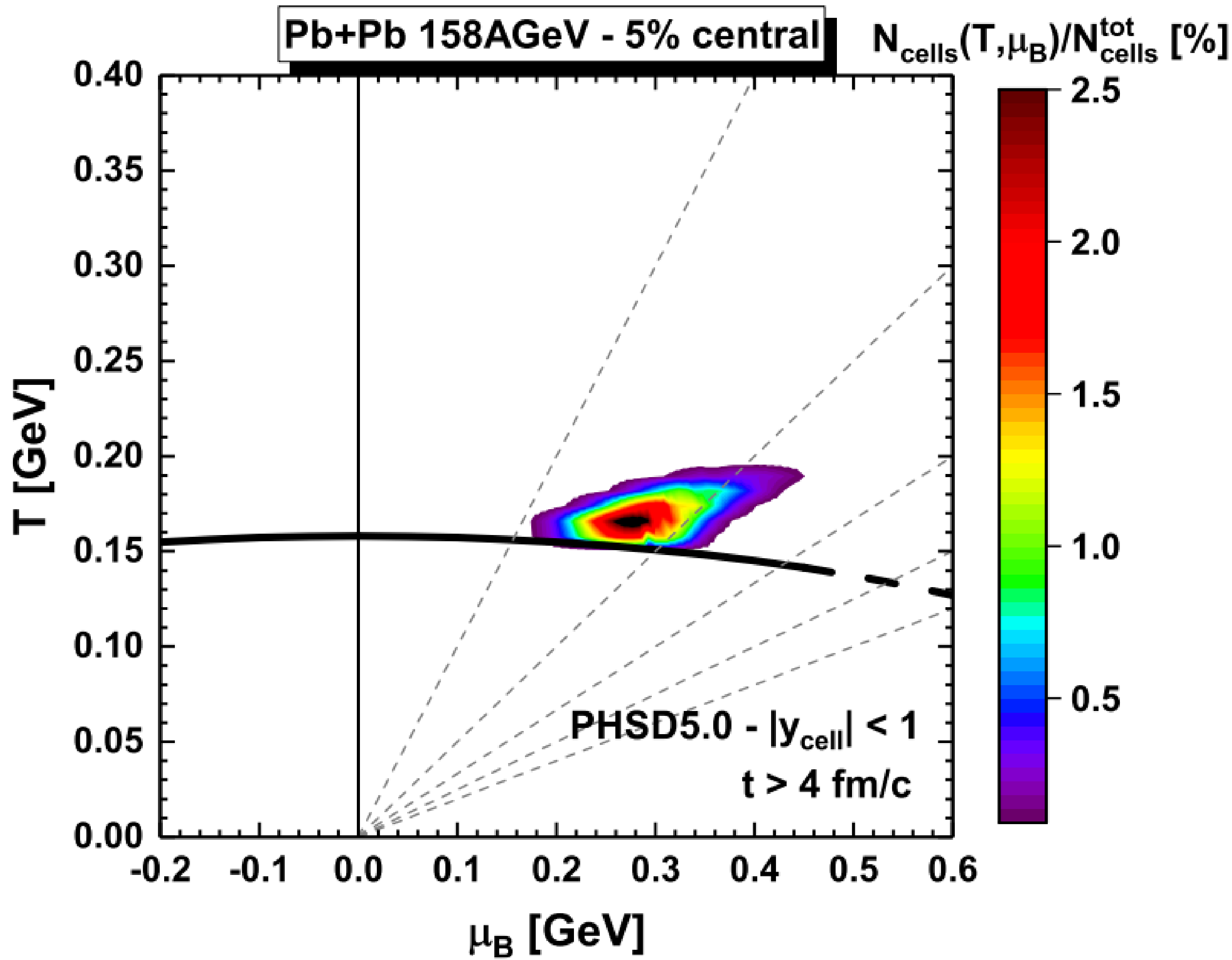

Illustration for HIC ($\sqrt{s_{NN}} = 200$ GeV)

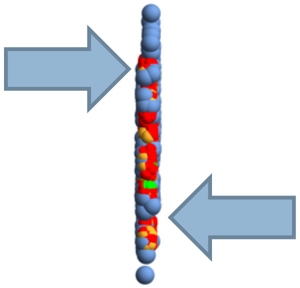

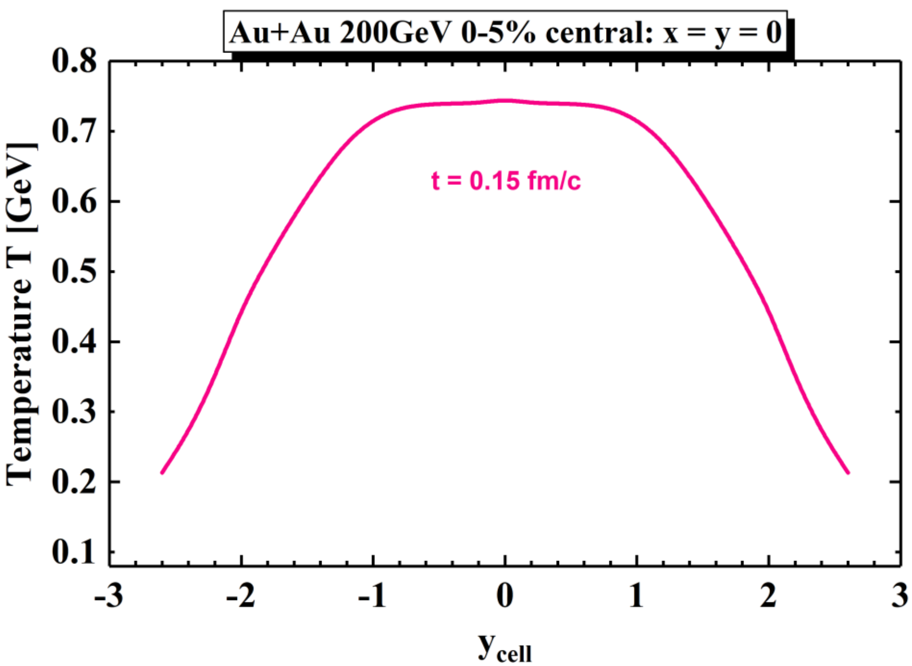

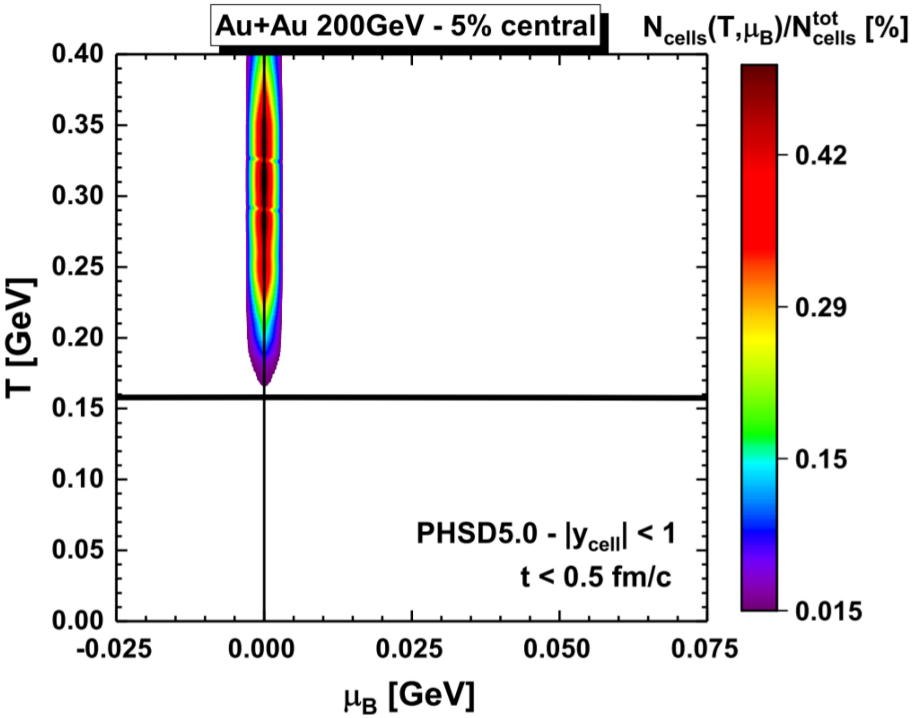

Illustration for HIC ($\sqrt{s_{NN}} = 200$ GeV)

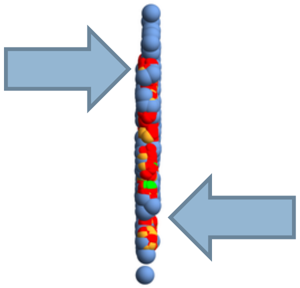

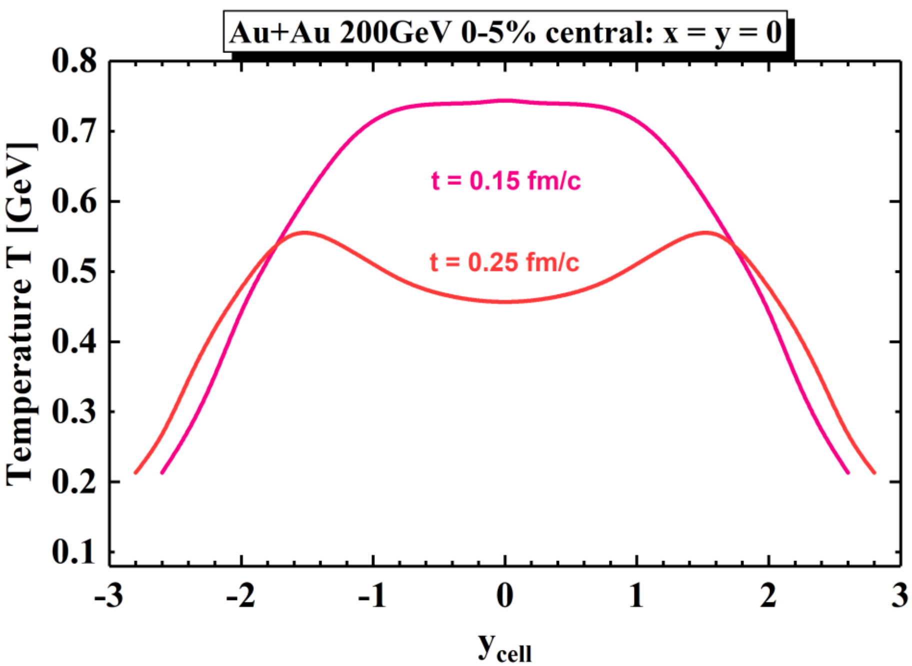

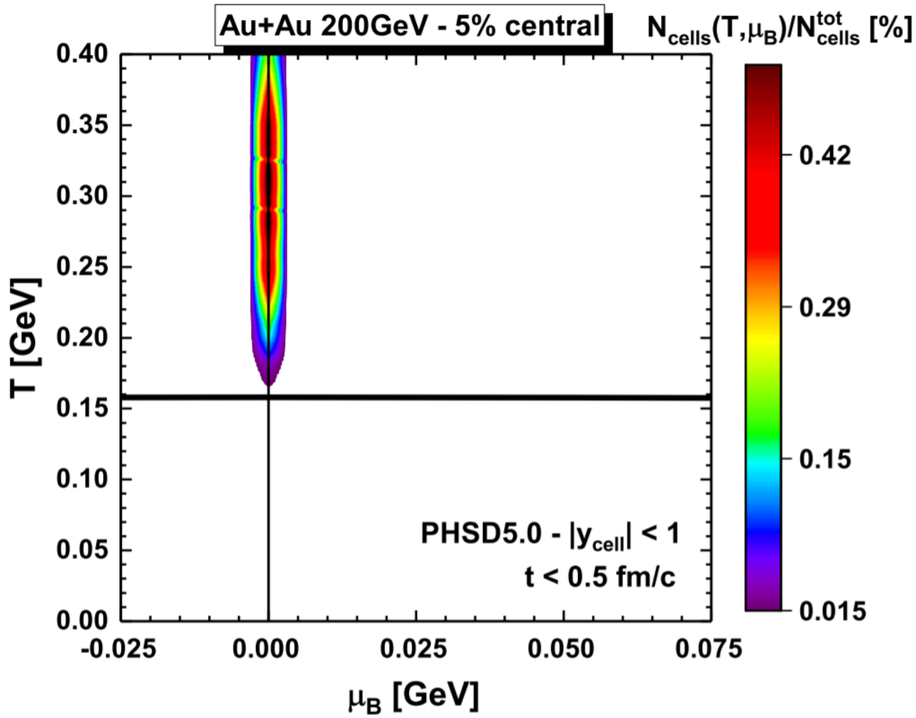

Illustration for HIC ($\sqrt{s_{NN}} = 200$ GeV)

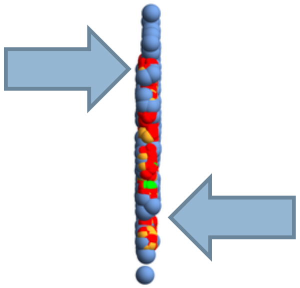

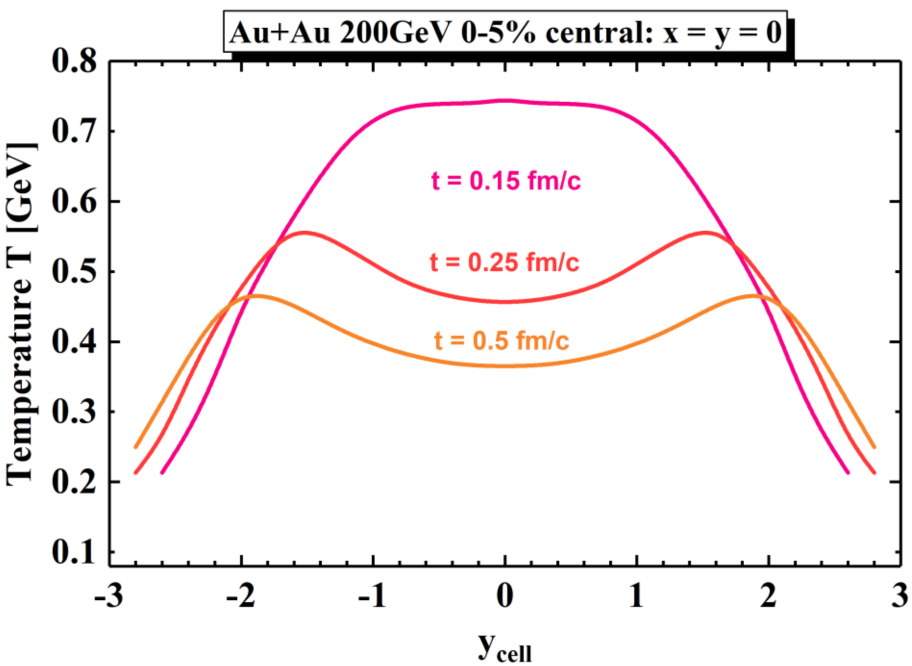

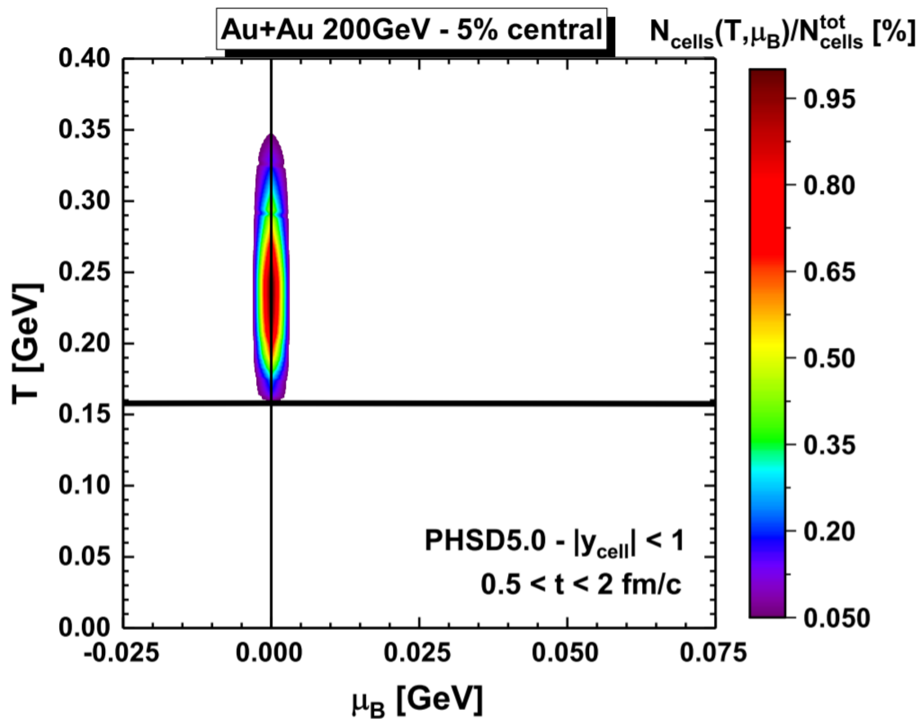

Illustration for HIC ($\sqrt{s_{NN}} = 200$ GeV)

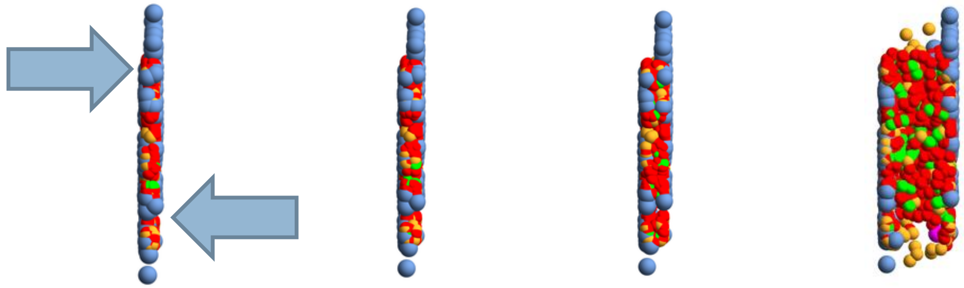

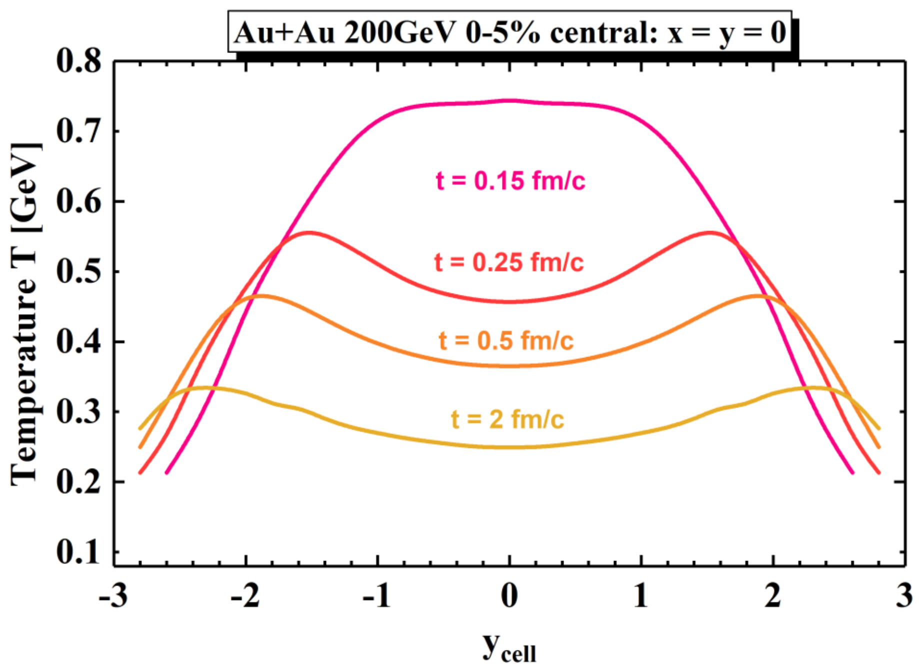

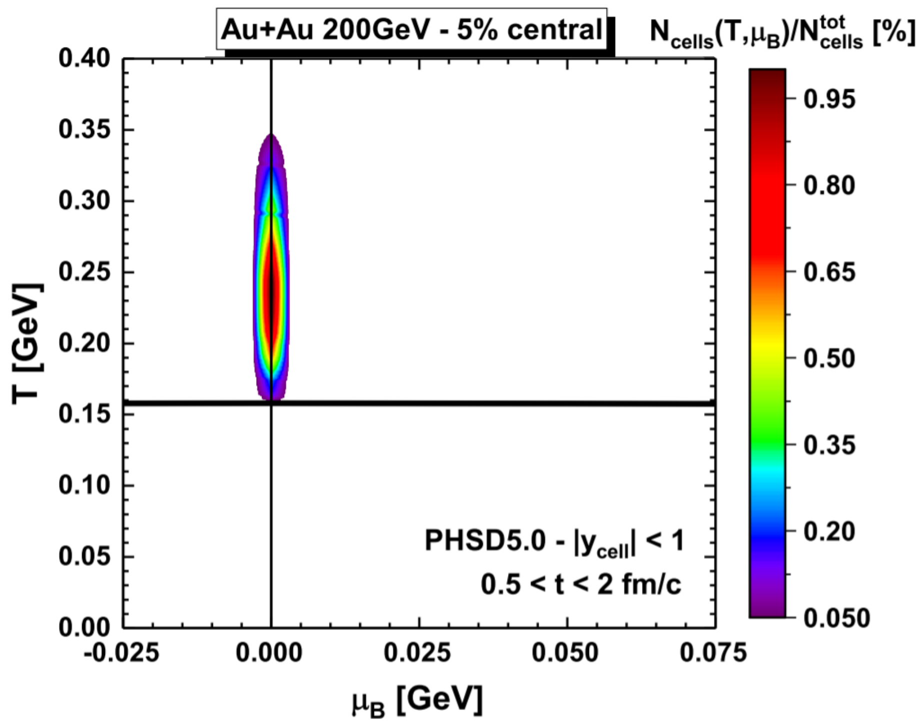

Illustration for HIC ($\sqrt{s_{NN}} = 200$ GeV)

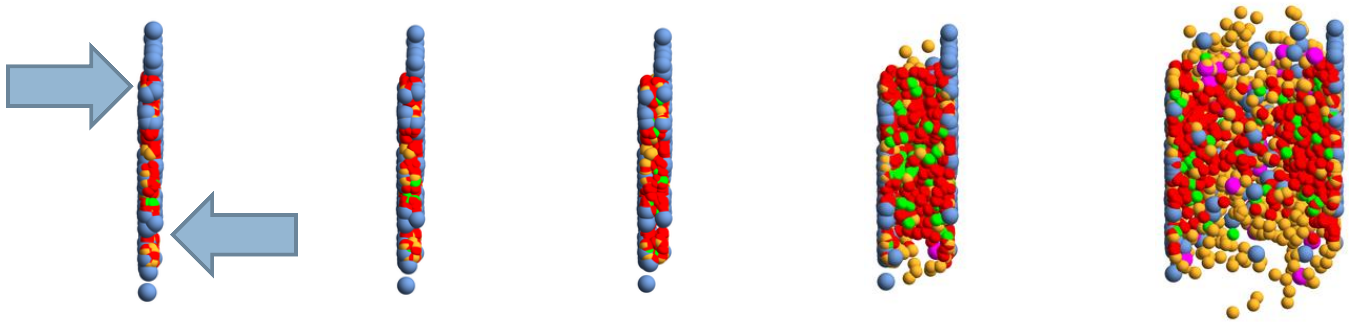

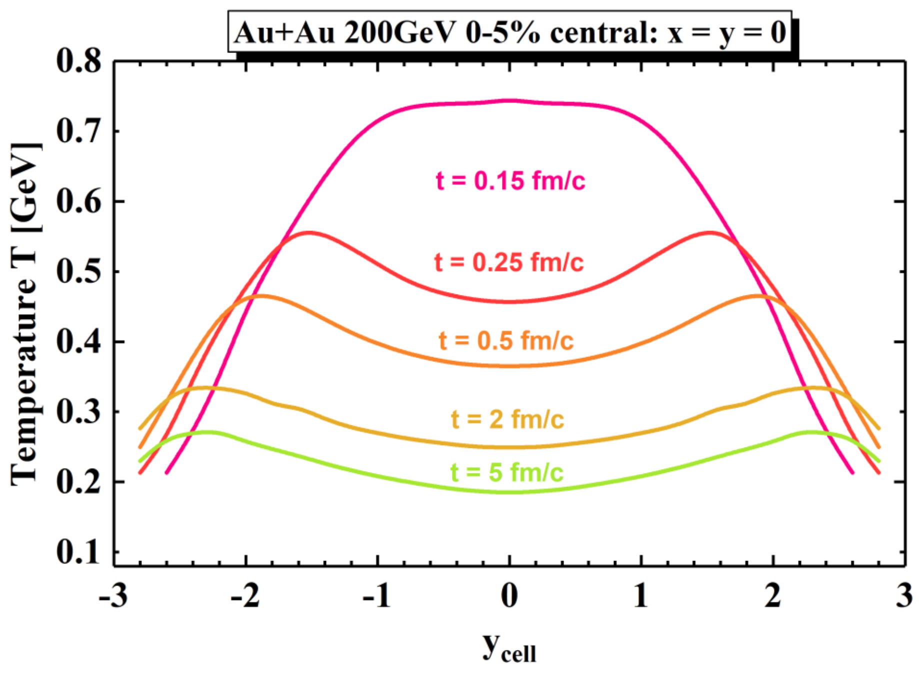

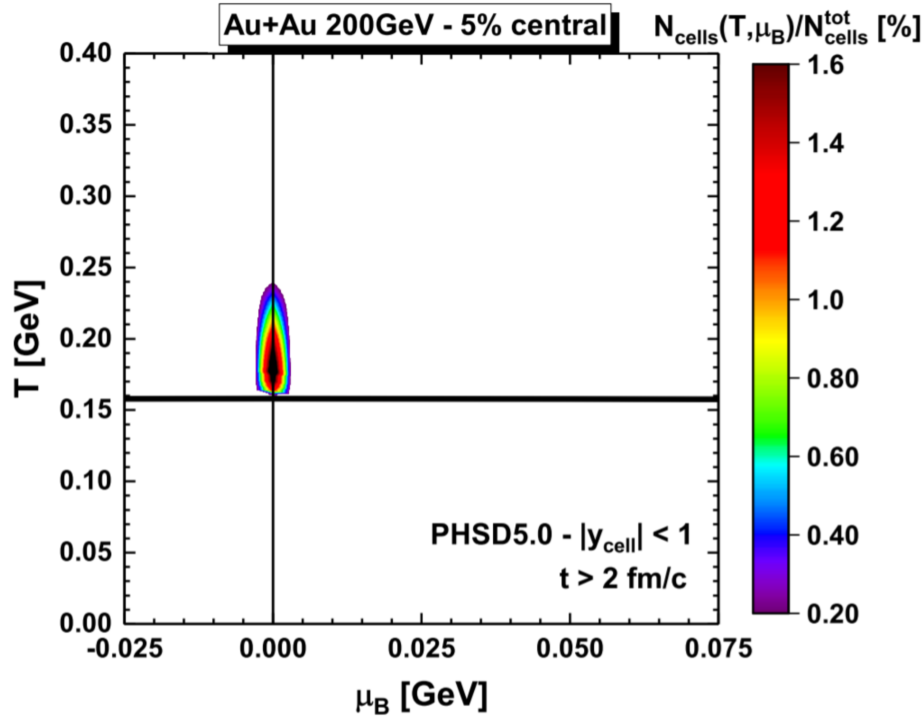

Illustration for HIC ($\sqrt{s_{NN}} = 200$ GeV)

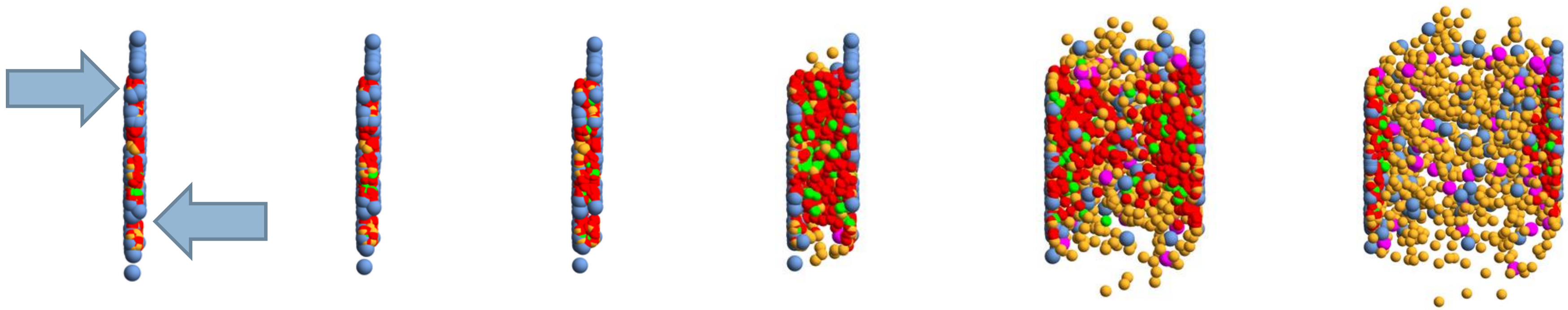

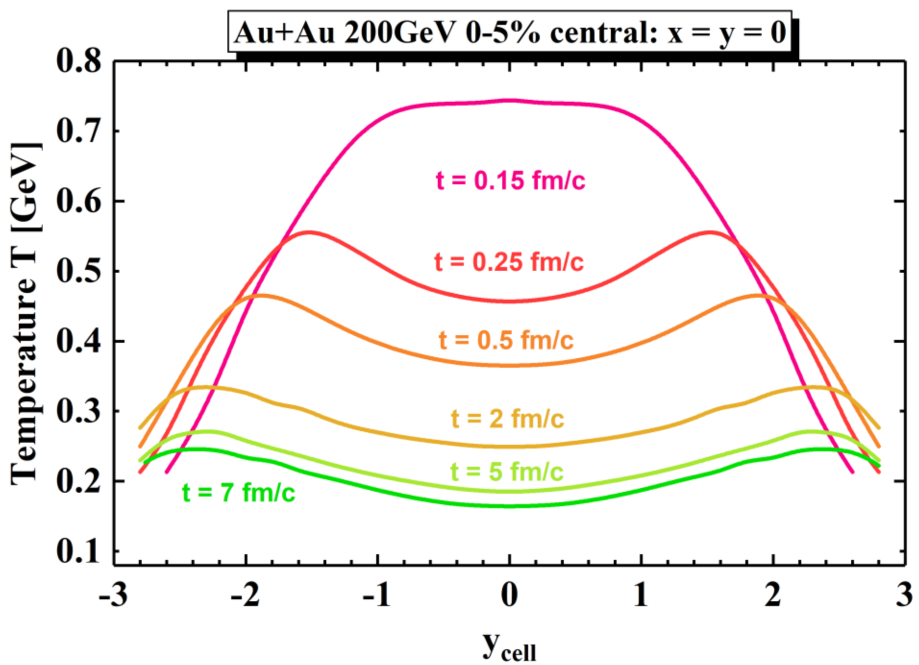

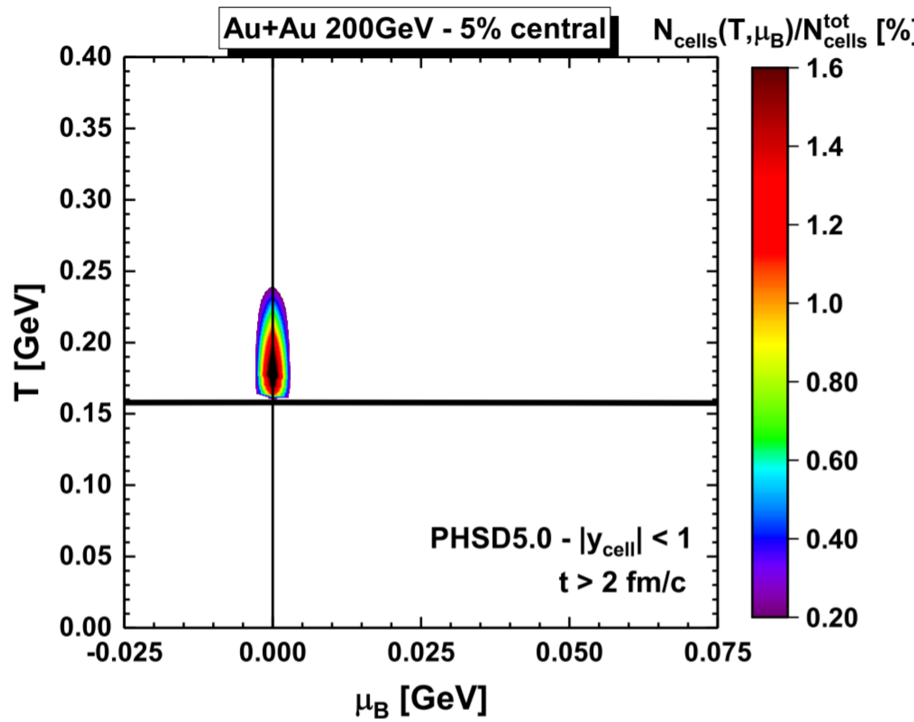

μ_B-dependence as a function of $\sqrt{s_{NN}}$

- **Comparison between:**
  - **μ_B obtained from a statistical analysis of exp. data**
  - **μ_B probed in PHSD simulations around the chemical freeze out temperature T_{ch}**
- **Two completely different quantities!!!**

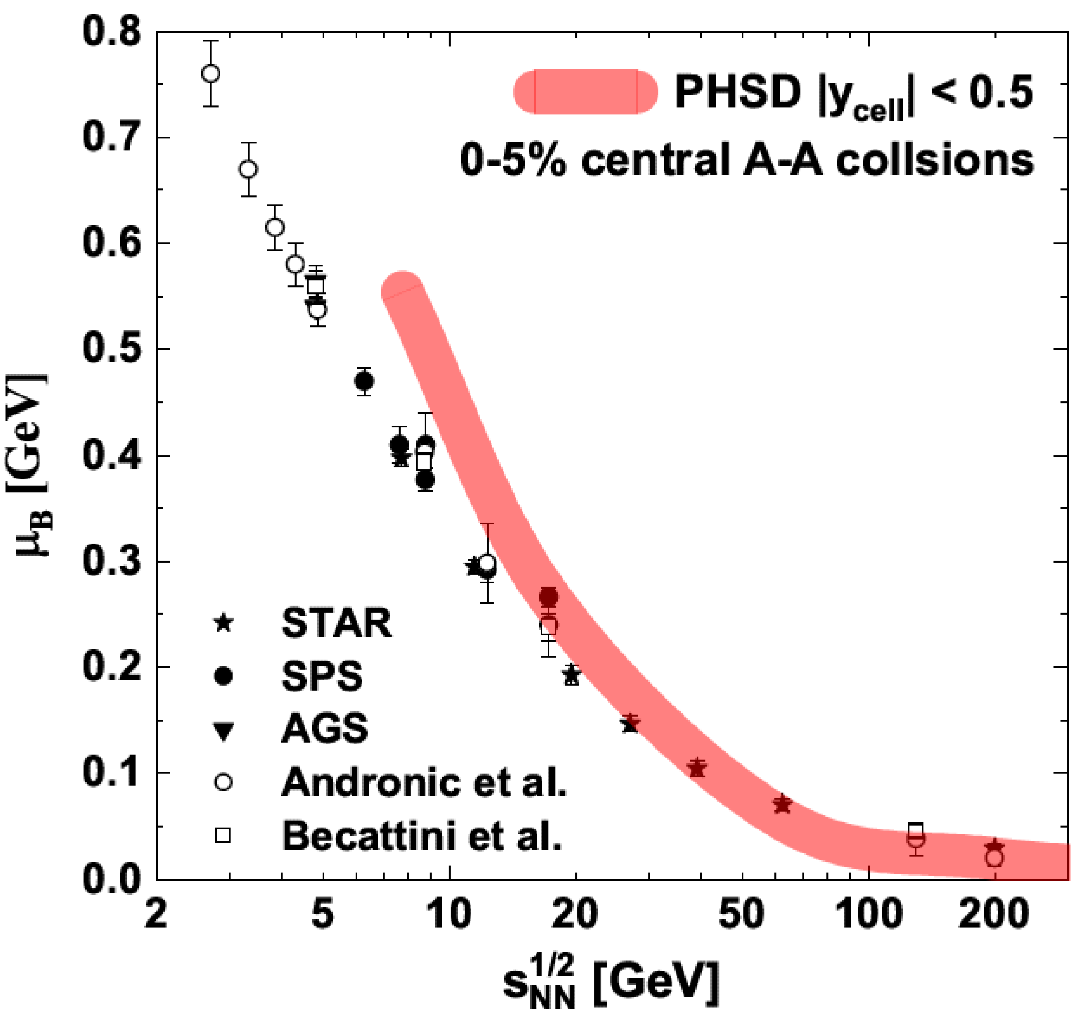

Traces of the QGP at finite μ_B in observables of heavy-ion collsions

Results for HIC

CRC-TR 211
Strong-interaction matter under extreme conditions

- **Comparison between three different results:**

1) **PHSD 4.0 : only $\sigma(T)$ and $M(T)$**
2) **PHSD 5.0 : with $\sigma\left(\sqrt{s}, T, \mu_B = 0\right)$ and $M(T, \mu_B = 0)$**
3) **PHSD 5.0 : with $\sigma\left(\sqrt{s}, T, \mu_B\right)$ and $M(T, \mu_B)$**

Results for HIC ($\sqrt{s_{NN}} = 200$ GeV)

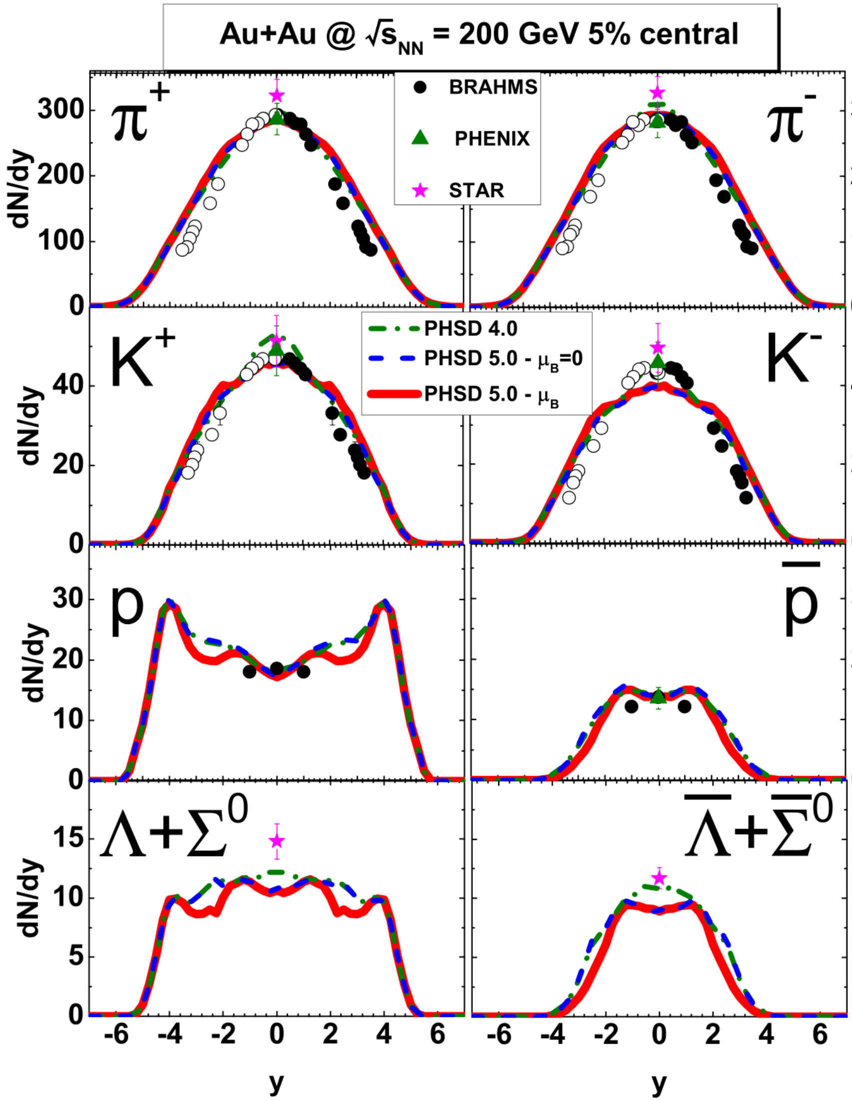

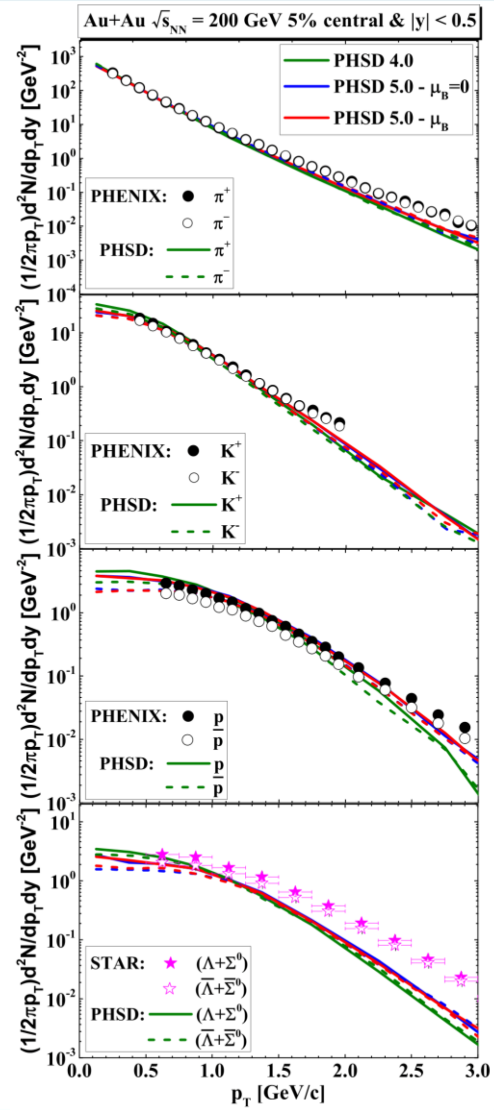

Results for HIC ($\sqrt{s_{NN}} = 17$ GeV)

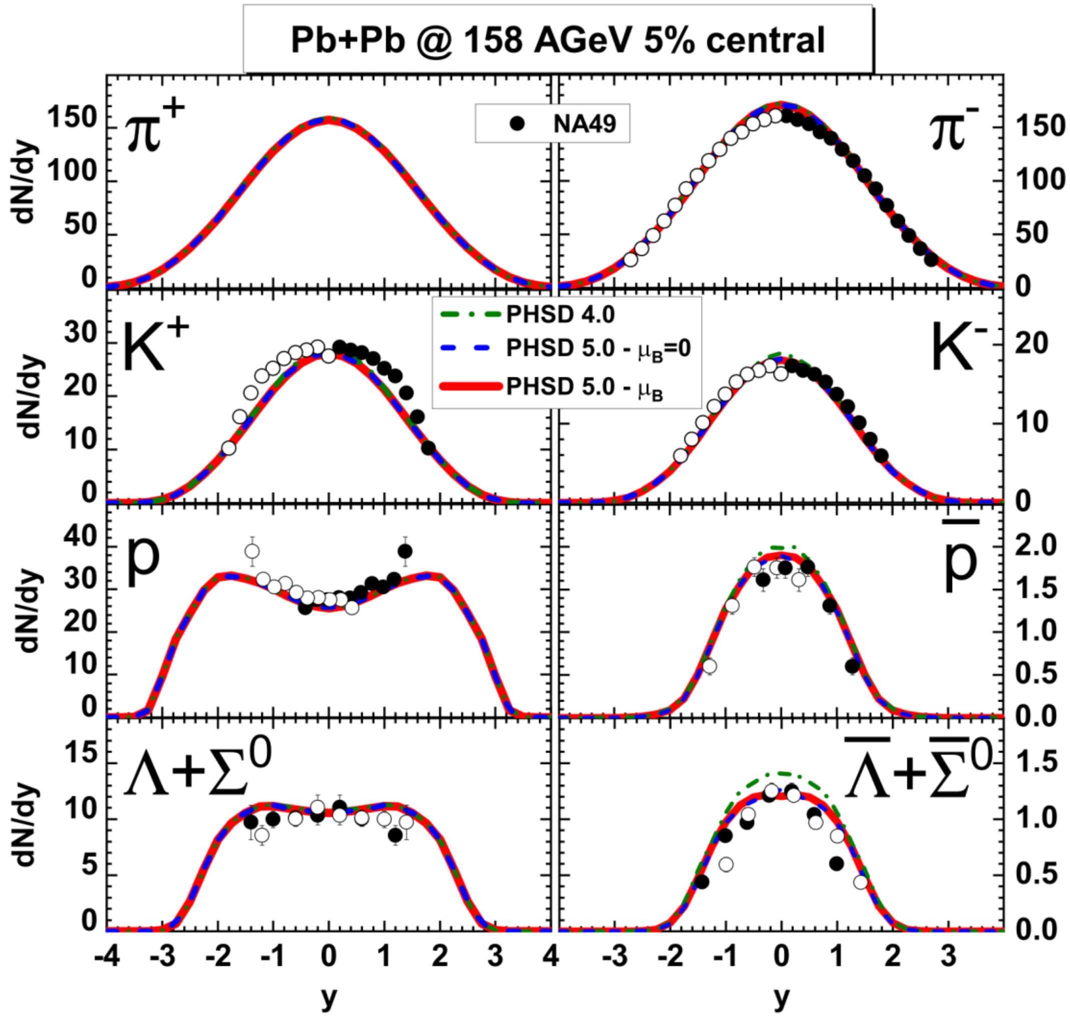

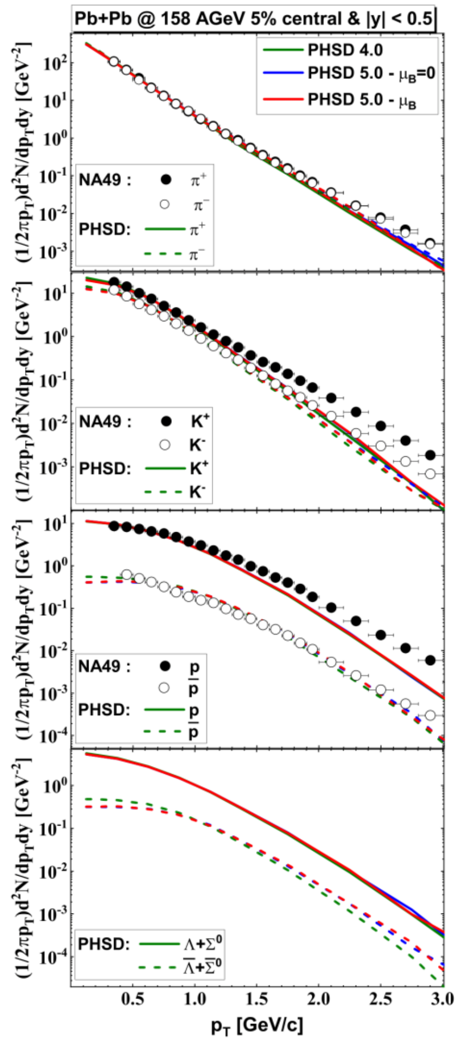

Results for HIC ($\sqrt{s_{NN}} = 7.6$ GeV)

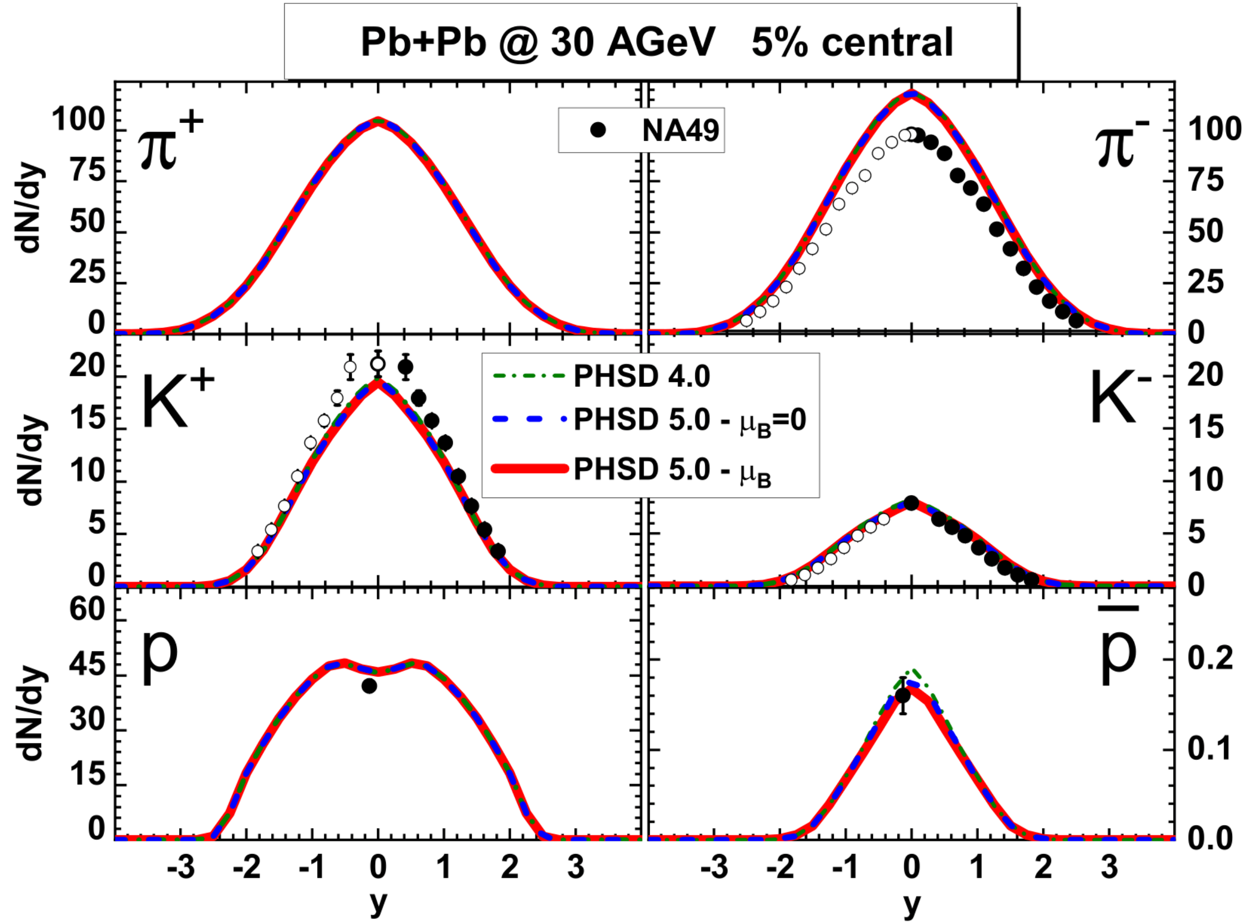

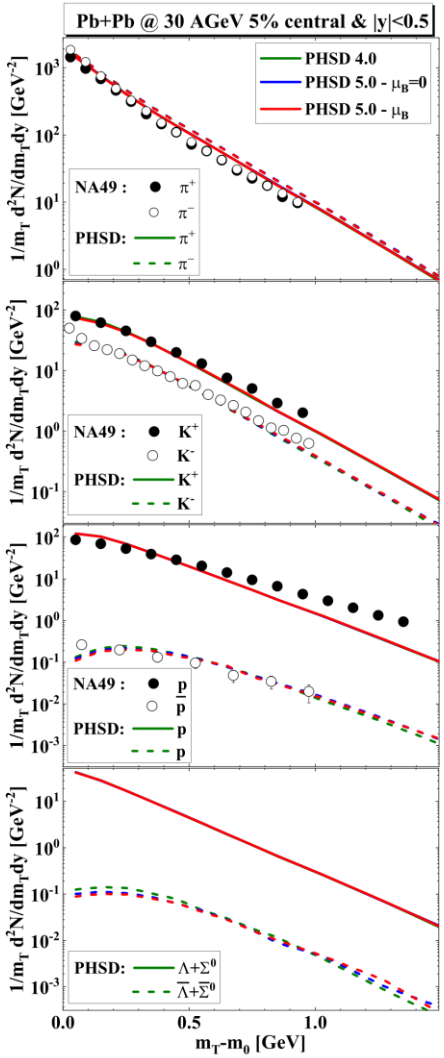

Summary / Outlook

CRC-TR 211
Strong-interaction matter under extreme conditions

- (T, μ_B)-dependent cross sections and masses have been implemented in PHSD
- High-μ_B regions are probed at low $\sqrt{s_{NN}}$ or high rapidity regions
- But, QGP fraction is small at low $\sqrt{s_{NN}}$: no effects seen in bulk observables

- **Outlook:**
  - Study more sensitive probes to finite-μ_B dynamics
  - Use of a more sophisticated QuasiParticle Model with momentum dependent masses and widths
  - Possible 1st order phase transition at larger μ_B ?

Thank you for your attention!

Energy density and baryon density

- Illustration of the **energy density** and **baryon density**